Empowering Decision Trees via Shape Function Branching

Nakul Upadhya, Eldan Cohen
Department of Mechanical and Industrial Engineering
University of Toronto, Toronto, Canada
nakul.upadhya@mail.utoronto.ca, eldan.cohen@utoronto.ca

Abstract

Decision trees are prized for their interpretability and strong performance on tabular data. Yet, their reliance on simple axis-aligned linear splits often forces deep, complex structures to capture non-linear feature effects, undermining human comprehension of the constructed tree. To address this limitation, we propose a novel generalization of a decision tree, the Shape Generalized Tree (SGT), in which each internal node applies a learnable axis-aligned shape function to a single feature, enabling rich, non-linear partitioning in one split. As users can easily visualize each node's shape function, SGTs are inherently interpretable and provide intuitive, visual explanations of the model's decision mechanisms. To learn SGTs from data, we propose ShapeCART, an efficient induction algorithm for SGTs. We further extend the SGT framework to bivariate shape functions (S^2GT) and multi-way trees (SGT_K), and present Shape^2CART and $\mathrm{ShapeCART}_K$, extensions to ShapeCART for learning S^2GTs and SGT_Ks, respectively. Experiments on various datasets show that SGTs achieve superior performance with reduced model size compared to traditional axis-aligned linear trees.

1 Introduction

Tabular datasets are collections of data organized into rows and columns, containing distinct features that can be continuous, categorical, or ordinal and remain among the most widely used dataset types in machine learning [1, 2]. Decisions trees are one of the most widely used approaches on these tabular datasets [3], largely due to their inherent interpretability [4] and robust performance [3]. These characteristics have established them as a favored choice in high-stakes domains such as healthcare [5, 6], finance [7, 8], and manufacturing [9, 10], where the ability to understand the model predictions is often just as important as high predictive accuracy. Structurally, decision trees organize nodes hierarchically, with internal nodes responsible for routing data samples based on defined criteria and terminal (leaf) nodes providing the final predictions. A common type of tree is the *binary axis-aligned linear tree*, where each internal node routes data to a left or right child node based on a simple threshold comparison involving only a single feature: $x_d \leq \theta$ (send to left if feature d is less than or equal to threshold θ).

While axis-aligned linear trees are simple and interpretable, the impact of feature values on the target is often non-linear, requiring repeated splits on the same features at different levels of the tree to represent the feature-target relationship adequately (see Figure 1b). However, repeatedly employing a single feature across multiple nodes in a decision path can hinder end-user comprehension of the model's learned relationship for that feature [11] and necessitate a larger tree with greater depth and node count to attain sufficient performance. This increase in size directly impacts interpretability, with empirical evidence confirming that tree comprehensibility is highly sensitive to the depth of decision paths and the number of leaves [4]. Furthermore, deeper trees inherently generate larger,

39th Conference on Neural Information Processing Systems (NeurIPS 2025).

less interpretable local explanations [12, 13]. Finally, larger trees are also challenging to visualize effectively, often requiring complex, interactive tools to gain insights [12, 14].

Generalized Additive Models (GAMs) [15] are another class of interpretable models where predictions are the result of the sum of individual feature contributions, each defined by a potentially non-linear *shape function*. Researchers have parameterized these shape functions using diverse model classes such as splines [15], trees [16, 17], and neural networks [18–20], enabling powerful modeling capabilities. Shape functions offer a key interpretability benefit as their flexibility enables GAMs to closely capture the true feature–target dynamics in the data [21] while still allowing practitioners to visualize each function independently, faithfully conveying the learned relationship [15, 21]. GAMs have also been extended to incorporate pairwise feature interactions [17, 19, 20, 22] by adding bivariate shape functions, creating GA^{2}Ms. Bivariate shape functions can be visualized via heatmaps, improving modelling capacity as they can capture second-order feature interaction effects.

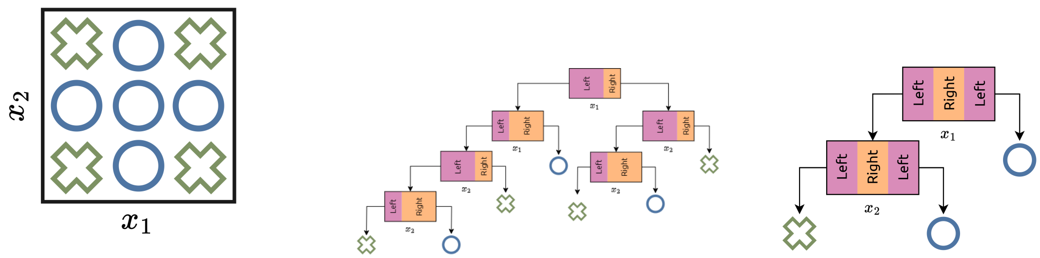

(a) Plus Sign dataset. (b) Linear Axis-Aligned Tree (c) SGT

Figure 1: Demonstration of an SGT on a simple toy dataset. As seen here, the SGT can achieve perfect accuracy with a smaller depth and number of nodes compared to the linear axis-aligned tree.

In this work, we introduce the *Shape Generalized Tree (SGT)*, a novel class of decision tree models where each internal node utilizes an axis-aligned shape function to determine the routing of samples to child nodes. As shape functions can be parametrized by a variety of rich models, they provide the capability to capture non-linear decision boundaries with respect to a chosen feature in each node. The benefit of increasing the capabilities of individual nodes can be seen clearly in Figure 1. Figure 1a visualizes a simple two dimensional synthetic dataset. A traditional axis-aligned linear tree requires six splits with a maximum depth of four (Figure 1b) to represent decision boundaries in this dataset, while the SGT can achieve the same result with only two nodes with a maximum depth of two (Figure 1c). To build SGTs, we propose *ShapeCART*, a novel and efficient SGT induction algorithm modeled after the CART framework [23] that constructs shape functions in each node via internal decision trees. Furthermore, we extend the SGT framework by incorporating bivariate shape functions in each node, resulting in S^{2}GT, and by enabling the construction of trees with higher branching factors (i.e., multi-way trees), resulting in SGT$_K$. Correspondingly, we extend the ShapeCART algorithm to accommodate these extensions, resulting in Shape^{2}CART and ShapeCART$_K$.

Overall our contributions are as follows: *(1) We introduce Shape Generalized Trees (SGTs), a new family of decision trees where internal node splits are governed by interpretable axis-aligned shape functions that can capture non-linear feature effects; (2) We introduce ShapeCART, a novel and efficient top-down induction algorithm for constructing SGTs; (3) We extend the SGT Framework to accommodate multi-way trees (SGT$_K$) and bivariate shape functions in each node (S^{2}GT) and modify ShapeCART accordingly; (4) We demonstrate across a range of datasets that SGTs achieve superior performance with more compact trees compared to traditional linear trees.*

2 Background

2.1 Decision Trees

Consider a supervised learning setting where we are given a dataset consisting of N data points $\mathcal{X} = \{\mathbf{x}_n\}_{n=1}^{N}$, where each $\mathbf{x}_n \in \mathbb{R}^D$ is a D-dimensional feature vector, and their corresponding labels $\mathcal{Y} = \{y_n\}_{n=1}^N$. Within a decision tree framework, let $\mathcal{D} \subseteq \mathcal{X} \times \mathcal{Y}$ represent the subset of training data that reaches a specific internal node. The core mechanism of a decision tree involves recursively partitioning the data $\mathcal{D}$ at each internal node based on a defined splitting criterion. Among the most common type of decision trees is the binary axis-aligned linear tree:

Definition 1 (Binary Axis-Aligned Linear Tree). *In a binary axis-aligned linear tree, internal nodes partition the data $\mathcal{D}$ into two subsets, $\mathcal{D}^l$ and $\mathcal{D}^r$, based on a threshold θ applied to a single feature encoded by a one-hot vector $\mathbf{w}$:*

$$\mathcal{D}^l = \{(\mathbf{x}_n, y_n) \in \mathcal{D} \mid \mathbf{w}^\top \mathbf{x}_n \leq \theta;\ \mathbf{w} \in \{0,1\}^D, \|\mathbf{w}\|_0 = 1, \theta \in \mathbb{R}\} \quad \mathcal{D}^r = \mathcal{D}/\mathcal{D}^l \tag{1}$$

A common paradigm for learning binary-axis aligned trees is the Top-Down Induction of Decision Trees (TDIDT) strategy, a greedy procedure that recursively partitions data to minimize a predefined impurity measure, used in algorithms like the widely adopted Classification and Regression Tree (CART) [23]. The appeal of these approaches lies in their empirical performance and efficiency, allowing trees to be trained quickly and scale well. Extensions like SERDT [13] incorporate inductive biases to encourage path-level sparsity and improve interpretability. Other methods refine trees after initial training, such as Tree Alternating Optimization (TAO) [24] which iteratively updates nodes to boost predictive performance and prune the tree, and Hierarchical Shrinkage [25] which modifies the empirical target distributions in each leaf based on the parents of each leaf. Alternatively, global optimization methods such as DL8.5 [26], GOSDT [27], and OMT [28] aim to learn optimal trees but typically scale poorly on large datasets [26, 27] and often require pre-discretization of continuous features [26–28]. Recently, there has been work on developing non-greedy *near-optimal* tree induction methods. Some notable approaches include DPDT [29], which formulates tree construction as an MDP, and SPLIT [30], which reduces the runtime of GOSDT [27] via lookahead methods.

Another important type of decision trees aims to enhance node expressivity by utilizing oblique splits, which allow internal nodes to split on linear combinations of multiple features:

Definition 2 (Binary M-variate Oblique Tree). *In a Binary M-variate oblique tree, nodes use a linear combination of at most M features to partition the data:*

$$\mathcal{D}^l = \{(\mathbf{x}_n, y_n) \in \mathcal{D} \mid \mathbf{w}^\top \mathbf{x}_n \leq \theta;\ \mathbf{w} \in \mathbb{R}^D, \|\mathbf{w}\|_0 \leq M, \theta \in \mathbb{R}\} \tag{2}$$

However, oblique trees are difficult to interpret on most datasets due to the high dimensionality of each cut, making it difficult for users to reason about model decisions. Some notable approaches for learning unconstrained oblique trees ($M = D$) include utilizing the TAO [24] framework and soft decision trees, which use a continuous relaxation of the binary oblique cut to learn a tree using gradient descent. Of particular relevance to our work are pairwise oblique models ($M = 2$) such as BiCART [31], BiTAO [31], and BiDT [32], which restrict each split to consider linear combinations between exactly two input features. This restriction allows the decision boundary in each node to be visualizable, unlike higher-order ($M > 2$) oblique trees, and have shown promise in constructing accurate and compact trees.

2.2 Interpretability

Model interpretability, revealing the internal mechanisms driving predictions, is crucial for fostering trust and enabling effective deployment, especially in high-stakes domains. Interpretability is typically understood across two primary scopes: global interpretability, concerning the model's overall logic and the relationships it has learned across the entire dataset, and local interpretability, explaining the model's prediction for a specific instance and the effect of small input perturbations [33]. Approaches to achieving interpretability fall into two main categories: intrinsic model-based interpretability, where the model itself is structured to allow for direct understanding and reasoning about its predictions, and post-hoc interpretability, which uses external methods after training to approximate explanations for models lacking this inherent transparency [12, 34]. Intrinsic model-based interpretability, which allows for understanding at both local and global scopes, is facilitated by specific structural properties of the model, including: *Modularity* (or composability) where different parts of the model can be interpreted independently [34, 35]; *Simulability*, where users can reason about and faithfully trace the model's decision process; [33, 34]; and *Sparsity*, where the complexity of the model is constrained, through both reducing the number of features used and constraining the number of distinct model components a user must analyze [34, 35].

Decision trees are considered modular and simulable models, and provide model-based interpretability when their sparsity is enforced through limiting the total number of features used [13, 34] and restricting the size of the tree, measured by node count and maximum depth [4, 12, 13, 36]. Further discussion on the interpretability of trees in comparison to other models can be found in Appendix A.

3 Shape Generalized Tree

While effective in many scenarios, linear splitting criterion may result in a feature being used multiple times in a given decision path, leading to larger trees where the learned relation between the feature and the target is difficult for users to understand. To address this drawback, we propose a novel generalization of linear trees, the **Shape Generalized Tree (SGT)**, that can represent non-linear decisions within a single node. More formally, we define a binary axis-aligned SGT as follows:

Definition 3 (Binary Axis-Aligned Shape Generalized Tree (SGT)). *In a Shape Generalized Tree, internal nodes partition the data based on the output of a flexible shape function applied to a single selected feature:*

$$\mathcal{D}^l = \{(\mathbf{x}_n, y_n) \in \mathcal{D} \mid f_\Theta(\mathbf{w}^\top \mathbf{x}_n) \leq 0.0; \mathbf{w} \in \{0,1\}^D; \|\mathbf{w}\|_0 = 1\} \tag{3}$$

Here, $\mathbf{w}$ *is a one-hot feature selection vector where* $d = \arg\max(\mathbf{w})$ *is the selected feature, and* $f_\Theta : dom(\mathcal{X}_d) \to \mathbb{R};$ *is a flexible shape function parameterized by* Θ. f *can be drawn from richer function classes, enabling the capture of more intricate, non-linear decision boundaries. As* f *operates only on one feature, the shape function is easily visualized and interpreted.*

Additionally, we propose extending this generalization to accommodate bivariate shape functions in each node, leading to the Binary Bivariate Shape Generalized Tree (S^2GT) model:

Definition 4 (Binary Bivariate Shape Generalized Tree (S^2GT)). *In an* S^2GT*, internal nodes partition the data based on a shape function that utilizes at most two features:*

$$\begin{aligned}\mathcal{D}^l = \{(\mathbf{x}_n, y_n) \in \mathcal{D} \mid f^2_\Theta(\mathbf{w}_0^\top \mathbf{x}_n, \mathbf{w}_2^\top \mathbf{x}_n, \Theta) \leq 0.0;\\ \mathbf{w}_1, \mathbf{w}_2 \in \{0,1\}^D; \|\mathbf{w}_1\|_0, \|\mathbf{w}_2\|_0 = 1\}\end{aligned} \tag{4}$$

Here, $\mathbf{w}_1, \mathbf{w}_2$ *are one-hot feature selection vectors where* $d_1 = \arg\max \mathbf{w}_1, d_2 = \arg\max \mathbf{w}_2$ *are the selected features, and* $f^2_\Theta : dom(\mathcal{X}_{d_1}) \times dom(\mathcal{X}_{d_2}) \to \mathbb{R}$ *is a shape function that maps the pair of features to an output branch. The Binary Bivariate Oblique Cut (Definition 2) can be seen as a special case where* $f_\Theta(z_1, z_2) = \Theta_1 z_1 + \Theta_2 z_2 - \Theta_0$.

One significant advantage of employing shape functions is that they can be extended to accommodate multi-way branching (i.e. routing data into $K > 2$ child nodes simultaneously). This facilitates the creation of the K-Way Axis-Aligned Shape Generalized Tree (SGT_K) model:

Definition 5 (Multi-Way Axis-Aligned Shape Generalized Tree (SGT_K)). *In an* SGT_K*, internal nodes partition the data into up to* K *distinct subsets based on the output of a vector-valued shape function applied to a single feature:*

$$\mathcal{D}^k = \{(\mathbf{x}_n, y_n) \in \mathcal{D} \mid \underset{k \in \{1,\ldots,K\}}{\arg\max} \left(f^{(K)}_\Theta(\mathbf{w}^\top \mathbf{x}_n)\right) = k; \mathbf{w} \in \{0,1\}^D, \|\mathbf{w}\|_0 \leq 1\} \tag{5}$$

Here, the shape function $f^{(K)} : dom(\mathcal{X}_d) \to \mathbb{R}^K; d = \arg\max \mathbf{w}$ *maps the selected feature value to a* K*-dimensional vector, and the argmax operation determines the branch assignment.*

Although our model naturally extends to any K, we limit our exploration of SGT_K to $K = 3$ to maintain sparsity and, consequently, a high degree of interpretability. By integrating the bivariate splitting and K-way branching, we obtain S^2GT_K trees, which support multi-way splits based on non-linear interactions between two features (formal definition in Appendix B).

Expressiveness Guarantees for SGTs We formally establish that SGTs are more expressive than binary axis-aligned linear trees by showing that: (1) SGTs are at least as expressive as binary axis-aligned linear trees with a similar number of decision nodes; (2) SGTs can be strictly more expressive than axis-aligned linear trees with a similar number of decision nodes. More formally:

Theorem 1. *Every function that can be represented by a binary axis-aligned linear tree (Definition 1), can be represented by an SGT (Definition 3) with the same number of decision nodes.*

Algorithm 1: Selecting Shape Function (Node Level Outer Problem)

Input : Features $\mathcal{X}$, Target $\mathcal{Y}$, Branching Factor K, Pairwise Candidate Limit P, Coordinate Descent Iterations R, Pairwise Reg. γ, Branching Reg. λ, Impurity $\mathcal{H}(\cdot)$, Weighted Impurity $\mathcal{L}(\cdot)$
Output : Set of branching partitions $\boldsymbol{D}^*$, Best Shape Function $f^*(\cdot)$, Best Weighted Impurity $\boldsymbol{L}^*$

```
L* ← ∞; f*(·) ← None; D* ← None                                    // Initialize
for d ← 1 to D do                                          // Iterate through all features
    L_d, f_d(·), D_d ← FitShapeFunction(X, Y, H(·), K, λ, R, d)
    if L_d < L* then
        L* ← L_d; f*(·) ← f_d(·); D* ← D_d
end
if P > 0 then
    for (d_1, d_2) ∈ PairwiseCombinations(D) do        // Filter Interactions (Section 4.2)

        D_Intersect ← {D^i ∩ D^j ∀(D^i, D^j) ∈ D_{d_1} × D_{d_2}}
        δ_(d_1,d_2) ← L(D_Intersect);
    end
    Δ_P ← P Best δ values
    for (d_1, d_2) ∈ Δ_P do                  // Iterate through candidate pairs of features
        L_(d_1,d_2), f_(d_1,d_2)(·), D_(d_1,d_2) ← FitShapeFunction(X, Y, H(·), K, λ, R, (d_1, d_2))
        L_(d_1,d_2) ← L_(d_1,d_2) + γ                                // Add Pairwise Penalty
        if L_(d_1,d_2) < L* then
            L* ← L_d; f*(·) ← f_(d_1,d_2)(·); D* ← D_(d_1,d_2)
    end
return D*, L*, f*(·)
```

Theorem 2. *For every $B \in \mathbb{N}$, there exists a function for which a binary axis-aligned tree requires at least B additional decision nodes to represent, compared to an SGT.*

To prove Theorem 1, we demonstrate that axis-aligned linear trees are a special case of SGTs. To prove Theorem 2, we construct a family of one-dimensional labeling functions with periodic boundaries and show that an SGT can represent any function in this family using a fixed number of nodes, while an axis-aligned linear tree requires a number of nodes that grows linearly with the number of intervals. Complete proofs for both theorems can be found in Appendix C.

4 ShapeCART

To learn SGTs from data, we propose *ShapeCART*, a novel and efficient tree-induction algorithm inspired by the classic Classification and Regression Tree (CART) framework [23]. Furthermore, we extend the core ShapeCART algorithm to learn SGT$_K$s and S^{2}GTs, creating ShapeCART$_K$ and Shape^{2}CART respectively. For simplicity, we present our methods in the classification setting, where each label $y_n \in \mathcal{Y}$ takes values in a finite class set $\mathcal{C}$, but provide a detailed description of the regression variant in Appendix J. ShapeCART constructs a decision tree via the TDIDT paradigm (Pseudocode in Appendix K), decomposing the global optimization into greedy, recursive node-level learning tasks similar to CART. At each node, we aim to learn feature selection parameters $\mathbf{w}$ and shape-function parameters Θ that minimize the weighted impurity of the empirical class distributions in the resulting child nodes. We pose this node-level problem as a bi-level optimization: (1) An inner problem to learn the optimal shape-function parameters for each candidate feature and (2) an outer problem to select the shape function that yields the lowest impurity:

$$\min_{\mathbf{w}\in\{0,1\}^D, \|\mathbf{w}\|\leq 1} \sum_{d=1}^{D} w_d \min_{\Theta_d} \left[\mathcal{L}\left(\{\mathcal{D}_d^{\mathrm{l}}, \mathcal{D}_d^{\mathrm{r}}\}\right)\right] \tag{6}$$
$$\text{s.t.} \quad \mathcal{D}_d^{\mathrm{l}} = \{(\mathbf{x}_n, y_n) \in \mathcal{D} \mid f_d(x_{n,d}) \leq 0.0\}$$

Here, $f_d(\cdot) \equiv f_{\Theta_d}(\cdot)$ and $\mathcal{L}(\cdot)$ is the weighted impurity of the resulting branches, defined for any superadditive impurity measure $\mathcal{H}$ (e.g. Gini [23] or entropy [37]) as:

$$\mathcal{L}(\boldsymbol{D}) = \sum_{\mathcal{D}\in\boldsymbol{D}} |\mathcal{D}|\mathcal{H}(\Pi(\mathcal{D})); \quad \Pi(\mathcal{D})_c = \frac{1}{|\mathcal{D}|} \sum_{(x_n,y_n)\in\mathcal{D}} \mathbf{1}(y_n = c)\ \forall c \in \mathcal{C} \tag{7}$$

To solve this problem, we construct shape functions for each feature and select the one with the lowest weighted impurity (node level pseudocode in Algorithm 1). Additionally, this formulation naturally extends to implementing SGT_K (Equation 5) by adopting a multi-way shape function in lieu of the binary one, creating ShapeCART_K.

Extending to Shape^{2}CART To extend ShapeCART to Shape^{2}CART, we extend the above formulation to consider both individual feature shape functions and bivariate shape functions. The resulting bi-level optimization problem is as follows:

$$\begin{aligned}
\min_{\mathbf{w},\mathbf{W}} \quad & \sum_{d=1}^{D} w_d \min_{\Theta_d} \left[\mathcal{L}\left(\{\mathcal{D}_d^{\mathtt{l}}, \mathcal{D}_d^{\mathtt{r}}\}\right)\right] + && (8)\\
& \sum_{(d_1,d_2)\in\Delta} W_{(d_1,d_2)} \min_{\Theta_{(d_1,d_2)}} \left[\mathcal{L}\left(\{\mathcal{D}_{(d_1,d_2)}^{\mathtt{l}}, \mathcal{D}_{(d_1,d_2)}^{\mathtt{r}}\}\right)\right] + \gamma\|\mathbf{W}\|_0 \\
\text{s.t.} \quad & \mathcal{D}_d^{\mathtt{l}} = \{(\mathbf{x}_n, y_n) \in \mathcal{D} \mid f_d(x_{n,d}) \leq 0.0\} && (9)\\
& \mathcal{D}_{(d_1,d_2)}^{\mathtt{l}} = \{(\mathbf{x}_n, y_n) \in \mathcal{D} \mid f^2_{(d_1,d_2)}(x_{n,d_1}, x_{n,d_2}) \leq 0.0\} \\
& \|\mathbf{w}\|_0 + \|\mathbf{W}\|_0 = 1, \mathbf{w} \in \{0,1\}^D, \mathbf{W} \in \{0,1\}^{D\times D}
\end{aligned}$$

Here, $\mathbf{w}$ is a one-hot univariate feature selection vector, $\mathbf{W}$ is a one-hot bivariate interaction selection matrix, Δ is a set representing all pairs of features, and γ is a tuneable regularization hyperparameter added to penalize selection of a bivariate shape function to encourage choosing axis-aligned splits unless the bivariate function leads to a significantly lower loss.

4.1 Learning Shape Functions

Recall that for a given feature or pair of features, we would like to learn a shape function $f_d(\cdot)$ (or $f_{(d_1,d_2)}$ for bivariate trees) that assigns samples to a branch (e.g., `left`/`right` or $1,\ldots,K$ in the multi-way case) such that we minimize the impurity of the empirical class distributions of the resultant branches. To learn this shape function efficiently, we propose a two-stage approximation strategy:

1. We first learn a function $\mathbf{T}(\cdot) : \mathbb{R} \to \{1,\ldots,L\}$ that maps samples to L mutually exclusive bins based on the value of the d-th feature (or (d_1, d_2) for bivariate shape functions).
2. We then compute an assignment of bins to branches (e.g., `left`/`right`) that minimizes the impurity over the induced partitioning of the data.

4.1.1 Binning the samples

We choose to represent the binning function $\mathbf{T}(\cdot)$ via an internal decision tree. For univariate shape functions, we use CART to train a binary axis-aligned linear tree only on the relevant feature and the target to construct L mutually exclusive bins that approximately minimize the chosen impurity criteria $\mathcal{H}$. For bivariate shape functions, we instead train a binary bivariate oblique tree using BiCART [31] on the pair of features under consideration and the target. The use of CART and BiCART affords us control over model complexity; by constraining parameters such as the number of leaves and the minimum of samples in each leaf tree depth, one can ensure that the resulting piecewise-constant shape function comprises a bounded number of meaningful segments. Each bin $\ell = 1,\ldots,L$ stores its empirical class distribution $\pi_\ell \in \mathbb{R}^{|\mathcal{C}|}$ and weight $W_\ell \in \mathbb{R}$, representing the number of samples that fall into the bin. Note that while we utilize CART, this step can be performed with a variety of approaches, and we provide results using an alternative tree induction algorithm (DPDT [29]) in Appendix I.

4.1.2 Mapping Bins to Branches

Given the bins from the first stage, our goal is to assign each bin ℓ to an output branch (e.g. $\mathtt{l},\mathtt{r}$) such that we minimize the weighted impurity of the resultant branches. Formally, let $\mathbf{a} \in \{\mathtt{l},\mathtt{r}\}^L$ denote the branch assignment vector. We aim to solve the following discrete optimization problem:

$$\min_{\mathbf{a}} \quad W_{\mathbf{l}}\mathcal{H}(\Pi_{\mathbf{l}}) + W_{\mathbf{r}} \cdot \mathcal{H}(\Pi_{\mathbf{r}}) \tag{10}$$

$$\text{s.t.} \quad W_k = \sum_{\ell=1}^{L} \mathbf{1}(\mathbf{a}_\ell = k)W^\ell, \quad \Pi^k = \frac{\sum_{\ell=1}^{L} \mathbf{1}(\mathbf{a}_\ell = k)(W^\ell \pi^\ell)}{W_k} \tag{11}$$

To solve this optimization problem in a scalable manner, we adopt a coordinate descent procedure. At each step, we determine the assignment of a single bin ℓ while keeping all other assignments fixed. This reduces the optimization problem to iteratively evaluating the impurity resulting from assigning ℓ to each possible branch and selecting the assignment that minimizes the objective. The process is repeated for R iterations, with the order of leaf updates randomly shuffled in each pass to mitigate ordering bias (Pseudocode in Appendix K). Coordinate descent guarantees monotonic objective decrease and finite convergence given the discrete search space [38], with time complexity scaling linearly in the number of leaves (Appendix D). However, its sensitivity to initialization can lead to suboptimal local minima [38]. To obtain a strong initialization, we choose the better of the following two strategies for setting $\mathbf{a}$: (1) cluster assignments obtained by applying Weighted K-Means to the empirical distributions of the bins π_ℓ, weighted by W_ℓ; or (2) bin assignments based on whether each bin falls to the left or right of the root node in the inner CART tree.

Based on the procedure detailed above, we can derive a lower-bound on the information gain at each decision node with respect to the information gain at each node in CART:

Lemma 1. *Let t be an individual node in T, let $\mathcal{IG}(t)$ denote the information gain obtained by an axis-aligned (threshold) split on the samples in t from CART, and let $\mathcal{IG}_f(t)$ denote the information gain obtained by a shape function split from ShapeCART on the samples in t. We show that $\mathcal{IG}_f(t) \geq \mathcal{IG}(t)$.*

Given this lemma, ShapeCART inherits the bound on information gain for any terminal node of the tree established for CART by Klusowski and Tian [39]. Proof of Lemma 1 can be found in Appendix C.2.

Algorithm 2: Fit Shape Function

Input : $\mathcal{X},\ \mathcal{Y},\ R,\ K,\ \lambda,\ \mathcal{H}(\cdot),\ d$ or (d_1, d_2),
Output: $\boldsymbol{L}_{k^*},\ f_d(\cdot)$

```
if d was provided then
  | T ← FitCART(X_d, Y) ;
else
  | T ← FitBiCART(X_{d_1}, X_{d_2}, Y)
end
(W_1, ..., W_L), (π_1, ..., π_L) ← ExtractBinStats(T)
a_{(0),root}, L^{(0)}_root ← ExtractRootAssignments(T)
for k ← 2 to K do
  | a^k_{(0),WKM}, L^{(0)}_{k,WKM} ← WeightedKMeans([π_1, ..., π_L];
  |                                   [W_1, ..., W_L]; k)
  | if L^{(0)}_root < L^{(0)}_{k,WKM} then
  |   | a^k_{(0)} ← a_{(0),root}
  | else
  |   | a^k_{(0)} ← a^k_{(0),WKM}
  | end
  | (a^k, L_k) ← CoordDescent(a^k_{(0)}; [π_1, ..., π_L];
  |                           [W_1, ..., W_L]; k; H(·); R)
end
k* ← argmin_{k=2,...,K} (L_k + λ(k − 2))
{D^1, ..., D^{k*}} ← RetrieveBranchAssignments(X, T, a^{k*})
f(·) ← a^{k*}_{T(·)}
return L_{k*}, f(·), {D^1, ..., D^{k*}}
```

Extending to Multi-Way Branching ShapeCART can be adapted to the multi-way setting, ShapeCART$_K$, by increasing the number of clusters in the Weighted K-Means initialization and considering more options for $\mathbf{a}_\ell$ in each step of the coordinate descent procedure. To regularize ShapeCART$_K$ and prevent the creation of branches that do not provide a significant impurity decrease, we run the Weighted K-Means initialization and Coordinate Descent procedure for each $k \in \{2, \ldots, K\}$ and add a penalty term $\lambda(k-2)$ to the weighted impurity of the assignments for that k, where λ is a hyperparameter. We then select the k with the minimum penalized impurity.

In summary, the shape function for a given feature $f_d(\cdot)$ is represented jointly by an internal tree $\mathbf{T}_d(\cdot)$ which maps samples to bins, and a lookup vector $\mathbf{a}$ which maps bins to branches (Pseudocode in Algorithm 2). The time complexity of constructing a shape function is $\mathcal{O}\left(NC\log N + K^2LC\right)$ where C is the number of classes (see Appendix D for detailed analysis).

4.2 Limiting Bivariate Shape Function Construction

Recall that to solve the optimization problem presented in Equations 8, we need to construct all univariate and bivariate shape functions to select the one that minimizes the weighted impurity of the resultant branches. A naive approach of constructing a shape function for each pair of features will require constructing $\mathcal{O}(D^2)$ shape functions, incurring significant computational cost. Instead, we propose a heuristic that utilizes the computation of univariate shape functions to identify a few promising pairs for which a shape function will be constructed. We first construct univariate shape functions $f_1, \ldots, f_D$ and denote the set of branches resultant from applying each feature's shape functions on the input data as $\boldsymbol{D}_d = \{\mathcal{D}_d^{\mathrm{l}}, \mathcal{D}_d^{\mathrm{r}}\}\ \forall d = 1, \ldots, D$ (or $\boldsymbol{D}_d = \{\mathcal{D}_d^1, \ldots, \mathcal{D}_d^K\}$ in the multi-way case). Our goal is to identify pairs of features (d_1, d_2) that have the potential to have an impurity that is significantly lower than the best impurity of the individual features. We achieve this by calculating the weighted impurity of the sets induced by the Cartesian product of the branching sets of a pair of features and subtracting this value from the best impurity obtained from the univariate shape functions in the pair:

$$\delta_{(d_1,d_2)} = \min(\mathcal{L}(\boldsymbol{D}_{d_1}), \mathcal{L}(\boldsymbol{D}_{d_2})) - \mathcal{L}(\{\mathcal{D}^i \cap \mathcal{D}^j | (\mathcal{D}^i, \mathcal{D}^j) \in \boldsymbol{D}_{d_1} \times \boldsymbol{D}_{d_2}\}) \tag{12}$$

We retain the P pairs with the highest δ values and denote this set as Δ_P, which we use in lieu of the full set of pairs (Δ) in Equation 8. With our heuristic, we only require $\mathcal{O}((N + CK^2)D^2)$ operations to construct the intersection of sets followed by the construction of P shape functions ($\mathcal{O}(P(NC \log N + K^2 LC))$ vs. $\mathcal{O}(D^2(NC \log N + K^2 LC))$). Assuming $P \ll D^2$, this heuristic can significantly reduce runtime (evaluated in Appendix G.2.3). The choice of P is guided by the user's computational preferences; higher P increases runtime in return for increased performance.

4.3 Post-Processing

TDIDT approaches are efficient and allow trees to be trained quickly. However, one downside of TDIDT approaches is their greedy behavior, potentially resulting in globally-suboptimal trees [24, 29]. To overcome this, we globally refine the tree constructed via ShapeCART using Tree Alternating Optimization (TAO) [24, 31]. This post-processing procedure refits the shape function at each internal node of the constructed tree using the predictions of the subtrees rooted at the node's children, while also pruning nodes that do not significantly reduce error. While the original TAO algorithm is restricted to binary trees, we extend it to support K-way branching. Full implementation details and our modifications to TAO are provided in Appendix F.

5 Experimental Evaluation

In this section, we evaluate the performance of trees induced by ShapeCART (SGT-C), ShapeCART$_3$ (SGT$_3$-C), Shape^{2}CART (S^{2}GT-C) and Shape^{2}CART$_3$ (S^{2}GT$_3$-C) against various benchmark approaches on a range of 26 real-world classification datasets (details in Appendix E). We also present results on the TAO refined ShapeCART models - denoted as SGT-T, SGT$_3$-T, S^{2}GT-T, and S^{2}GT$_3$-T. We benchmark our axis-aligned approaches against CART [23], SERDT [13], HSTree [25], Axis-Aligned TAO (AxTAO) [24], DPDT [29], and SPLIT [30]. We evaluate our bivariate approaches against the newly proposed BiCART and BiTAO algorithms [31]. CART, SERDT, HSTree, and BiCART are greedy TDIDT induction approaches, while AxTAO, DPDT, SPLIT and BiTAO are non-greedy induction approaches. Implementation details for all models evaluated can be found in Appendix F.

Hyperparameter Search and Evaluation In our experiments, we report results for all approaches across reasonable tree depths (2–6), following Souza et al. [13] and for the overall best model. Each dataset is split into three folds using a 70/30 train/validation–test split, with the non-training data further divided in the same ratio. Hyperparameters are optimized via Bayesian search with Optuna [40] using 50 trials per model and depth to ensure fairness across differing search spaces. Each configuration is scored by mean validation accuracy, and we retain the best per depth and overall. Training time is limited to 15 minutes for univariate and 30 minutes for bivariate models. All runs are executed on GCP N2 instances (8 vCPUs, 32 GB RAM). Hyperparameter search spaces for all evaluated approaches and hyperparameter importance analyses for all ShapeCART variants appear in Appendix F.1. We present average test accuracy results across datasets below, and additional evaluations and ablations are presented in Appendix G.

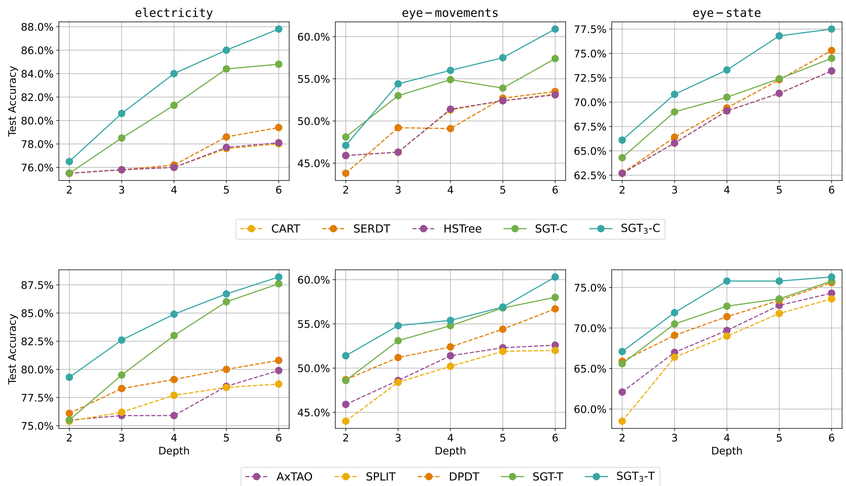

Figure 2: Test accuracy per depth for axis-aligned approaches on `eye-movements`, `electricity`, and `eye-state`. Top: TDIDT-Approaches. Bottom: Non-Greedy Approaches.

Table 1: Average Test Accuracy (%) across the datasets tested. Top: TDIDT approaches, Bottom: Non-Greedy Approaches. Best approach per block is **bolded** and second best is *italicized*.

(a) Axis-Aligned Approaches

Model	2	3	4	5	6	Best
CART	83.9	81.6	82.3	84.0	85.1	85.2
SERDT	83.7	80.9	81.7	83.7	85.1	85.1
HSTree	83.9	81.6	82.4	84.0	85.1	85.1
SGT-C	*84.5*	*82.5*	*83.7*	*84.9*	*86.2*	*86.3*
SGT$_3$-C	**85.7**	**84.6**	**85.9**	**87.3**	**87.8**	**87.8**
AxTAO	83.9	82.1	82.8	84.5	85.5	85.4
DPDT	84.9	83.4	83.8	85.2	86.2	86.2
SPLIT	81.7	76.6	77.9	79.5	80.2	80.3
SGT-T	*85.0*	*83.5*	*84.6*	*85.9*	*86.8*	*86.8*
SGT$_3$-T	**86.4**	**85.1**	**86.2**	**87.5**	**88.0**	**88.0**

(b) Bivariate Approaches

Model	2	3	4	5	6	Best
BiCART	87.3	87.6	87.9	88.7	89.6	89.6
S^{2}GT-C	*89.3*	*89.1*	*89.5*	*90.5*	*91.3*	*91.4*
S^{2}GT$_3$-C	**90.0**	**90.2**	**91.1**	**91.8**	**91.5**	**91.7**
BiTAO	87.9	88.1	88.4	89.3	90.1	90.0
S^{2}GT-T	*89.7*	*90.0*	*90.2*	*91.2*	*91.7*	*91.6*
S^{2}GT$_3$-T	**90.2**	**90.6**	**91.2**	**91.7**	**92.4**	**91.9**

Results on Axis-Aligned Trees Table 1a reports the average test accuracy of axis-aligned approaches across all datasets. We observe that SGT-C consistently outperforms all baseline TDIDT methods at every evaluated depth. Moreover, SGT$_3$-C achieves superior performance both overall and at each depth, highlighting the benefit of higher branching factors. It is important to note that despite the increase in the number of nodes, ternary trees have the same size of local explanation as binary trees of the same depth [13]. Among non-greedy methods, we observe that the TAO-refined SGTs attain the highest performance across all axis-aligned approaches. At the dataset level (Figure 2), SGT-C often matches or exceeds the maximum-depth accuracy of other TDIDT methods with substantially shallower trees. A similar, though less pronounced, pattern is observed for SGT-T when compared to deeper non-greedy methods.

Results on Bivariate Trees In our evaluation of bivariate approaches, we exclude Covertype, Eucalyptus, and Higgs as BiCART and BiTAO require more than the 32GB of available memory on these datasets. When looking at the average performance of the bivariate models on the remaining datasets (Table 1b), we observe that S^{2}GT-C and S^{2}GT-T consistently outperform BiCART and BiTAO, respectively, across all depths as well as overall. Like in the univariate case, we observe that a higher branching factor helps improve expressivity as both S^{2}GT$_3$-C and S^{2}GT$_3$-T outperform S^{2}GT-C and S^{2}GT-T respectively. We also observe that bivariate shape function branching can significantly compress needed tree size in many cases. More specifically, we observe that on the `eye-movements` and `electricity` datasets (See Figure G.4 in Appendix), S^{2}GT-C with a depth of two achieves similar performance to both BiTAO and BiCART with depths of six.

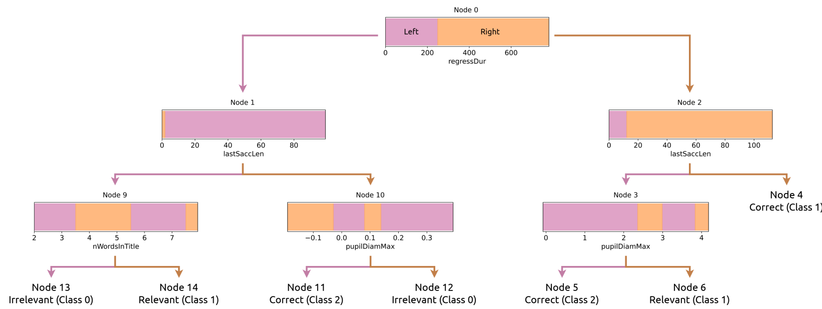

Figure 3: Visualization of a SGT induced via ShapeCART (max depth 3) trained on the `eye-movements` dataset. Purple indicates regions where samples will be directed to the left child; Orange directed to the right.

Visualization To illustrate the interpretability of SGTs, we visualize a trained ShapeCART model on the `eye-movements` dataset [41] in Figure 3. We observe that multiple nodes benefit from non-linear shape functions. For example, the decisions represented in Nodes 3, 9, and 10 would each require at least three additional splits in a linear axis-aligned tree. Additional examples, including visualized Shape^{2}CART, ShapeCART$_3$, and Shape^{2}CART$_3$ trees, are provided in Appendix H.

6 Conclusion

This paper introduces the Shape Generalized Tree (SGT), a novel generalization of traditional linear decision trees that empowers each node with shape-function branching. Shape Generalized Trees retain the inherent interpretability that makes decision trees a leading approach as the shape functions learned at each node can be easily visualized, allowing users to understand an SGT's internal decision mechanisms. We also introduce ShapeCART, an efficient top-down induction algorithm to construct these SGT models. Additionally, we extend our framework to support bivariate SGTs (S^{2}GT) and multi-way SGTs (SGT$_K$), and present the corresponding ShapeCART variants (Shape^{2}CART and ShapeCART$_K$). Overall, we show that SGTs outperform linear trees on various datasets across various model sizes.

Limitations As tree-based models, Shape Generalized Trees (SGTs) inherit intrinsic constraints of traditional decision trees, most notably that they are designed primarily for tabular data. Furthermore, interpreting the shape functions at each node can be more challenging than understanding axis-aligned linear splits, potentially increasing the cognitive effort required for analysis. Nevertheless, SGTs preserve essential interpretability properties, including simulability and modularity, while their enhanced expressiveness enables the construction of smaller trees without compromising predictive performance, thereby improving the sparsity of local explanations. Despite these advantages, further work is needed to systematically evaluate the interpretability of SGTs, and human-subject studies, similar to those conducted for GAMs [42], present a valuable direction for future research.

Broader Impact SGTs constitute an inherently interpretable class of models, and our promising results inducing them via ShapeCART may inspire other future inherently interpretable approaches, thereby enhancing transparency and accountability in machine learning systems. Exploring alternative shape function representations representations, such as neural networks used in GAMs [18–20], and developing clustering SGTs [43–45] are promising directions for future work. Furthermore, our work opens interesting directions for future work to further theoretically characterize SGTs and ShapeCART, including extending theoretical properties of CART such as consistency rate [39, 46], the impact of sparsity [47], and tighter empirical risk bounds [39].

Acknowledgments and Disclosure of Funding

This research was supported by grant number DSI-CGY3R1P18 from the Data Sciences Institute at the University of Toronto. The authors also gratefully acknowledge funding from the Natural Sciences and Engineering Research Council of Canada (NSERC).

References

[1] Duncan McElfresh, Sujay Khandagale, Jonathan Valverde, Vishak Prasad C, Ganesh Ramakrishnan, Micah Goldblum, and Colin White. When do neural nets outperform boosted trees on tabular data? *Advances in Neural Information Processing Systems*, 36:76336–76369, 2023.

[2] Ravid Shwartz-Ziv and Amitai Armon. Tabular data: Deep learning is not all you need. *Information Fusion*, 81:84–90, 2022.

[3] Léo Grinsztajn, Edouard Oyallon, and Gaël Varoquaux. Why do tree-based models still outperform deep learning on typical tabular data? *Advances in neural information processing systems*, 35:507–520, 2022.

[4] Mitja Luštrek, Matjaž Gams, Sanda Martinčić-Ipšić, et al. What makes classification trees comprehensible? *Expert Systems with Applications*, 62:333–346, 2016.

[5] Gregor Stiglic, Primoz Kocbek, Nino Fijacko, Marinka Zitnik, Katrien Verbert, and Leona Cilar. Interpretability of machine learning-based prediction models in healthcare. *Wiley Interdisciplinary Reviews: Data Mining and Knowledge Discovery*, 10(5):e1379, 2020.

[6] K. Srinivas, G. Raghavendra Rao, and A. Govardhan. Analysis of coronary heart disease and prediction of heart attack in coal mining regions using data mining techniques. In *2010 5th International Conference on Computer Science & Education*, pages 1344–1349, 2010. doi: 10.1109/ICCSE.2010.5593711.

[7] Jozef Zurada. Could decision trees improve the classification accuracy and interpretability of loan granting decisions? In *2010 43rd Hawaii International Conference on System Sciences*, pages 1–9. IEEE, 2010.

[8] Pan Tang, Tiantian Tang, and Chennuo Lu. Predicting systemic financial risk with interpretable machine learning. *The North American Journal of Economics and Finance*, 71:102088, 2024. ISSN 1062-9408. doi: https://doi.org/10.1016/j.najef.2024.102088. URL `https://www.sciencedirect.com/science/article/pii/S1062940824000123`.

[9] Choi Sungsu, Battulga Lkhagvadorj, Aziz Nasridinov, Kwan-Hee Yoo, et al. A decision tree approach for identifying defective products in the manufacturing process. *International Journal of Contents*, 13(2):57–65, 2017.

[10] Sadeq Heydarbakian and Mehran Spehri. Interpretable machine learning to improve supply chain resilience, an industry 4.0 recipe. *IFAC-PapersOnLine*, 55(10):2834–2839, 2022. ISSN 2405-8963. doi: https://doi.org/10.1016/j.ifacol.2022.10.160. URL `https://www.sciencedirect.com/science/article/pii/S2405896322021747`. 10th IFAC Conference on Manufacturing Modelling, Management and Control MIM 2022.

[11] Federica Di Castro and Enrico Bertini. Surrogate decision tree visualization. In *IUI Workshops*, 2019.

[12] Christoph Molnar. *Interpretable machine learning*. Lulu. com, 2020.

[13] Victor Feitosa Souza, Ferdinando Cicalese, Eduardo Laber, and Marco Molinaro. Decision trees with short explainable rules. In S. Koyejo, S. Mohamed, A. Agarwal, D. Belgrave, K. Cho, and A. Oh, editors, *Advances in Neural Information Processing Systems*, volume 35, pages 12365–12379. Curran Associates, Inc., 2022. URL `https://proceedings.neurips.cc/paper_files/paper/2022/file/500637d931d4feb99d5cce84af1f53ba-Paper-Conference.pdf`.

[14] Yan Liu and Gavriel Salvendy. Design and evaluation of visualization support to facilitate decision trees classification. *International journal of human-computer studies*, 65(2):95–110, 2007.

[15] Trevor J Hastie. Generalized additive models. *Statistical models in S*, pages 249–307, 2017.

[16] Harsha Nori, Samuel Jenkins, Paul Koch, and Rich Caruana. Interpretml: A unified framework for machine learning interpretability. *arXiv preprint arXiv:1909.09223*, 2019.

[17] Chun-Hao Chang, Rich Caruana, and Anna Goldenberg. Node-gam: Neural generalized additive model for interpretable deep learning. *arXiv preprint arXiv:2106.01613*, 2021.

[18] Rishabh Agarwal, Levi Melnick, Nicholas Frosst, Xuezhou Zhang, Ben Lengerich, Rich Caruana, and Geoffrey E Hinton. Neural additive models: Interpretable machine learning with neural nets. *Advances in neural information processing systems*, 34:4699–4711, 2021.

[19] Filip Radenovic, Abhimanyu Dubey, and Dhruv Mahajan. Neural basis models for interpretability. *Advances in Neural Information Processing Systems*, 35:8414–8426, 2022.

[20] Nakul Upadhya and Eldan Cohen. Neurcam: Interpretable neural clustering via additive models. In *ECAI*, 2024.

[21] Chun-Hao Chang, Sarah Tan, Ben Lengerich, Anna Goldenberg, and Rich Caruana. How interpretable and trustworthy are gams? In *Proceedings of the 27th ACM SIGKDD conference on knowledge discovery & data mining*, pages 95–105, 2021.

[22] Yin Lou, Rich Caruana, Johannes Gehrke, and Giles Hooker. Accurate intelligible models with pairwise interactions. In *Proceedings of the 19th ACM SIGKDD international conference on Knowledge discovery and data mining*, pages 623–631, 2013.

[23] Leo Breiman. *Classification and regression trees*. Routledge, 2017.

[24] Miguel A Carreira-Perpinán and Pooya Tavallali. Alternating optimization of decision trees, with application to learning sparse oblique trees. *Advances in neural information processing systems*, 31, 2018.

[25] Abhineet Agarwal, Yan Shuo Tan, Omer Ronen, Chandan Singh, and Bin Yu. Hierarchical shrinkage: Improving the accuracy and interpretability of tree-based models. In *International Conference on Machine Learning*, pages 111–135. PMLR, 2022.

[26] Gaël Aglin, Siegfried Nijssen, and Pierre Schaus. Learning optimal decision trees using caching branch-and-bound search. In *Proceedings of the AAAI conference on artificial intelligence*, volume 34, pages 3146–3153, 2020.

[27] Jimmy Lin, Chudi Zhong, Diane Hu, Cynthia Rudin, and Margo Seltzer. Generalized and scalable optimal sparse decision trees. In *International conference on machine learning*, pages 6150–6160. PMLR, 2020.

[28] Shivaram Subramanian and Wei Sun. Scalable optimal multiway-split decision trees with constraints. In *Proceedings of the AAAI Conference on Artificial Intelligence*, volume 37, pages 9891–9899, 2023.

[29] Hector Kohler, Riad Akrour, and Philippe Preux. Breiman meets bellman: Non-greedy decision trees with mdps. In *KDD 2025-The 31st ACM SIGKDD Conference on Knowledge Discovery and Data Mining*, 2025.

[30] Varun Babbar, Hayden McTavish, Cynthia Rudin, and Margo Seltzer. Near optimal decision trees in a split second. *arXiv preprint arXiv:2502.15988*, 2025.

[31] Rasul Kairgeldin and Miguel Á Carreira-Perpiñán. Bivariate decision trees: Smaller, interpretable, more accurate. In *Proceedings of the 30th ACM SIGKDD Conference on Knowledge Discovery and Data Mining*, pages 1336–1347, 2024.

[32] Ferdinand Bollwein and Stephan Westphal. A branch & bound algorithm to determine optimal bivariate splits for oblique decision tree induction. *Applied Intelligence*, 51(10):7552–7572, 2021.

[33] Dylan Slack, Sorelle A Friedler, Carlos Scheidegger, and Chitradeep Dutta Roy. Assessing the local interpretability of machine learning models. *arXiv preprint arXiv:1902.03501*, 2019.

[34] W James Murdoch, Chandan Singh, Karl Kumbier, Reza Abbasi-Asl, and Bin Yu. Definitions, methods, and applications in interpretable machine learning. *Proceedings of the National Academy of Sciences*, 116(44):22071–22080, 2019.

[35] Finale Doshi-Velez and Been Kim. Towards a rigorous science of interpretable machine learning. *arXiv preprint arXiv:1702.08608*, 2017.

[36] Dimitris Bertsimas and Jack Dunn. Optimal classification trees. *Machine Learning*, 106: 1039–1082, 2017.

[37] J. Ross Quinlan. Induction of decision trees. *Machine learning*, 1:81–106, 1986.

[38] Stephen J Wright. Coordinate descent algorithms. *Mathematical programming*, 151(1):3–34, 2015.

[39] Jason M Klusowski and Peter M Tian. Large scale prediction with decision trees. *Journal of the American Statistical Association*, 119(545):525–537, 2024.

[40] Takuya Akiba, Shotaro Sano, Toshihiko Yanase, Takeru Ohta, and Masanori Koyama. Optuna: A next-generation hyperparameter optimization framework. In *Proceedings of the 25th ACM SIGKDD international conference on knowledge discovery & data mining*, pages 2623–2631, 2019.

[41] Jarkko Salojärvi, Kai Puolamäki, Jaana Simola, Lauri Kovanen, Ilpo Kojo, and Samuel Kaski. Inferring relevance from eye movements: Feature extraction. In *Workshop at NIPS*, page 45, 2005.

[42] Stefan Hegselmann, Thomas Volkert, Hendrik Ohlenburg, Antje Gottschalk, Martin Dugas, and Christian Ertmer. An evaluation of the doctor-interpretability of generalized additive models with interactions. In *Machine Learning for Healthcare Conference*, pages 46–79. PMLR, 2020.

[43] Eldan Cohen. Interpretable clustering via soft clustering trees. In *International Conference on Integration of Constraint Programming, Artificial Intelligence, and Operations Research*, pages 281–298. Springer, 2023.

[44] Nave Frost, Michal Moshkovitz, and Cyrus Rashtchian. Exkmc: Expanding explainable k-means clustering. *arXiv preprint arXiv:2006.02399*, 2020.

[45] Pouya Shati, Yuliang Song, Eldan Cohen, and Sheila McIlraith. Optimal decision trees for interpretable and constrained clustering. *Journal of Artificial Intelligence Research*, 84, 2025.

[46] Qin-Cheng Zheng, Shen-Huan Lyu, Shao-Qun Zhang, Yuan Jiang, and Zhi-Hua Zhou. On the consistency rate of decision tree learning algorithms. In *International Conference on Artificial Intelligence and Statistics*, pages 7824–7848. PMLR, 2023.

[47] Jason Klusowski. Sparse learning with cart. *Advances in Neural Information Processing Systems*, 33:11612–11622, 2020.

[48] Trevor Hastie, Robert Tibshirani, Jerome Friedman, et al. The elements of statistical learning, 2009.

[49] F. Pedregosa, G. Varoquaux, A. Gramfort, V. Michel, B. Thirion, O. Grisel, M. Blondel, P. Prettenhofer, R. Weiss, V. Dubourg, J. Vanderplas, A. Passos, D. Cournapeau, M. Brucher, M. Perrot, and E. Duchesnay. Scikit-learn: Machine learning in Python. *Journal of Machine Learning Research*, 12:2825–2830, 2011.

[50] Habiba Muhammad Sani, Ci Lei, and Daniel Neagu. Computational complexity analysis of decision tree algorithms. In Max Bramer and Miltos Petridis, editors, *Artificial Intelligence XXXV*, pages 191–197, Cham, 2018. Springer International Publishing. ISBN 978-3-030-04191-5.

[51] Sebastian Raschka. Stat 451: Machine learning lecture notes. *University of Wisconsin–Madison*, 2020.

[52] Greg Hamerly and Jonathan Drake. Accelerating lloyd's algorithm for k-means clustering. *Partitional clustering algorithms*, pages 41–78, 2015.

[53] Chandan Singh, Keyan Nasseri, Yan Shuo Tan, Tiffany Tang, and Bin Yu. imodels: a python package for fitting interpretable models, 2021. URL `https://doi.org/10.21105/joss.03192`.

NeurIPS Paper Checklist

1. **Claims**

   Question: Do the main claims made in the abstract and introduction accurately reflect the paper's contributions and scope?

   Answer: [Yes]

   Justification: We describe all main claims in our abstract and provide a list of contributions in our introduction.

2. **Limitations**

   Question: Does the paper discuss the limitations of the work performed by the authors?

   Answer: [Yes]

   Justification: See Conclusion

3. **Theory assumptions and proofs**

   Question: For each theoretical result, does the paper provide the full set of assumptions and a complete (and correct) proof?

   Answer: [Yes]

   Justification: See Appendix for time complexity proof.

4. **Experimental result reproducibility**

   Question: Does the paper fully disclose all the information needed to reproduce the main experimental results of the paper to the extent that it affects the main claims and/or conclusions of the paper (regardless of whether the code and data are provided or not)?

   Answer: [Yes]

   Justification: We provide detailed instructions on our experimental configuration, allowing others to reproduce our experiments if needed. Additionally, we provide detailed pseudocode on how to implement our algorithm.

5. **Open access to data and code**

   Question: Does the paper provide open access to the data and code, with sufficient instructions to faithfully reproduce the main experimental results, as described in supplemental material?

   Answer: [Yes]

   Justification: We utilize open source datasets in our experiments and provide code to replicate our experiments.

6. **Experimental setting/details**

   Question: Does the paper specify all the training and test details (e.g., data splits, hyperparameters, how they were chosen, type of optimizer, etc.) necessary to understand the results?

   Answer: [Yes]

   Justification: See Section 5.

7. **Experiment statistical significance**

   Question: Does the paper report error bars suitably and correctly defined or other appropriate information about the statistical significance of the experiments?

   Answer: [Yes]

   Justification: We provide standard deviation across folds when applicable in our per-dataset results in the supplementary material.

8. **Experiments compute resources**

   Question: For each experiment, does the paper provide sufficient information on the computer resources (type of compute workers, memory, time of execution) needed to reproduce the experiments?

   Answer: [Yes]

Justification: See Section 5 for compute resources used.

9. **Code of ethics**

   Question: Does the research conducted in the paper conform, in every respect, with the NeurIPS Code of Ethics `https://neurips.cc/public/EthicsGuidelines`?

   Answer: [Yes]

   Justification: We agree and confirm our work follows the NeurIPS code of ethics.

10. **Broader impacts**

    Question: Does the paper discuss both potential positive societal impacts and negative societal impacts of the work performed?

    Answer: [Yes]

    Justification: The goal of our work is to provide an improved decision tree algorithm that addresses many of the interpretability concerns with binary axis-aligned trees. As discussed in the introduction, increased interpretability is important in high-stakes, sensitive fields, and improving interpretability has a positive societal impact.

11. **Safeguards**

    Question: Does the paper describe safeguards that have been put in place for responsible release of data or models that have a high risk for misuse (e.g., pretrained language models, image generators, or scraped datasets)?

    Answer: [NA]

    Justification: Our approach has minor risk of misuse and we only consider open source datasets.

12. **Licenses for existing assets**

    Question: Are the creators or original owners of assets (e.g., code, data, models), used in the paper, properly credited and are the license and terms of use explicitly mentioned and properly respected?

    Answer: [Yes]

    Justification: Original producers of relevant code are cited.

13. **New assets**

    Question: Are new assets introduced in the paper well documented and is the documentation provided alongside the assets?

    Answer: [NA]

    Justification: No assets introduced

14. **Crowdsourcing and research with human subjects**

    Question: For crowdsourcing experiments and research with human subjects, does the paper include the full text of instructions given to participants and screenshots, if applicable, as well as details about compensation (if any)?

    Answer: [NA]

    Justification: No human subjects used.

15. **Institutional review board (IRB) approvals or equivalent for research with human subjects**

    Question: Does the paper describe potential risks incurred by study participants, whether such risks were disclosed to the subjects, and whether Institutional Review Board (IRB) approvals (or an equivalent approval/review based on the requirements of your country or institution) were obtained?

    Answer: [NA]

    Justification: No study participants.

16. **Declaration of LLM usage**

Question: Does the paper describe the usage of LLMs if it is an important, original, or non-standard component of the core methods in this research? Note that if the LLM is used only for writing, editing, or formatting purposes and does not impact the core methodology, scientific rigorousness, or originality of the research, declaration is not required.

Answer: [NA]

Justification: LLMs are not a core part of our work.

A Interpretability Discussion

Decision trees are widely regarded as modular and simulable models, offering model-based interpretability when their complexity is controlled through constraints on the number of features used [13, 34] and through structural restrictions such as limiting the total node count and maximum depth [4, 12, 13, 36]. As a decision tree variant, the SGT inherits this modularity, while the restriction that each internal node operates on only one or two features preserves simulability. In particular, each node's shape function can be directly visualized and queried to support transparent predictions. For example, consider the SGT trained on the eye-movements dataset (Figure 3). For a sample with `regressDur` = 100, `lastSaccLen` = 0, and `nWordsInTitle` = 4, the tree yields a local explanation of the form: "The model predicted (Relevant, Class 1) because regressDur < 220, lastSaccLen < 5, and nWordsInTitle $\in [4, 5]$." Moreover, the enhanced expressivity of SGTs enables them to achieve comparable or superior performance with smaller trees, thereby improving sparsity in the resulting explanations and aligning with the desiderata for interpretability proposed by Murdoch et al. [34]. Note that higher-order oblique trees (more than 2 features per node) are not naturally visualizable and are considered less interpretable [31]. We similarly excluded SGTs with higher-order shape functions beyond bivariate for the same reason.

One benefit of decision trees that the SGT inherits is that the local explanation length of an SGT is naturally bounded: a user needs to examine at most one piecewise-constant shape function per decision node along a path, bounding the explanation's size to the tree's depth. Consequently, interpretability is preserved only if the maximum depth is sufficiently small. For this reason, and following prior work on compact decision trees [13, 29, 30], we cap the depth of our models at six.

SGTs and GAMs: Despite being inspired by the feature specific transformations of GAMs, SGTs and GAMs are not directly comparable. In GAMs, a separate shape function is learned for each feature (and for each class in multi-class settings, yielding $|\mathcal{C}|$ shape functions per feature). As a result, the size of a local explanation in a GAM is identical to its global explanation, since all shape functions must be considered simultaneously. In contrast, decision trees bound the size of a local explanation by the depth of the tree, and the global explanation by the number of nodes (at most $2^d - 1$ for depth d). Due to these reasons, GAMs are not directly comparable to trees and we do not include them in our evaluation.

B S^{2}GT$_K$ Formulation

Definition 6 (Binary Multi-Way Shape Generalized Tree (S^{2}GT$_K$)). *In an S^2GT_K, internal nodes partition the data into at most K distinct subsets based on the output of a vector-valued shape function that utilizes at most two features:*

$$\begin{aligned}\mathcal{D}^k = \{(\mathbf{x}_n, y_n) \in \mathcal{D} \mid \underset{k\in\{1,\dots,K\}}{\arg\max} \left(f_\Theta^{2,(K)}(\mathbf{w}_0^\top \mathbf{x}_n, \mathbf{w}_2^\top \mathbf{x}_n, \Theta)\right) = k;\\ \mathbf{w}_1, \mathbf{w}_2 \in \{0,1\}^D; \|\mathbf{w}_1\|_0, \|\mathbf{w}_2\|_0 = 1\}\end{aligned} \tag{13}$$

Here, $\mathbf{w}_1, \mathbf{w}_2$ are one-hot feature selection vectors where $d_1 = \arg\max \mathbf{w}_1, d_2 = \arg\max \mathbf{w}_2$ are the selected features, and $f_\Theta^{2,(K)} : dom(\mathcal{X}_{d_1}) \times dom(\mathcal{X}_{d_2}) \to \mathbb{R}^K$ is a shape function that maps the selected features to a K-dimensional vector, and the argmax operation determines the branch assignment.

C Proofs

C.1 Expressiveness Guarantees

Theorem 1. *Every function that can be represented by a binary axis-aligned linear tree (Definition 1), can be represented by an SGT (Definition 3) with the same number of decision nodes.*

Proof. Given a binary axis-aligned linear tree, we construct an SGT with similar structure where the shape function in each decision node takes the form $f_\Theta(\mathbf{w}^\top \mathbf{x}) = \mathbf{w}^\top \mathbf{x}_n - \Theta$ where $\mathbf{w}$ and Θ match the values in the corresponding decision node in the axis-aligned linear tree. $\square$

Definition 7 (ω-Bars Labeling Function). *Let $\omega \in \mathbb{N}$ be a frequency parameter. We define the Bars Labeling function $g : [0, 1] \to \{0, 1\}$ as follows:*

$$g(x) = \begin{cases} 1 & \textit{if } \cos(2\pi\omega x_1) \leq 0, \\ 0 & \textit{otherwise}. \end{cases} \tag{14}$$

The ω-Bars Labeling Function partitions the unit interval $[0, 1]$ into alternating subintervals according to the sign of $\cos(2\pi\omega x)$. Within $[0, 1]$, the cosine function completes ω full oscillations, producing $\omega + 1$ zero-crossings and hence $\omega + 2$ disjoint subintervals of equal width. These subintervals alternate between label 1 and label 0.

We show that an SGT can directly utilize nonlinear shape functions to represent all functions in this family in a fixed number of nodes, while the number of nodes required by an axis-aligned linear tree scales linearly with the number of rectangles utilized by each function.

Lemma 2. *The ω-Bars labelling function can be represented by an SGT with one internal node for any value of ω.*

Proof. The ω-Bars Labelling function can be represented by an SGT in single node by utilizing a shape function of the form $f_\Theta(z) = \cos(2\pi\Theta z)$, where Θ is a learnable parameter. Recall that samples are assigned to the left partition if $f_\Theta(\mathbf{w}^\top \mathbf{x}_n) \leq 0.0$. As this is a univariate dataset, we select the only feature by setting $\mathbf{w} = [1]$. Additionally, we set $\Theta = \omega$, therefore samples satisfying $f_\Theta(x_1) = \cos(2\pi\omega x_1) \leq 0$ form the left subset, which is assigned to the positive class. The remaining points form the right subset and are assigned to the negative class. The resulting tree matches the definition of the Bars labelling function. □

Lemma 3. *A binary axis-aligned linear tree requires at least $\omega + 1$ internal nodes to represent the Bars labelling function.*

Proof. A binary axis-aligned decision tree partitions the input space into disjoint intervals, each corresponding to a leaf [23]. Since each subinterval of $[0, 1]$ under g is class-constant, and adjacent subintervals differ in label, every subinterval must correspond to a distinct leaf. Thus, a tree that represents g requires at least $\omega + 2$ leaves. In a binary tree, the number of internal nodes is always one less than the number of leaves. Therefore, the exact representation of the ω-Bars Labeling Function requires at least $\omega + 1$ internal nodes. □

Theorem 2. *For every $B \in \mathbb{N}$, there exists a function for which a binary axis-aligned tree requires at least B additional decision nodes to represent, compared to an SGT.*

Proof. For a given $\omega \in \mathbb{N}$, the binary axis-aligned linear tree requires $\omega + 1$ decision nodes while the SGT requires only one to perfectly represent the ω-Bars labelling function. To obtain a function in which the binary axis-aligned linear tree requires at least B additional decision nodes to represent, we can simply set $\omega = B$. □

C.2 Information Gain Guarantees

Lemma 1. *Let t be an individual node in T, let $\mathcal{IG}(t)$ denote the information gain obtained by an axis-aligned (threshold) split on the samples in t from CART, and let $\mathcal{IG}_f(t)$ denote the information gain obtained by a shape function split from ShapeCART on the samples in t. We show that $\mathcal{IG}_f(t) \geq \mathcal{IG}(t)$*

To construct the shape function f_j for each feature j, we begin by fitting a univariate CART tree that partitions the data along x_j. The root node of this tree provides the best axis-aligned split, with associated information gain $\mathcal{IG}(t, j)$. For the initial bin-to-branch assignment, we consider two alternatives: (1) the left/right partition induced by the root split, and (2) a clustering-based assignment obtained via Weighted K-Means. By selecting the better of these two, we guarantee that the initialization of coordinate descent achieves at least $\mathcal{IG}(t, j)$. Since coordinate descent monotonically improves the objective, the resulting shape function satisfies $\mathcal{IG}_f(f_j, t) \geq \mathcal{IG}(t, j), \quad \forall j$. Because ShapeCART employs a line search to select the feature shape function, it follows that

$$\mathcal{IG}_f(t) \;=\; \max_j \mathcal{IG}_f(f_j, t) \;\geq\; \max_j \mathcal{IG}(t, j) \;=\; \mathcal{IG}(t).$$

D Time Complexity Analysis

In this section, we provide the time-complexity of splitting a node using a shape function with respect to the number of samples N, number of classes C, branching factor K, and number of bins (internal tree leaves) L.

Internal Tree Construction To assign samples to L bins, an internal tree is constructed using the CART algorithm [23], trained on a single feature and the target variable. We can break down the analysis of tree construction into four components: sorting the samples, tabulating class counts, calculating impurity, and the recursive relation.

1. **Sorting**: Sorting the samples takes $\mathcal{O}(N \log N)$ time. This only needs to be done once for the whole tree as we operate only on one feature and samples retain their relative ordering when assigned to children nodes. [48–50].
2. **Class Count Tabulation** Once the samples are sorted, CART calculates a cumulative class count at each split point. This involves a scan of all possible splits (N at most).
3. **Impurity Calculation:** Once class counts are tabulated, we need to calculate the impurity for the class counts of each candidate split. Calculating the impurity of a single distribution scales linearly with C, which we repeat N times, resulting in a complexity of $\mathcal{O}(NC)$.
4. **Recursive Relation**: To simplify our runtime analysis, we assume the induced decision tree remains approximately balanced (similar to [51]), such that its maximum depth is on the order of $\log L$, where L denotes the number of leaves. Once a node is split, the cumulative class tabulations (Step 2) and impurity evaluations (Step 3) must be recomputed for the resulting child nodes. However, the total number of samples processed across all nodes at any given depth remains constant at N, since each split simply redistributes the same data among child nodes. Recall that Steps 2 and 3 have per-node complexities of $\mathcal{O}(N)$ and $\mathcal{O}(NC)$, respectively. Consequently, the total cost of class tabulation and impurity computation across all nodes at a given depth remains $\mathcal{O}(N+NC) \approx \mathcal{O}(NC)$. Aggregating over all levels of the tree yields a total complexity of $\mathcal{O}(NC \log L)$, which we can further simplify to $\mathcal{O}(NC \log N)$ as $L \leq N$ in all cases.

As result, the total complexity of fitting CART on a single feature is $\mathcal{O}(N \log N + NC \log N) \approx \mathcal{O}(NC \log N)$.

Bin-to-Branch Optimization Mapping bins (tree leaves) to branches involves running Weighted K-Means on the empirical distributions of the L bins to discover an initial assignment solution, then running coordinate descent to optimize the the assignments to minimize the weighted impurity of the resultant branches.

- For a given branching factor k, we run Weighted K-Means on the empirical class distributions of the L leaves/bins to group the bins into k groups. This is equivalent to running Weighted K-Means on L, C-dimensional samples, which has a time complexity of $\mathcal{O}(kLTC)$ where T is the number of iterations the algorithm runs for [49, 52].
- Our coordinate descent procedure optimizes the partition assignment for each bin independently, iterating over all leaves R times and evaluates the impurity for $k-1$ values for each leaf assignment. The cost of testing a new branch assignment for a bin does not scale with the number of branches as we only need to recalculate the impurity and weights of the current and new branch while the impurity of the other branches are frozen and can be treated as one unit. Therefore, the number of impurity evaluations in our coordinate descent is $\approx kLR$. The cost of impurity evaluation scales linearly with the number of classes ($\mathcal{O}(C)$) for both Gini impurity and entropy, therefore the time complexity of our coordinate descent procedure is $\mathcal{O}(kLRC)$.

As we repeat K-Means and coordinate descent for $k = 2, \ldots, K$, the time complexity of the bin-to-branch optimization is $\mathcal{O}(K^2LTC + K^2LRC)$. As T and R are algorithmic constants, we remove them from consideration for simplicity resulting in a time complexity of $\mathcal{O}(K^2LC)$.

The total time complexity of fitting a univariate shape function can then be obtained by adding up the two steps together, resulting in a complexity of $\mathcal{O}(NC \log N + K^2LC)$. As we construct shape functions for each of the D features, the total time complexity of fitting an internal node is:

$$\mathcal{O}\left(D(NC\log N + K^2LC)\right) \tag{15}$$

D.1 Shape^{2}CART

For Shape^{2}CART and its variants, we utilize BiCART to construct the internal tree for each pair of features. This algorithm creates H augmented features for each pair of features, then constructs a tree using this augmented feature and passes them into CART [31]. We can analyze the cost of internal tree construction using BiCART as a CART tree with H features. The runtime of CART scales linearly with the number of features [48–51] as each step (sorting, tabulating class counts, and evaluating impurity) needs to be done once for each feature. As such, the complexity of fitting bicart is simply $\mathcal{O}(HNC\log N)$, which we can further simplify back to $\mathcal{O}(NC\log N)$ as we only consider small, fixed values of H. In the naive approach of constructing shape functions for each pair of features, the time-complexity of splitting a node is $\mathcal{O}\left(D^2(NC\log N + K^2LC)\right)$.

When using our pairwise selection heuristic, the complexity can be broken down into the time to score each pair of features and the time to construct shape functions of the top P pairs. To evaluate pairs of features, we take the Cartesian product of the branching decisions provided from fitting the univariate shape functions, resulting in K^2 sets. We then calculate the empirical class distribution of each partition, which can be done efficiently in a single scan of the data. We then evaluate the impurity of each of the K^2 partitions' empirical class distributions, resulting in a complexity of $\mathcal{O}(N + CK^2)$ for each pair of features, and $\mathcal{O}((N + CK^2)D^2)$ when aggregated across all pairs. We then take the top P pairs of features and fit bivariate shape functions for these terms, resulting in a time complexity of:

$$\mathcal{O}\left(\underbrace{D(NC\log N + K^2LC)}_{\text{Univariate Shape Function Construction}} + \underbrace{(N + CK^2)D^2}_{\text{Pair Tests}} + \underbrace{P\left(NC\log N + K^2LC\right)}_{\text{Bivariate Shape Function Construction}}\right)$$
$$= \mathcal{O}\left((D+P)(NC\log N + K^2LC) + (N + CK^2)D^2\right)$$

Empirical evaluation of the runtime benefits of limiting pairs is provided in Section G.2.3.

E Dataset Information

Table 2: Dataset Information. Dimensionality refers to the number of columns after one-hot encoding.

Dataset	N	$\lvert\mathcal{C}\rvert$	Dimensionality	D	# Cat.	# Num./Binary
adult	45222	2	108	13	11	2
avila	20867	12	10	10	0	10
bank	1372	2	4	4	0	4
bean	13611	7	16	16	0	16
bidding	6321	2	9	9	0	9
covtype	581012	7	52	12	2	10
electricity	45312	2	13	8	1	7
eucalyptus	736	5	1487	19	14	5
eye-movements	10936	3	27	27	0	27
eye-state	14980	2	14	14	0	14
fault	1941	7	27	27	0	27
gas-drift	13910	6	128	128	0	128
higgs	11,000,000	2	29	29	0	29
htru	17898	2	8	8	0	8
magic	13376	2	10	10	0	10
mini-boone	130064	2	50	50	0	50
mushroom	8124	2	94	21	16	5
occupancy	20560	2	5	5	0	5
page	5473	5	10	10	0	10
pendigits	10992	10	16	16	0	16

Table 2 continued from previous page

Dataset	N	$\|\mathcal{C}\|$	Dimensionality	D	# Cat.	# Num./Binary
raisin	900	2	7	7	0	7
rice	3810	2	7	7	0	7
room	10129	4	16	16	0	16
segment	2310	7	18	18	0	18
skin	245057	2	3	3	0	3
wilt	4839	2	5	5	0	5

F Model Implementation Details

All models are implemented in Python. For CART, we utilize the implementation found in the Scikit-Learn [49]. For Axis-Aligned TAO and HSTree, we utilize the implementation found in the imodels [53] package. For SERDT, we utilize the implementation provided by the original authors [13] found at `https://github.com/user-anonymous-researcher/interpretable-dts`. For DPDT, we utilize the official implementation provided by the original authors [29] found at `https://github.com/KohlerHECTOR/DPDTreeEstimator`. For SPLIT, we utilize the official implementation provided by the original authors found at `https://github.com/VarunBabbar/SPLIT-ICML`. As noted in Section 2.1, some optimal methods, including GOSDT [27] and SPLIT [30] (which builds on GOSDT), require pre-binarization of continuous features. Similar to the setting from the original work [30], we set `binarize=True` when running SPLIT, which applies Threshold Guessing to produce a sparse set of binary features. While full binarization over all thresholds may improve performance, it is orders of magnitude more computationally expensive [30].

Categorical Variables Since all baseline methods require numerical inputs, we one-hot encode categorical variables when relevant. Unlike the baselines that are limited to split on one (axis-aligned) or two (bivariate) levels at a time, we note that ShapeCART and its variants support superset branching on categorical variables owing to the flexibility of their shape functions. This is achieved by passing all relevant columns of the one-hot encoded categorical variable into the internal tree.

BiCART and BiTAO As there are no available pre-existing implementations of the BiCART and BiTAO models, we do our best to replicate these approaches following the methods outlined by Kairgeldin and Carreira-Perpiñán [31] in their original paper. For each pair of features (d_1, d_2), BiCART and BiTAO create H pre-computed linear combination features. They do this by creating a small, fixed subset of line orientation $\mathbf{W} \in \mathbb{R}^{2\times H}$, sampled uniformly in two directions by rotating it around the origin H times, within a range of 0-180 degrees. The augmented feature set for d_1, d_2 is then computed as $\mathbf{X}^{\text{aug}}_{(d_1,d_2)} = \mathbf{X}_{(d_1,d_2)}\mathbf{W}$ where $\mathbf{X}_{(d_1,d_2)} \in \mathbb{R}^{N\times 2}$ is the matrix containing the relevant pair of features. In BiCART, we utilize this augmented feature along with the original features to induce a tree via the CART algorithm [31]. For BiTAO, we utilize TAO to refine a bivariate tree constructed by BiCART, finding the best linear split for nodes in a reverse depth order. For pseudocode of this procedure, we refer reads to Kairgeldin and Carreira-Perpiñán [31] Figure 3.

ShapeTAO To implement ShapeTAO (and Shape^{2}TAO), we train a ShapeCART (and Shape^{2}CART) tree and refine it using TAO. Unlike Axis-Aligned TAO and BiTAO, our `FindBestSplit` function trains a decision tree via CART (BiCART for Shape^{2}TAO) on the "care" set of samples when refining each node. More formally, we follow the pseudocode provided by Kairgeldin and Carreira-Perpiñán [31] Figure 3 and modify the solving procedure of the reduced problem (Kairgeldin and Carreira-Perpiñán [31] Equation 3) from considering linear splits, to instead training a decision tree via CART/BiCART. For Shape^{2}TAO, we only consider pairs of features that were considered in the node under refinement during the initial induction process. To extend TAO to multi-way branching, we make two key changes:

1. In the standard TAO procedure, each sample is assigned to a single "correct" branch, which is then used as its pseudolabel. In the multi-way setting, however, a sample may correspond to multiple valid branches. To accommodate this, we modify the pseudolabeling procedure by duplicating each sample across its valid branches and passing the new upsampled dataset to CART.

2. To evaluate whether an updated decision function improves upon the previous one, we adapt the accuracy metric to reflect the multi-way setting. Specifically, a prediction is deemed correct if the decision function assigns the sample to any branch that is among the set of valid branches for that sample.

Source code for for ShapeCART, ShapeTAO, and its variants can be found at https://github.com/optimal-uoft/Empowering-DTs-via-Shape-Functions.

F.1 Hyperparameter Information

For all models, we vary the maximum depth between 2-6. Below are the other parameters we tune for each model. Note that when models share hyperparameters, we utilize the same values across all modesl.

- **CART**: `criterion`: {gini, entropy}, `min_samples_split`: {2,4,8,16,32}, `min_samples_leaf`: [1,32], `min_impurity_decrease`: {0.0, 1e-4, 5e-4, 1e-3, 5e-3, 0.01}, `ccp_alpha`: {0.0, 1e-4, 5e-4, 1e-3, 5e-3, 0.01}
- **SERDT**: `min_samples_stop`: {2,4,8,16,32}, `gini_factor`: {0.9, 0.91, ..., 0.99}, `gamma_factor`: {0.5, 0.65, 0.8}
- **HSTree**: `criterion`: {gini, entropy}, `min_samples_split`: {2,4,8,16,32}, `min_samples_leaf`: [1,32], `min_impurity_decrease`: {0.0, 1e-4, 5e-4, 1e-3, 5e-3, 0.01}, `ccp_alpha`: {0.0, 1e-4, 5e-4, 1e-3, 5e-3, 0.01}, `reg_param` (different from TAO): {1e-2, 5e-2, 1e-1, 5e-1, 1.0, 5.0, 10, 50}
- **AxTAO**: `criterion`: {gini, entropy}, `min_samples_split`: {2,4,8,16,32}, `min_samples_leaf`: [1,32], `min_impurity_decrease`: {0.0, 1e-4, 5e-4, 1e-3, 5e-3, 0.01}, `reg_param/lambda_`: {0.0, 1e-4, 5e-4, 1e-3, 5e-3, 0.01}
- **DPDT**: `criterion`: {gini, entropy}, `min_samples_split`: {2,4,8,16,32}, `min_samples_leaf`: [1,32], `min_impurity_decrease`: {0.0, 1e-4, 5e-4, 1e-3, 5e-3, 0.01}, `cart_nodes_list`: {(8,3,), (32,), (4,3,), (16,6,), (16,4,), (4,4), (3,3), (6,6)}
- **SPLIT**: `reg`: {1e-3, 1e-2, .1}, `lookahead_depth`: {2,..., maximum depth of tree}, `gbdt_n_est`: {10, 20, ..., 100}
- **BiCART**: `criterion`: {gini, entropy}, `min_samples_split`: {2,4,8,16,32}, `min_samples_leaf`: [1,32], `min_impurity_decrease`: {0.0, 1e-4, 5e-4, 1e-3, 5e-3, 0.01}, `ccp_alpha`: {0.0, 1e-4, 5e-4, 1e-3, 5e-3, 0.01}, H: {5,6,7,8}
- **BiTAO**: `criterion`: {gini, entropy}, `min_samples_split`: {2,4,8,16,32}, `min_samples_leaf`: [1,32], `min_impurity_decrease`: {0.0, 1e-4, 5e-4, 1e-3, 5e-3, 0.01}, `reg_param/lambda_`: {0.0, 1e-4, 5e-4, 1e-3, 5e-3, 0.01}, H: {5,6,7,8}
- **ShapeCART/ ShapeCART$_3$**: `criterion`: {gini, entropy}, `min_samples_split`: {2,4,8,16,32}, `min_samples_leaf`: [1,32], `min_impurity_decrease`: {0.0, 1e-4, 5e-4, 1e-3, 5e-3, 0.01}, `inner_max_leaf_nodes` (aka L): {4,8,12,...,64}, `inner_min_samples_leaf`: {1, 1e-4, 5e-4, 1e-3, 5e-3, 1e-2}, `branching_penalty` (aka λ): {0.0, 1e-4, 5e-4, 1e-3, 5e-3, 0.01}
- **ShapeTAO / ShapeTAO$_3$**: `criterion`: {gini, entropy}, `min_samples_split`: {2,4,8,16,32}, `min_samples_leaf`: [1,32],`min_impurity_decrease`: {0.0, 1e-4, 5e-4, 1e-3, 5e-3, 0.01}, `reg_param/lambda_`: {0.0, 1e-4, 5e-4, 1e-3, 5e-3, 0.01}, `inner_max_leaf_nodes` (aka L): {4,8,12,...,64}, `inner_min_samples_leaf`: {1, 1e-4, 5e-4, 1e-3, 5e-3, 1e-2}
- **Shape^{2}CART / Shape^{2}CART$_3$**: `criterion`: {gini, entropy}, `min_samples_split`: {2,4,8,16,32}, `min_samples_leaf`: [1,32], `min_impurity_decrease`: {0.0, 1e-4, 5e-4, 1e-3, 5e-3, 0.01}, `inner_max_leaf_nodes` (aka L): {4,8,12,...,64}, `inner_min_samples_leaf`: {1, 1e-4, 5e-4, 1e-3, 5e-3, 1e-2}, `branching_penalty` (aka λ), H: {5,6,7,8}
- **Shape^{2}TAO / Shape^{2}TAO$_3$**: `criterion`: {gini, entropy}, `min_samples_split`: {2,4,8,16,32}, `min_samples_leaf`: [1,32],`min_impurity_decrease`: {0.0, 1e-4, 5e-4, 1e-3, 5e-3, 0.01}, `reg_param/lambda_`: {0.0, 1e-4, 5e-4, 1e-3, 5e-3, 0.01},

`inner_max_leaf_nodes` (aka L): {4,8,12,...,64}, `inner_min_samples_leaf`: {1, 1e-4, 5e-4, 1e-3, 5e-3, 1e-2}, H: {5,6,7,8}

Note on H: The choice of H was predicated on ensuring computational tractability. While prior work by [31] examined H values from 30 to 90, our evaluation revealed that these higher values imposed unmanageable memory burdens, preventing successful execution on any dataset. Accordingly, a more computationally conservative value for H was selected. Despite this restriction, three datasets (Eucalyptus, Higgs, and Covertype) still were not able to run on BiCART and BiTAO given our 32GB RAM limit.

F.1.1 Hyperparameter Importance

In this section, we analyze the important hyperparameters for our approaches. Following [2] and [3], we normalize the test accuracy within each model and dataset and train a Random Forest regressor to predict test Z-scores from the model hyperparameters and provide the feature importance in Table 3

Table 3: Hyperparameter Importance of ShapeCART and its variants.

	ShapeCART	ShapeCART$_3$	Shape^{2}CART	Shape^{2}CART$_3$	ShapeTAO	ShapeTAO$_3$	Shape^{2}TAO	Shape^{2}TAO$_3$
max_depth	0.35	0.24	0.179	0.095	0.359	0.221	0.142	0.085
criterion	0.038	0.035	0.033	0.034	0.035	0.025	0.038	0.035
min_samples_split	0.079	0.082	0.08	0.081	0.075	0.075	0.078	0.069
min_samples_leaf	0.182	0.178	0.188	0.189	0.154	0.179	0.17	0.159
min_impurity_decrease	0.094	0.08	0.094	0.08	0.074	0.079	0.082	0.078
inner_max_leaf_nodes	0.169	0.192	0.167	0.19	0.137	0.172	0.154	0.195
inner_min_samples_leaf	0.088	0.098	0.094	0.088	0.082	0.084	0.096	0.089
branching_penalty	—	0.095	—	0.088	—	0.079	—	0.082
H	—	—	0.066	0.062	—	—	0.069	0.054
pairwise_penalty	—	—	0.098	0.094	—	—	0.088	0.084

G Extra results

In this section, we provide results for all approaches across all datasets as well as results from more empirical evaluations.

G.1 Full Results

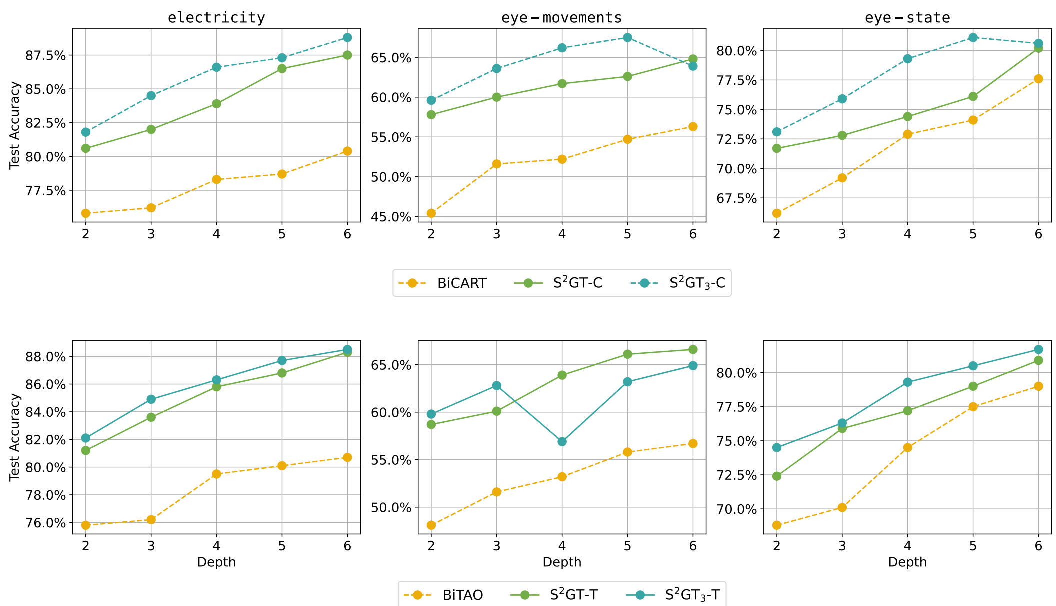

Figure G.4: Test accuracy per depth for Bivariate models on `eye-movements`, `electricity`, and `eye-state`. Top: TDIDT-Approaches. Bottom: Non-Greedy Approaches.

Table 4: Test Accuracy (% ± std.) for all axis-aligned approaches separated into TDIDT and Non-Greedy approaches by dashed lines per dataset. Best approach is **bolded**, second-best is *italicized*.

dataset	model	2	3	4	5	6	Best
adult	CART	*82.60 ± 0.20*	*82.60 ± 0.30*	83.20 ± 0.30	83.60 ± 0.30	83.60 ± 0.30	83.60 ± 0.30
	HSTree	*82.60 ± 0.20*	*82.60 ± 0.30*	83.20 ± 0.30	83.60 ± 0.30	83.70 ± 0.50	83.70 ± 0.50
	SERDT	*82.60 ± 0.20*	*82.60 ± 0.20*	82.60 ± 0.20	83.00 ± 0.20	83.10 ± 0.30	83.10 ± 0.30
	SGT-C	**82.80 ± 0.20**	**84.10 ± 0.30**	*84.00 ± 0.30*	*84.30 ± 0.40*	*84.60 ± 0.60*	*84.60 ± 0.60*
	SGT$_3$-C	**82.80 ± 0.20**	**84.10 ± 0.30**	**84.10 ± 0.40**	**84.50 ± 0.60**	**84.80 ± 0.40**	**84.80 ± 0.40**
	AxTAO	*82.60 ± 0.20*	82.60 ± 0.30	83.30 ± 0.30	83.50 ± 0.50	83.90 ± 0.20	83.90 ± 0.20
	DPDT	*82.60 ± 0.20*	83.20 ± 0.20	83.50 ± 0.40	83.50 ± 0.30	83.90 ± 0.40	83.90 ± 0.40
	SPLIT	78.00 ± 0.30	82.60 ± 0.20	83.50 ± 0.30	84.00 ± 0.30	84.20 ± 0.30	84.20 ± 0.30
	SGT-T	**82.90 ± 0.20**	**84.10 ± 0.30**	*84.10 ± 0.30*	*84.40 ± 0.20*	*84.80 ± 0.60*	*84.80 ± 0.60*
	SGT$_3$-T	**82.90 ± 0.20**	**84.10 ± 0.30**	**84.50 ± 0.40**	**84.80 ± 0.50**	**85.00 ± 0.50**	**85.00 ± 0.50**
avila	CART	—	—	57.60 ± 1.20	62.30 ± 0.90	65.20 ± 0.90	65.20 ± 0.90
	HSTree	—	—	57.60 ± 1.20	62.30 ± 0.90	65.20 ± 0.90	65.20 ± 0.90
	SERDT	—	—	58.10 ± 0.30	61.90 ± 0.70	66.60 ± 1.90	66.60 ± 1.90
	SGT-C	—	—	*64.50 ± 2.90*	*71.70 ± 1.80*	*82.00 ± 2.10*	*82.00 ± 2.10*
	SGT$_3$-C	—	—	**87.00 ± 1.50**	**98.00 ± 0.50**	**99.70 ± 0.10**	**99.70 ± 0.10**
	AxTAO	—	—	58.00 ± 0.60	64.10 ± 1.10	67.00 ± 0.80	67.00 ± 0.80
	DPDT	—	—	61.00 ± 0.60	64.70 ± 1.00	68.70 ± 0.00	68.70 ± 0.00
	SPLIT	—	—	52.90 ± 0.30	56.50 ± 0.40	58.30 ± 1.10	58.30 ± 1.10
	SGT-T	—	—	*69.60 ± 1.40*	*77.00 ± 0.60*	*84.40 ± 1.70*	*84.40 ± 1.70*
	SGT$_3$-T	—	—	**87.50 ± 1.80**	**98.10 ± 0.60**	**99.60 ± 0.30**	**99.60 ± 0.30**
bank	CART	*89.10 ± 1.30*	*94.40 ± 0.40*	95.80 ± 0.60	96.00 ± 2.00	**97.90 ± 0.90**	**97.90 ± 0.90**
	HSTree	*89.10 ± 1.30*	*94.40 ± 0.40*	94.80 ± 2.00	96.20 ± 1.80	**97.90 ± 0.90**	96.20 ± 1.80
	SERDT	88.80 ± 1.30	93.20 ± 2.60	94.70 ± 2.00	96.10 ± 2.10	*97.30 ± 1.30*	*97.30 ± 1.30*

	SGT-C	88.50 ± 2.30	89.50 ± 3.20	**97.00 ± 0.90**	*96.70 ± 0.00*	96.70 ± 0.00	97.00 ± 0.90
	SGT$_3$-C	**90.90 ± 0.70**	**97.00 ± 0.80**	*96.80 ± 1.90*	**96.80 ± 1.90**	96.80 ± 1.90	96.80 ± 1.90
	AxTAO	*88.80 ± 1.30*	95.40 ± 0.60	96.50 ± 1.40	*97.70 ± 1.80*	**98.80 ± 0.20**	*97.70 ± 1.80*
	DPDT	88.50 ± 1.50	*95.60 ± 1.00*	**97.80 ± 1.00**	**97.90 ± 1.20**	*98.40 ± 0.90*	**98.40 ± 0.90**
	SPLIT	82.70 ± 0.60	90.10 ± 1.40	96.50 ± 0.60	97.20 ± 0.80	97.10 ± 1.00	97.20 ± 0.80
	SGT-T	*88.80 ± 1.30*	92.00 ± 4.20	**97.80 ± 1.00**	*97.70 ± 0.80*	97.90 ± 0.60	*97.70 ± 0.80*
	SGT$_3$-T	**91.60 ± 1.30**	**96.40 ± 1.10**	*97.30 ± 1.40*	97.30 ± 1.40	97.30 ± 1.40	97.30 ± 1.40
bean	CART	—	79.90 ± 0.40	85.60 ± 0.10	89.60 ± 0.70	*90.30 ± 0.50*	*90.30 ± 0.50*
	HSTree	—	79.90 ± 0.40	85.60 ± 0.10	89.60 ± 0.60	*90.30 ± 0.40*	*90.30 ± 0.40*
	SERDT	—	77.10 ± 0.60	83.00 ± 0.70	88.20 ± 0.60	**90.70 ± 0.50**	**90.70 ± 0.50**
	SGT-C	—	*85.10 ± 1.20*	*88.80 ± 0.40*	*89.70 ± 0.40*	89.80 ± 0.10	89.80 ± 0.10
	SGT$_3$-C	—	**87.90 ± 0.50**	**90.40 ± 0.60**	**90.50 ± 0.20**	*90.30 ± 0.50*	*90.30 ± 0.50*
	AxTAO	—	81.90 ± 0.40	87.20 ± 0.10	90.00 ± 0.50	90.40 ± 0.40	90.40 ± 0.40
	DPDT	—	85.10 ± 0.30	*89.80 ± 0.30*	*90.80 ± 0.80*	**90.90 ± 0.20**	**90.90 ± 0.20**
	SPLIT	—	55.80 ± 0.40	66.80 ± 1.80	71.20 ± 1.00	72.80 ± 1.10	72.80 ± 1.10
	SGT-T	—	*85.70 ± 1.10*	88.80 ± 0.60	90.10 ± 0.80	*90.80 ± 0.70*	*90.80 ± 0.70*
	SGT$_3$-T	—	**88.20 ± 0.60**	**90.40 ± 0.70**	**90.90 ± 0.40**	90.00 ± 0.30	**90.90 ± 0.40**
bidding	CART	*98.10 ± 0.60*	98.10 ± 0.60	98.20 ± 0.50	**99.70 ± 0.30**	*99.60 ± 0.20*	**99.70 ± 0.30**
	HSTree	*98.10 ± 0.60*	98.10 ± 0.60	98.20 ± 0.50	**99.70 ± 0.30**	*99.60 ± 0.30*	**99.70 ± 0.30**
	SERDT	*98.10 ± 0.60*	98.10 ± 0.60	*99.60 ± 0.10*	**99.70 ± 0.30**	**99.70 ± 0.10**	**99.70 ± 0.10**
	SGT-C	*98.10 ± 0.70*	*98.40 ± 0.60*	**99.70 ± 0.20**	*99.60 ± 0.30*	*99.60 ± 0.10*	*99.60 ± 0.10*
	SGT$_3$-C	**99.10 ± 0.10**	**99.60 ± 0.20**	*99.60 ± 0.20*	*99.60 ± 0.20*	*99.60 ± 0.20*	*99.60 ± 0.20*
	AxTAO	*98.10 ± 0.60*	98.20 ± 0.60	98.30 ± 0.40	99.50 ± 0.00	99.50 ± 0.20	*99.50 ± 0.00*
	DPDT	*98.10 ± 0.60*	**99.50 ± 0.10**	**99.70 ± 0.30**	*99.60 ± 0.10*	**99.80 ± 0.10**	**99.70 ± 0.30**
	SPLIT	97.30 ± 0.60	98.10 ± 0.60	*99.40 ± 0.10*	**99.70 ± 0.30**	*99.70 ± 0.30*	**99.70 ± 0.30**
	SGT-T	*98.10 ± 0.60*	98.50 ± 0.70	*99.40 ± 0.20*	*99.60 ± 0.10*	99.60 ± 0.20	99.40 ± 0.20
	SGT$_3$-T	**99.10 ± 0.10**	*99.30 ± 0.20*	*99.40 ± 0.20*	99.40 ± 0.20	99.40 ± 0.20	99.40 ± 0.20
covtype	CART	—	67.70 ± 0.00	70.10 ± 0.10	70.20 ± 0.10	71.50 ± 0.00	71.50 ± 0.00
	HSTree	—	67.70 ± 0.00	70.10 ± 0.10	70.20 ± 0.10	71.50 ± 0.00	71.50 ± 0.00
	SERDT	—	67.40 ± 0.00	69.00 ± 0.10	69.90 ± 0.30	71.80 ± 0.20	71.80 ± 0.20
	SGT-C	—	*68.90 ± 0.20*	*70.40 ± 0.10*	*72.10 ± 0.50*	*73.70 ± 0.20*	*73.70 ± 0.20*
	SGT$_3$-C	—	**71.00 ± 0.20**	**72.60 ± 0.20**	**75.40 ± 0.20**	**78.10 ± 0.30**	**78.10 ± 0.30**
	AxTAO	—	67.90 ± 0.10	70.10 ± 0.10	70.30 ± 0.10	72.00 ± 0.20	72.00 ± 0.20
	DPDT	—	68.60 ± 0.00	70.80 ± 0.10	71.60 ± 0.20	73.20 ± 0.20	73.20 ± 0.20
	SPLIT	—	63.60 ± 0.10	63.60 ± 0.10	63.60 ± 0.10	63.60 ± 0.10	63.60 ± 0.10
	SGT-T	—	*69.50 ± 0.20*	*70.90 ± 0.50*	*72.50 ± 0.40*	*74.40 ± 0.20*	*74.40 ± 0.20*
	SGT$_3$-T	—	**71.20 ± 0.10**	**73.30 ± 0.30**	**76.20 ± 0.00**	**79.30 ± 0.40**	**79.30 ± 0.40**
electricity	CART	*75.50 ± 0.10*	75.80 ± 0.20	76.00 ± 0.20	77.60 ± 0.20	78.00 ± 0.10	78.00 ± 0.10
	HSTree	*75.50 ± 0.10*	75.80 ± 0.20	76.00 ± 0.20	77.70 ± 0.10	78.10 ± 0.10	78.10 ± 0.10
	SERDT	*75.50 ± 0.10*	75.80 ± 0.20	76.20 ± 0.10	78.60 ± 0.80	79.40 ± 0.30	79.40 ± 0.30
	SGT-C	*75.50 ± 0.10*	*78.50 ± 0.40*	*81.30 ± 0.80*	*84.40 ± 0.10*	*84.80 ± 0.60*	*84.80 ± 0.60*
	SGT$_3$-C	**76.50 ± 0.30**	**80.60 ± 0.60**	**84.00 ± 1.20**	**86.00 ± 0.40**	**87.80 ± 1.00**	**87.80 ± 1.00**
	AxTAO	75.50 ± 0.10	75.90 ± 0.10	75.90 ± 0.30	78.50 ± 0.80	79.90 ± 0.20	79.90 ± 0.20
	DPDT	*76.10 ± 0.20*	78.30 ± 0.20	79.10 ± 0.20	80.00 ± 0.30	80.80 ± 0.50	80.80 ± 0.50
	SPLIT	75.40 ± 0.10	76.20 ± 0.10	77.70 ± 0.50	78.40 ± 0.20	78.70 ± 0.30	78.70 ± 0.30
	SGT-T	75.50 ± 0.10	*79.50 ± 0.40*	*83.00 ± 0.40*	*86.00 ± 0.40*	*87.60 ± 0.50*	*87.60 ± 0.50*
	SGT$_3$-T	**79.30 ± 0.30**	**82.60 ± 0.60**	**84.90 ± 0.60**	**86.70 ± 0.60**	**88.20 ± 0.30**	**88.20 ± 0.30**
eucalyptus	CART	—	50.90 ± 4.50	52.50 ± 3.80	52.00 ± 5.40	*55.20 ± 5.00*	*55.20 ± 5.00*
	HSTree	—	50.90 ± 4.50	52.50 ± 3.80	52.00 ± 5.40	54.10 ± 5.10	54.10 ± 5.10
	SERDT	—	46.80 ± 2.70	44.60 ± 1.80	47.10 ± 3.70	51.40 ± 1.80	51.40 ± 1.80
	SGT-C	—	*53.60 ± 3.30*	**55.90 ± 4.00**	**56.30 ± 4.60**	**58.80 ± 7.20**	**58.80 ± 7.20**
	SGT$_3$-C	—	**55.00 ± 2.70**	*53.40 ± 4.10*	*55.40 ± 6.80*	54.70 ± 4.90	53.40 ± 4.10
	AxTAO	—	*50.90 ± 4.50*	51.80 ± 5.50	52.00 ± 5.40	54.70 ± 3.80	54.70 ± 3.80
	DPDT	—	49.80 ± 4.90	*52.50 ± 3.80*	*53.80 ± 3.20*	*55.20 ± 3.00*	*55.20 ± 3.00*
	SPLIT	—	29.30 ± 2.60	36.70 ± 2.10	36.30 ± 2.20	34.20 ± 4.50	34.20 ± 4.50
	SGT-T	—	**55.40 ± 4.10**	**57.20 ± 2.00**	**57.00 ± 3.00**	*55.20 ± 4.80*	*55.20 ± 4.80*
	SGT$_3$-T	—	**55.40 ± 1.80**	50.00 ± 2.90	**57.00 ± 2.80**	**57.00 ± 2.80**	**55.40 ± 1.80**
eye-movements	CART	45.90 ± 0.30	46.30 ± 2.60	51.30 ± 0.20	52.40 ± 1.40	53.20 ± 0.70	53.20 ± 0.70
	HSTree	45.90 ± 0.30	46.30 ± 2.60	51.40 ± 0.20	52.40 ± 1.40	53.10 ± 0.70	53.10 ± 0.70

	SERDT	43.80 ± 0.30	49.20 ± 0.20	49.10 ± 0.40	52.70 ± 1.00	53.50 ± 0.60	53.50 ± 0.60
	SGT-C	**48.10 ± 2.10**	*53.00 ± 0.70*	*54.90 ± 1.20*	*53.90 ± 0.70*	*57.40 ± 1.20*	*57.40 ± 1.20*
	SGT$_3$-C	*47.10 ± 0.50*	**54.40 ± 0.80**	**56.00 ± 0.30**	**57.50 ± 1.60**	**60.90 ± 2.60**	**60.90 ± 2.60**
	AxTAO	45.90 ± 0.30	48.60 ± 0.80	51.40 ± 0.30	52.30 ± 1.20	52.60 ± 1.60	52.60 ± 1.60
	DPDT	*48.70 ± 0.40*	51.20 ± 0.30	52.40 ± 0.80	54.40 ± 1.20	56.70 ± 1.20	56.70 ± 1.20
	SPLIT	44.00 ± 0.70	48.40 ± 0.30	50.20 ± 0.60	51.90 ± 0.20	52.00 ± 0.50	51.90 ± 0.20
	SGT-T	48.60 ± 2.40	*53.10 ± 1.50*	*54.80 ± 0.50*	*56.80 ± 2.80*	*58.00 ± 1.40*	*58.00 ± 1.40*
	SGT$_3$-T	**51.40 ± 0.90**	**54.80 ± 0.30**	**55.40 ± 0.80**	**56.90 ± 2.50**	**60.30 ± 2.90**	**60.30 ± 2.90**
eye-state	CART	62.70 ± 0.60	65.80 ± 1.30	69.10 ± 1.60	70.90 ± 0.30	73.20 ± 1.40	73.20 ± 1.40
	HSTree	62.70 ± 0.60	65.80 ± 1.30	69.10 ± 1.60	70.90 ± 0.30	73.20 ± 1.40	73.20 ± 1.40
	SERDT	62.70 ± 0.60	66.40 ± 1.50	69.40 ± 0.90	72.30 ± 0.70	*75.30 ± 0.50*	*75.30 ± 0.50*
	SGT-C	*64.30 ± 0.90*	*69.00 ± 0.20*	*70.50 ± 1.20*	*72.40 ± 1.30*	74.50 ± 1.10	74.50 ± 1.10
	SGT$_3$-C	**66.10 ± 0.70**	**70.80 ± 1.40**	**73.30 ± 1.00**	**76.80 ± 1.30**	**77.50 ± 0.50**	**77.50 ± 0.50**
	AxTAO	62.10 ± 1.40	67.00 ± 1.00	69.70 ± 1.20	72.80 ± 0.70	74.30 ± 1.60	74.30 ± 1.60
	DPDT	*65.90 ± 0.50*	69.10 ± 1.90	71.40 ± 1.30	73.40 ± 0.50	75.60 ± 0.90	75.60 ± 0.90
	SPLIT	58.50 ± 0.40	66.40 ± 0.30	69.00 ± 1.30	71.80 ± 1.10	73.60 ± 0.30	73.60 ± 0.30
	SGT-T	65.60 ± 1.20	*70.50 ± 0.60*	*72.70 ± 0.40*	*73.60 ± 1.20*	*75.80 ± 0.90*	*75.80 ± 0.90*
	SGT$_3$-T	**67.10 ± 0.50**	**71.90 ± 0.60**	**75.80 ± 0.60**	**75.80 ± 0.90**	**76.30 ± 1.20**	**76.30 ± 1.20**
fault	CART	—	61.50 ± 4.50	*66.30 ± 1.30*	67.10 ± 1.60	*70.30 ± 2.30*	*70.30 ± 2.30*
	HSTree	—	61.50 ± 4.50	*66.30 ± 1.30*	67.60 ± 2.30	*70.30 ± 2.30*	*70.30 ± 2.30*
	SERDT	—	*63.60 ± 0.90*	64.80 ± 0.80	67.00 ± 1.20	**70.50 ± 1.00**	**70.50 ± 1.00**
	SGT-C	—	59.70 ± 3.90	65.30 ± 1.80	*68.00 ± 0.40*	69.70 ± 3.60	69.70 ± 3.60
	SGT$_3$-C	—	**65.20 ± 5.10**	**69.60 ± 2.30**	**69.70 ± 1.30**	69.10 ± 3.40	69.10 ± 3.40
	AxTAO	—	61.50 ± 4.50	66.40 ± 1.70	68.40 ± 2.00	69.80 ± 1.30	69.80 ± 1.30
	DPDT	—	*67.40 ± 2.10*	66.90 ± 2.20	**71.00 ± 2.10**	**70.90 ± 2.80**	**70.90 ± 2.80**
	SPLIT	—	47.00 ± 2.30	59.50 ± 1.00	61.90 ± 2.10	67.10 ± 3.50	67.10 ± 3.50
	SGT-T	—	65.70 ± 1.40	*68.00 ± 3.30*	*70.10 ± 3.10*	*70.70 ± 5.20*	*70.70 ± 5.20*
	SGT$_3$-T	—	**69.30 ± 1.60**	**70.40 ± 2.20**	69.20 ± 2.50	69.20 ± 3.40	69.20 ± 3.40
gas-drift	CART	—	65.40 ± 0.80	72.30 ± 2.10	81.00 ± 0.10	86.90 ± 1.70	86.90 ± 1.70
	HSTree	—	65.40 ± 0.80	72.30 ± 2.10	81.00 ± 0.10	86.80 ± 1.60	86.80 ± 1.60
	SERDT	—	65.50 ± 0.30	74.70 ± 1.00	81.70 ± 0.10	87.60 ± 0.90	87.60 ± 0.90
	SGT-C	—	*66.30 ± 1.30*	*76.00 ± 1.00*	*83.10 ± 2.00*	*89.00 ± 0.90*	*89.00 ± 0.90*
	SGT$_3$-C	—	**81.00 ± 1.00**	**87.90 ± 1.90**	**93.00 ± 1.60**	**94.70 ± 1.20**	**94.70 ± 1.20**
	AxTAO	—	66.90 ± 1.00	76.10 ± 1.80	83.50 ± 2.90	89.50 ± 1.30	89.50 ± 1.30
	DPDT	—	70.20 ± 0.80	78.50 ± 1.30	*86.60 ± 0.80*	*91.90 ± 0.90*	*91.90 ± 0.90*
	SPLIT	—	51.20 ± 0.90	59.00 ± 1.00	64.50 ± 1.80	69.00 ± 1.50	69.00 ± 1.50
	SGT-T	—	*70.90 ± 3.30*	*80.00 ± 1.60*	86.40 ± 0.70	91.10 ± 1.30	91.10 ± 1.30
	SGT$_3$-T	—	**83.00 ± 0.60**	**89.20 ± 0.80**	**92.80 ± 1.60**	**94.80 ± 0.30**	**94.80 ± 0.30**
higgs	CART	**64.70 ± 0.30**	**65.60 ± 0.60**	**66.00 ± 0.80**	*66.30 ± 1.20*	**67.60 ± 0.30**	**67.60 ± 0.30**
	HSTree	**64.70 ± 0.20**	**65.60 ± 0.70**	**66.00 ± 0.80**	**66.50 ± 1.20**	*67.10 ± 0.20*	*67.10 ± 0.20*
	SERDT	**64.70 ± 0.20**	**65.60 ± 0.60**	*65.70 ± 1.30*	66.20 ± 1.10	66.80 ± 0.40	66.80 ± 0.40
	SGT-C	*64.40 ± 0.20*	63.50 ± 0.50	64.10 ± 1.70	64.90 ± 1.30	63.70 ± 1.80	64.90 ± 1.70
	SGT$_3$-C	63.50 ± 0.70	*64.70 ± 0.70*	63.30 ± 1.20	63.00 ± 0.90	64.30 ± 0.60	64.30 ± 0.90
	AxTAO	62.60 ± 0.20	64.90 ± 0.30	65.00 ± 0.70	**67.40 ± 0.40**	65.40 ± 0.40	65.40 ± 0.40
	DPDT	**64.70 ± 0.60**	**66.80 ± 0.90**	*65.50 ± 1.80*	65.50 ± 0.60	**66.40 ± 1.40**	**66.40 ± 1.40**
	SPLIT	61.90 ± 0.60	*65.10 ± 0.30*	*65.50 ± 1.10*	*66.80 ± 1.50*	*66.00 ± 2.00*	*66.00 ± 2.00*
	SGT-T	*63.80 ± 0.10*	64.60 ± 1.00	**65.90 ± 1.30**	65.00 ± 2.10	63.90 ± 2.60	63.90 ± 2.60
	SGT$_3$-T	62.90 ± 0.10	*65.10 ± 0.60*	64.70 ± 0.90	63.70 ± 1.00	64.30 ± 1.00	64.30 ± 1.00
htru	CART	**97.80 ± 0.10**	**97.80 ± 0.20**	*97.90 ± 0.10*	*97.90 ± 0.10*	*97.80 ± 0.00*	*97.90 ± 0.10*
	HSTree	**97.80 ± 0.10**	**97.80 ± 0.10**	**98.00 ± 0.10**	*97.90 ± 0.10*	*97.80 ± 0.00*	*97.90 ± 0.10*
	SERDT	**97.80 ± 0.10**	**97.80 ± 0.10**	**98.00 ± 0.10**	**98.00 ± 0.10**	**98.00 ± 0.10**	**98.00 ± 0.10**
	SGT-C	**97.80 ± 0.10**	**97.80 ± 0.10**	97.80 ± 0.20	*97.90 ± 0.20*	97.60 ± 0.10	97.80 ± 0.10
	SGT$_3$-C	*97.70 ± 0.10*	*97.70 ± 0.10*	97.80 ± 0.10	*97.90 ± 0.20*	97.70 ± 0.10	97.80 ± 0.10
	AxTAO	*97.80 ± 0.10*	**97.80 ± 0.10**	**98.00 ± 0.20**	*97.90 ± 0.10*	*97.90 ± 0.10*	*97.90 ± 0.10*
	DPDT	**98.00 ± 0.10**	**97.80 ± 0.10**	**98.00 ± 0.10**	*97.90 ± 0.10*	*97.90 ± 0.10*	**98.00 ± 0.10**
	SPLIT	*97.80 ± 0.10*	**97.80 ± 0.10**	*97.90 ± 0.20*	**98.00 ± 0.10**	**98.00 ± 0.10**	**98.00 ± 0.10**
	SGT-T	97.70 ± 0.10	**97.80 ± 0.10**	97.80 ± 0.10	97.80 ± 0.10	97.70 ± 0.10	97.70 ± 0.10
	SGT$_3$-T	97.70 ± 0.10	*97.70 ± 0.10*	97.70 ± 0.10	97.70 ± 0.10	97.70 ± 0.10	97.70 ± 0.10
magic	CART	73.70 ± 1.20	76.80 ± 0.90	78.90 ± 0.70	*80.10 ± 0.90*	*81.30 ± 0.90*	**81.30 ± 0.90**

	HSTree	73.70 ± 1.20	76.80 ± 0.90	78.90 ± 0.70	*80.10 ± 0.90*	*81.30 ± 0.90*	**81.30 ± 0.90**
	SERDT	73.70 ± 1.20	76.70 ± 1.00	78.70 ± 0.80	80.00 ± 1.20	81.10 ± 0.80	*81.10 ± 0.80*
	SGT-C	*73.90 ± 1.00*	*77.10 ± 0.10*	*79.60 ± 1.10*	*80.10 ± 1.70*	81.00 ± 0.50	81.00 ± 0.50
	SGT$_3$-C	**77.90 ± 1.20**	**78.40 ± 0.80**	**79.90 ± 0.50**	**81.10 ± 0.60**	**81.40 ± 0.40**	*81.10 ± 0.60*
	AxTAO	74.60 ± 0.90	76.90 ± 0.90	79.30 ± 0.80	**81.10 ± 1.30**	*82.10 ± 1.00*	*82.10 ± 1.00*
	DPDT	*76.50 ± 1.20*	*78.30 ± 0.90*	*80.30 ± 0.80*	**81.10 ± 0.30**	**82.30 ± 1.00**	**82.30 ± 1.00**
	SPLIT	72.00 ± 0.70	77.00 ± 1.10	78.70 ± 1.20	80.50 ± 0.90	81.20 ± 0.80	81.20 ± 0.80
	SGT-T	74.80 ± 1.00	78.00 ± 0.80	80.00 ± 0.70	80.30 ± 1.10	81.80 ± 1.30	81.80 ± 1.30
	SGT$_3$-T	**78.50 ± 1.20**	**78.70 ± 0.70**	**81.10 ± 0.60**	*81.00 ± 0.40*	81.00 ± 0.50	81.00 ± 0.50
mini-boone	CART	83.50 ± 0.20	86.60 ± 0.20	87.70 ± 0.10	89.00 ± 0.20	89.70 ± 0.10	89.70 ± 0.10
	HSTree	83.50 ± 0.20	86.60 ± 0.20	87.70 ± 0.10	89.00 ± 0.20	89.70 ± 0.10	89.70 ± 0.10
	SERDT	83.30 ± 0.10	86.40 ± 0.10	88.10 ± 0.10	89.00 ± 0.20	*89.80 ± 0.10*	*89.80 ± 0.10*
	SGT-C	*84.80 ± 0.20*	*87.10 ± 0.50*	*88.30 ± 0.30*	*89.20 ± 0.20*	89.70 ± 0.10	89.70 ± 0.10
	SGT$_3$-C	**85.60 ± 0.30**	**88.10 ± 0.50**	**89.10 ± 0.20**	**89.70 ± 0.10**	**89.90 ± 0.20**	**89.90 ± 0.20**
	AxTAO	83.50 ± 0.20	86.60 ± 0.10	88.00 ± 0.20	89.20 ± 0.30	89.70 ± 0.30	89.70 ± 0.30
	DPDT	*86.50 ± 0.20*	*88.00 ± 0.20*	88.30 ± 0.20	89.20 ± 0.20	*89.90 ± 0.10*	*89.90 ± 0.10*
	SPLIT	83.20 ± 0.20	86.80 ± 0.20	88.00 ± 0.30	88.60 ± 0.30	86.80 ± 0.20	88.60 ± 0.30
	SGT-T	85.80 ± 1.60	87.90 ± 0.20	*88.60 ± 0.10*	*89.40 ± 0.10*	*89.90 ± 0.10*	*89.90 ± 0.10*
	SGT$_3$-T	**87.10 ± 0.20**	**88.40 ± 0.10**	**89.20 ± 0.20**	**89.70 ± 0.20**	**90.10 ± 0.20**	**90.10 ± 0.20**
mushroom	CART	95.10 ± 0.40	98.30 ± 0.20	99.20 ± 0.20	**100.00 ± 0.00**	**100.00 ± 0.00**	**100.00 ± 0.00**
	HSTree	95.10 ± 0.40	98.30 ± 0.20	99.20 ± 0.20	**100.00 ± 0.00**	**100.00 ± 0.00**	**100.00 ± 0.00**
	SERDT	95.10 ± 0.40	98.30 ± 0.20	99.20 ± 0.20	99.60 ± 0.10	*99.90 ± 0.20*	*99.90 ± 0.20*
	SGT-C	*98.60 ± 0.30*	*99.30 ± 0.10*	*99.80 ± 0.20*	*99.90 ± 0.10*	*99.90 ± 0.10*	*99.90 ± 0.10*
	SGT$_3$-C	**99.40 ± 0.20**	**99.70 ± 0.20**	**100.00 ± 0.00**	**100.00 ± 0.00**	**100.00 ± 0.00**	**100.00 ± 0.00**
	AxTAO	95.10 ± 0.40	98.30 ± 0.20	99.20 ± 0.20	**100.00 ± 0.00**	**100.00 ± 0.00**	**100.00 ± 0.00**
	DPDT	96.90 ± 0.30	*99.00 ± 0.30*	**100.00 ± 0.00**	**100.00 ± 0.00**	**100.00 ± 0.00**	**100.00 ± 0.00**
	SPLIT	88.10 ± 1.10	96.90 ± 0.30	98.50 ± 0.10	*99.70 ± 0.30*	*99.70 ± 0.30*	*99.70 ± 0.30*
	SGT-T	*98.60 ± 0.30*	**99.60 ± 0.20**	*99.90 ± 0.10*	**100.00 ± 0.00**	**100.00 ± 0.00**	**100.00 ± 0.00**
	SGT$_3$-T	**99.40 ± 0.20**	**99.60 ± 0.20**	**100.00 ± 0.00**	**100.00 ± 0.00**	**100.00 ± 0.00**	**100.00 ± 0.00**
occupancy	CART	**99.00 ± 0.10**	**99.00 ± 0.10**	*99.00 ± 0.10*	99.00 ± 0.10	99.00 ± 0.10	99.00 ± 0.10
	HSTree	**99.00 ± 0.10**	**99.00 ± 0.10**	*99.00 ± 0.10*	99.00 ± 0.10	*99.10 ± 0.10*	*99.10 ± 0.10*
	SERDT	**99.00 ± 0.10**	**99.00 ± 0.10**	**99.10 ± 0.10**	*99.10 ± 0.10*	*99.10 ± 0.10*	*99.10 ± 0.10*
	SGT-C	**99.00 ± 0.10**	*98.90 ± 0.10*	*99.00 ± 0.10*	99.00 ± 0.20	**99.20 ± 0.20**	**99.20 ± 0.20**
	SGT$_3$-C	**99.00 ± 0.10**	*98.90 ± 0.10*	*99.00 ± 0.10*	**99.20 ± 0.20**	*99.10 ± 0.10*	99.00 ± 0.10
	AxTAO	**99.00 ± 0.10**	**99.00 ± 0.10**	*99.00 ± 0.10*	99.00 ± 0.10	99.10 ± 0.10	99.10 ± 0.10
	DPDT	**99.00 ± 0.10**	**99.00 ± 0.10**	**99.10 ± 0.20**	**99.20 ± 0.10**	*99.20 ± 0.20*	*99.20 ± 0.10*
	SPLIT	**99.00 ± 0.10**	**99.00 ± 0.10**	*99.00 ± 0.10*	*99.10 ± 0.20*	99.10 ± 0.20	99.10 ± 0.20
	SGT-T	**99.00 ± 0.10**	**99.00 ± 0.20**	**99.10 ± 0.20**	**99.20 ± 0.30**	**99.30 ± 0.20**	**99.30 ± 0.20**
	SGT$_3$-T	*98.90 ± 0.20*	**99.00 ± 0.20**	*99.00 ± 0.20*	*99.10 ± 0.20*	99.10 ± 0.10	99.10 ± 0.10
page	CART	—	*96.00 ± 0.30*	*96.50 ± 0.50*	**97.30 ± 0.60**	*97.20 ± 0.80*	**97.30 ± 0.60**
	HSTree	—	*96.00 ± 0.30*	*96.50 ± 0.50*	*97.20 ± 0.60*	**97.30 ± 0.50**	*97.20 ± 0.60*
	SERDT	—	**96.10 ± 0.20**	**96.60 ± 0.60**	96.90 ± 0.40	96.90 ± 0.20	96.90 ± 0.20
	SGT-C	—	95.20 ± 0.30	96.40 ± 0.20	96.30 ± 1.20	96.20 ± 0.40	96.30 ± 1.20
	SGT$_3$-C	—	95.60 ± 0.10	95.70 ± 0.30	96.30 ± 0.30	96.00 ± 0.10	96.30 ± 0.30
	AxTAO	—	*96.20 ± 0.50*	*96.70 ± 0.60*	**97.20 ± 0.60**	*97.10 ± 0.60*	*97.10 ± 0.60*
	DPDT	—	**96.70 ± 0.40**	**97.00 ± 0.30**	**97.20 ± 0.50**	**97.40 ± 0.60**	**97.40 ± 0.60**
	SPLIT	—	95.20 ± 0.20	96.10 ± 0.20	96.30 ± 1.00	96.20 ± 0.60	96.30 ± 1.00
	SGT-T	—	95.50 ± 0.00	96.30 ± 0.70	*96.50 ± 0.50*	96.30 ± 0.90	96.30 ± 0.90
	SGT$_3$-T	—	96.10 ± 0.10	96.50 ± 0.70	96.20 ± 0.40	95.70 ± 1.10	96.50 ± 0.70
pendigits	CART	—	—	77.20 ± 2.10	85.70 ± 1.50	*90.00 ± 0.60*	*90.00 ± 0.60*
	HSTree	—	—	77.20 ± 2.10	85.70 ± 1.50	*90.00 ± 0.60*	*90.00 ± 0.60*
	SERDT	—	—	77.60 ± 3.90	85.30 ± 3.00	89.30 ± 1.40	89.30 ± 1.40
	SGT-C	—	—	*79.30 ± 3.90*	*86.40 ± 0.70*	88.30 ± 1.20	88.30 ± 1.20
	SGT$_3$-C	—	—	**87.30 ± 0.50**	**90.80 ± 0.60**	**93.50 ± 0.40**	**93.50 ± 0.40**
	AxTAO	—	—	78.70 ± 2.40	86.00 ± 1.10	87.50 ± 0.60	87.50 ± 0.60
	DPDT	—	—	*82.70 ± 0.50*	*89.00 ± 0.50*	*93.10 ± 0.30*	*93.10 ± 0.30*
	SPLIT	—	—	57.90 ± 0.50	66.20 ± 0.60	70.70 ± 2.20	70.70 ± 2.20
	SGT-T	—	—	81.50 ± 3.90	87.50 ± 0.90	91.50 ± 0.60	91.50 ± 0.60
	SGT$_3$-T	—	—	**87.70 ± 0.40**	**92.50 ± 0.50**	**93.90 ± 0.50**	**93.90 ± 0.50**

raisin	CART	**85.90 ± 2.30**	85.90 ± 2.30	85.20 ± 1.20	**85.90 ± 2.00**	85.20 ± 1.20	85.20 ± 1.20
	HSTree	**85.90 ± 2.30**	*86.30 ± 3.10*	*85.90 ± 3.30*	*85.70 ± 2.20*	**86.10 ± 2.00**	*85.90 ± 3.30*
	SERDT	**85.90 ± 2.30**	**86.70 ± 2.00**	**86.30 ± 2.80**	85.60 ± 2.50	*85.60 ± 2.50*	**86.30 ± 2.80**
	SGT-C	*85.70 ± 1.40*	85.90 ± 2.30	84.30 ± 3.90	84.30 ± 2.90	84.40 ± 2.90	84.30 ± 2.90
	SGT$_3$-C	84.60 ± 2.30	85.20 ± 2.00	84.40 ± 3.10	84.60 ± 2.30	84.60 ± 2.30	85.20 ± 2.00
	AxTAO	**86.50 ± 2.70**	**86.50 ± 2.70**	**86.30 ± 2.20**	**86.10 ± 2.20**	**86.30 ± 2.20**	**86.30 ± 2.20**
	DPDT	**86.50 ± 2.30**	*86.10 ± 2.50*	*86.10 ± 3.10*	**86.10 ± 3.10**	85.90 ± 1.70	*85.90 ± 1.70*
	SPLIT	*86.10 ± 2.50*	85.70 ± 2.80	85.70 ± 3.10	*85.90 ± 2.50*	85.40 ± 2.20	85.70 ± 3.10
	SGT-T	85.00 ± 3.80	85.70 ± 2.20	85.40 ± 2.90	85.40 ± 2.90	85.40 ± 2.90	85.40 ± 2.90
	SGT$_3$-T	85.90 ± 1.30	85.60 ± 2.90	*86.10 ± 3.10*	**86.10 ± 3.10**	*86.10 ± 3.10*	85.60 ± 2.90
rice	CART	*93.10 ± 0.40*	*93.10 ± 0.40*	92.70 ± 0.50	92.50 ± 0.30	92.30 ± 0.30	92.50 ± 0.30
	HSTree	*93.10 ± 0.40*	*93.10 ± 0.40*	*93.00 ± 0.60*	*93.00 ± 0.20*	*92.80 ± 0.70*	*93.00 ± 0.60*
	SERDT	*93.10 ± 0.40*	*93.10 ± 0.40*	92.80 ± 0.50	92.80 ± 0.60	92.50 ± 0.80	92.80 ± 0.50
	SGT-C	*93.10 ± 0.40*	92.70 ± 0.80	92.50 ± 0.90	92.10 ± 0.90	92.50 ± 0.50	92.50 ± 0.50
	SGT$_3$-C	**93.20 ± 0.30**	**93.20 ± 0.40**	**93.20 ± 0.50**	**93.20 ± 0.50**	**93.20 ± 0.50**	**93.20 ± 0.30**
	AxTAO	*93.10 ± 0.40*	93.10 ± 0.40	*92.90 ± 0.50*	*92.90 ± 0.40*	*92.80 ± 0.30*	92.80 ± 0.30
	DPDT	93.00 ± 0.20	*93.20 ± 0.40*	*92.90 ± 0.50*	92.70 ± 0.40	92.70 ± 0.40	**93.20 ± 0.40**
	SPLIT	*93.10 ± 0.40*	**93.30 ± 0.20**	**93.20 ± 0.50**	**93.20 ± 0.50**	**93.20 ± 0.50**	*93.10 ± 0.40*
	SGT-T	*93.10 ± 0.40*	92.30 ± 0.50	92.70 ± 0.60	92.60 ± 0.60	92.30 ± 1.10	92.70 ± 0.60
	SGT$_3$-T	**93.20 ± 0.50**	93.00 ± 0.70	92.60 ± 0.20	92.60 ± 0.20	92.60 ± 0.20	92.60 ± 0.20
room	CART	92.50 ± 0.30	97.30 ± 0.50	98.70 ± 0.30	*99.40 ± 0.20*	99.30 ± 0.20	99.40 ± 0.20
	HSTree	92.50 ± 0.30	97.30 ± 0.50	98.70 ± 0.30	*99.40 ± 0.10*	99.40 ± 0.10	99.40 ± 0.10
	SERDT	92.50 ± 0.30	96.20 ± 0.60	98.90 ± 0.10	99.30 ± 0.20	*99.50 ± 0.20*	*99.50 ± 0.20*
	SGT-C	*93.00 ± 0.40*	*98.30 ± 0.20*	*99.40 ± 0.10*	*99.40 ± 0.00*	**99.60 ± 0.00**	**99.60 ± 0.00**
	SGT$_3$-C	**98.70 ± 0.10**	**99.50 ± 0.20**	**99.50 ± 0.20**	**99.50 ± 0.20**	*99.50 ± 0.20*	*99.50 ± 0.20*
	AxTAO	92.50 ± 0.30	98.80 ± 0.30	99.20 ± 0.00	*99.50 ± 0.20*	*99.40 ± 0.20*	99.40 ± 0.20
	DPDT	93.60 ± 1.10	99.00 ± 0.00	99.30 ± 0.20	**99.60 ± 0.10**	*99.40 ± 0.10*	**99.60 ± 0.10**
	SPLIT	88.80 ± 0.30	90.90 ± 0.30	92.40 ± 0.70	94.00 ± 0.70	94.20 ± 0.90	94.20 ± 0.90
	SGT-T	*96.90 ± 0.20*	**99.50 ± 0.10**	**99.60 ± 0.00**	*99.50 ± 0.20*	**99.50 ± 0.10**	*99.50 ± 0.10*
	SGT$_3$-T	**98.60 ± 0.30**	*99.30 ± 0.10*	*99.50 ± 0.20*	99.20 ± 0.30	**99.50 ± 0.10**	*99.50 ± 0.20*
segment	CART	—	81.30 ± 0.10	88.70 ± 1.10	90.90 ± 0.80	**93.40 ± 1.00**	**93.40 ± 1.00**
	HSTree	—	81.30 ± 0.10	88.70 ± 1.10	*91.30 ± 1.10*	**93.40 ± 1.20**	**93.40 ± 1.20**
	SERDT	—	67.00 ± 3.20	81.50 ± 0.20	88.70 ± 1.20	91.00 ± 1.80	91.00 ± 1.80
	SGT-C	—	*83.30 ± 3.60*	*88.90 ± 0.80*	89.80 ± 2.50	91.50 ± 1.90	91.50 ± 1.90
	SGT$_3$-C	—	**88.70 ± 0.20**	**91.20 ± 0.50**	**92.40 ± 1.00**	*92.90 ± 1.10*	*92.40 ± 1.00*
	AxTAO	—	81.70 ± 0.70	89.40 ± 1.00	*92.40 ± 0.90*	*93.30 ± 1.00*	*93.30 ± 1.00*
	DPDT	—	*87.10 ± 0.50*	*90.50 ± 0.60*	92.10 ± 0.30	**94.20 ± 0.70**	**94.20 ± 0.70**
	SPLIT	—	52.30 ± 2.50	61.90 ± 3.80	67.20 ± 3.50	67.70 ± 2.60	67.70 ± 2.60
	SGT-T	—	84.20 ± 3.40	89.80 ± 0.60	91.60 ± 1.50	90.80 ± 1.70	90.80 ± 1.70
	SGT$_3$-T	—	**89.30 ± 1.20**	**91.70 ± 0.10**	**93.00 ± 0.90**	92.90 ± 0.90	93.00 ± 0.90
skin	CART	90.80 ± 0.10	96.60 ± 0.10	97.40 ± 0.10	98.40 ± 0.10	98.90 ± 0.10	98.90 ± 0.10
	HSTree	90.80 ± 0.10	96.60 ± 0.10	97.50 ± 0.10	98.50 ± 0.00	99.00 ± 0.00	99.00 ± 0.00
	SERDT	90.80 ± 0.10	96.60 ± 0.10	97.80 ± 0.10	98.60 ± 0.10	*99.30 ± 0.00*	*99.30 ± 0.00*
	SGT-C	*93.20 ± 0.20*	*97.70 ± 0.10*	*98.50 ± 0.00*	*98.90 ± 0.10*	99.20 ± 0.20	99.20 ± 0.20
	SGT$_3$-C	**96.80 ± 0.10**	**98.80 ± 0.00**	**99.20 ± 0.10**	**99.60 ± 0.10**	**99.80 ± 0.00**	**99.80 ± 0.00**
	AxTAO	90.80 ± 0.10	96.60 ± 0.10	97.90 ± 0.00	98.70 ± 0.20	*99.60 ± 0.00*	*99.60 ± 0.00*
	DPDT	92.50 ± 0.10	96.60 ± 0.10	98.50 ± 0.00	*99.10 ± 0.00*	99.40 ± 0.10	99.40 ± 0.10
	SPLIT	88.40 ± 0.10	92.70 ± 0.00	96.50 ± 0.10	98.10 ± 0.10	98.50 ± 0.00	98.50 ± 0.00
	SGT-T	*93.20 ± 0.10*	*98.20 ± 0.00*	*99.20 ± 0.10*	**99.70 ± 0.10**	**99.80 ± 0.10**	**99.80 ± 0.10**
	SGT$_3$-T	**97.10 ± 0.10**	**98.80 ± 0.10**	**99.70 ± 0.10**	**99.70 ± 0.10**	**99.80 ± 0.00**	**99.80 ± 0.00**
wilt	CART	*97.30 ± 0.40*	**97.50 ± 0.20**	*97.80 ± 0.60*	*98.20 ± 0.50*	98.10 ± 0.70	98.20 ± 0.50
	HSTree	*97.30 ± 0.40*	**97.50 ± 0.20**	97.70 ± 0.70	*98.20 ± 0.50*	**98.40 ± 0.50**	**98.40 ± 0.50**
	SERDT	*97.30 ± 0.40*	**97.50 ± 0.20**	**97.90 ± 0.60**	**98.30 ± 0.40**	*98.30 ± 0.60*	*98.30 ± 0.40*
	SGT-C	97.10 ± 0.60	*97.10 ± 0.10*	**97.90 ± 0.50**	97.60 ± 0.20	97.60 ± 0.20	97.90 ± 0.50
	SGT$_3$-C	**97.50 ± 0.50**	**97.50 ± 0.20**	*97.80 ± 0.50*	97.60 ± 0.30	97.60 ± 0.30	97.50 ± 0.20
	AxTAO	**97.30 ± 0.40**	*97.50 ± 0.20*	*97.80 ± 0.70*	*98.10 ± 0.70*	*98.00 ± 0.10*	*98.10 ± 0.70*
	DPDT	*97.20 ± 0.40*	**97.80 ± 0.30**	**98.20 ± 0.40**	**98.20 ± 0.50**	**98.30 ± 0.60**	**98.30 ± 0.60**
	SPLIT	95.00 ± 0.40	97.30 ± 0.40	97.70 ± 0.20	97.80 ± 0.10	97.80 ± 0.10	97.80 ± 0.10
	SGT-T	**97.30 ± 0.40**	96.90 ± 0.40	97.40 ± 0.30	97.60 ± 0.50	97.60 ± 0.40	97.60 ± 0.40

SGT$_3$-T	**97.30 ± 0.60**	*97.50 ± 0.30*	97.70 ± 0.30	97.50 ± 0.20	97.50 ± 0.20	97.50 ± 0.20

Table 5: Test Accuracy (% ± std.) for all bivariate approaches separated into TDIDT and Non-Greedy approaches by dashed lines per dataset. Best approach is **bolded**, second-best is *italicized*.

dataset	model	2	3	4	5	6	Best
adult	BiCART	83.40 ± 0.30	83.60 ± 0.30	83.80 ± 0.40	84.10 ± 0.50	*84.10 ± 0.50*	*84.10 ± 0.50*
	S^{2}GT-C	*83.60 ± 0.30*	*83.80 ± 0.40*	*84.40 ± 0.50*	*84.90 ± 0.60*	**85.10 ± 0.60**	**85.10 ± 0.60**
	S^{2}GT$_3$-C	**84.30 ± 0.20**	**84.10 ± 0.50**	**84.60 ± 0.70**	**85.00 ± 0.40**	**85.10 ± 0.20**	**85.10 ± 0.20**
	BiTAO	83.60 ± 0.40	84.00 ± 0.30	84.20 ± 0.40	84.30 ± 0.50	84.30 ± 0.50	84.30 ± 0.50
	S^{2}GT-T	*83.90 ± 0.60*	*84.30 ± 0.40*	*84.90 ± 0.40*	*85.00 ± 0.70*	*84.90 ± 0.30*	*85.00 ± 0.70*
	S^{2}GT$_3$-T	**84.10 ± 0.40**	**84.50 ± 0.50**	**85.00 ± 0.40**	**85.10 ± 0.60**	**85.00 ± 0.40**	**85.10 ± 0.60**
avila	BiCART	—	—	59.80 ± 0.50	62.20 ± 0.60	66.90 ± 0.50	66.90 ± 0.50
	S^{2}GT-C	—	—	*80.20 ± 2.80*	*88.70 ± 4.30*	*95.30 ± 0.90*	*95.30 ± 0.90*
	S^{2}GT$_3$-C	—	—	**97.30 ± 0.90**	**99.90 ± 0.10**	**99.90 ± 0.10**	**99.90 ± 0.10**
	BiTAO	—	—	60.00 ± 0.40	66.00 ± 1.20	70.90 ± 1.50	70.90 ± 1.50
	S^{2}GT-T	—	—	*83.00 ± 0.70*	*90.90 ± 1.80*	*95.10 ± 1.10*	*95.10 ± 1.10*
	S^{2}GT$_3$-T	—	—	**97.10 ± 0.20**	**99.90 ± 0.10**	**99.80 ± 0.00**	**99.80 ± 0.00**
bank	BiCART	95.60 ± 1.90	*97.80 ± 2.00*	**99.40 ± 0.80**	**99.50 ± 0.80**	**99.30 ± 0.70**	**99.40 ± 0.80**
	S^{2}GT-C	*98.40 ± 0.80*	**98.40 ± 0.80**	*98.40 ± 0.80*	*98.40 ± 0.80*	*98.40 ± 0.80*	98.40 ± 0.80
	S^{2}GT$_3$-C	**98.50 ± 0.60**	**98.40 ± 0.60**	*98.40 ± 0.60*	*98.40 ± 0.60*	*98.40 ± 0.60*	*98.50 ± 0.60*
	BiTAO	95.40 ± 1.80	98.30 ± 0.80	**99.50 ± 0.60**	**99.50 ± 0.60**	**99.50 ± 0.60**	**99.50 ± 0.60**
	S^{2}GT-T	*97.80 ± 1.00*	**98.90 ± 0.40**	*98.90 ± 0.40*	*98.90 ± 0.40*	*98.90 ± 0.40*	*98.90 ± 0.40*
	S^{2}GT$_3$-T	**98.90 ± 1.00**	*98.50 ± 0.70*	98.50 ± 0.70	98.50 ± 0.70	98.50 ± 0.70	*98.90 ± 1.00*
bean	BiCART	—	89.80 ± 0.70	90.40 ± 0.30	**91.50 ± 0.00**	**91.80 ± 0.20**	**91.80 ± 0.20**
	S^{2}GT-C	—	*90.10 ± 0.50*	*90.60 ± 0.40*	*91.30 ± 0.30*	*91.30 ± 0.50*	*91.30 ± 0.50*
	S^{2}GT$_3$-C	—	**90.30 ± 0.90**	**91.10 ± 0.30**	*91.30 ± 0.50*	90.70 ± 0.30	91.10 ± 0.30
	BiTAO	—	90.20 ± 0.30	**91.00 ± 0.40**	*91.50 ± 0.30*	*91.70 ± 0.40*	*91.70 ± 0.40*
	S^{2}GT-T	—	**91.00 ± 0.30**	*90.90 ± 0.30*	**91.60 ± 0.40**	**91.80 ± 0.50**	**91.80 ± 0.50**
	S^{2}GT$_3$-T	—	*90.60 ± 0.30*	90.70 ± 0.60	91.20 ± 0.70	91.40 ± 0.40	91.20 ± 0.70
bidding	BiCART	97.90 ± 0.40	*99.60 ± 0.20*	**99.80 ± 0.10**	**99.80 ± 0.10**	**99.80 ± 0.10**	**99.80 ± 0.10**
	S^{2}GT-C	*99.50 ± 0.60*	**99.70 ± 0.20**	*99.70 ± 0.20*	*99.70 ± 0.20*	*99.70 ± 0.20*	*99.70 ± 0.20*
	S^{2}GT$_3$-C	**99.70 ± 0.30**	*99.60 ± 0.10*	99.60 ± 0.10	99.60 ± 0.10	99.60 ± 0.10	*99.70 ± 0.30*
	BiTAO	*98.00 ± 0.50*	*99.50 ± 0.20*	**99.80 ± 0.10**	**99.80 ± 0.10**	**99.80 ± 0.10**	**99.80 ± 0.10**
	S^{2}GT-T	**99.50 ± 0.10**	**99.80 ± 0.10**	**99.80 ± 0.10**	**99.80 ± 0.10**	**99.80 ± 0.10**	**99.80 ± 0.10**
	S^{2}GT$_3$-T	**99.50 ± 0.10**	*99.50 ± 0.20*	*99.50 ± 0.20*	*99.50 ± 0.20*	*99.50 ± 0.20*	*99.50 ± 0.20*
electricity	BiCART	75.80 ± 0.20	76.20 ± 0.10	78.30 ± 0.70	78.70 ± 0.30	80.40 ± 0.30	80.40 ± 0.30
	S^{2}GT-C	*80.60 ± 0.60*	*82.00 ± 0.60*	*83.90 ± 0.30*	*86.50 ± 1.20*	*87.50 ± 0.50*	*87.50 ± 0.50*
	S^{2}GT$_3$-C	**81.80 ± 0.20**	**84.50 ± 0.30**	**86.60 ± 0.80**	**87.30 ± 1.00**	**88.80 ± 0.20**	**88.80 ± 0.20**
	BiTAO	75.80 ± 0.20	76.20 ± 0.10	79.50 ± 0.50	80.10 ± 0.70	80.70 ± 0.40	80.70 ± 0.40
	S^{2}GT-T	*81.20 ± 0.50*	*83.60 ± 0.50*	*85.80 ± 0.80*	*86.80 ± 0.70*	*88.30 ± 0.80*	*88.30 ± 0.80*
	S^{2}GT$_3$-T	**82.10 ± 0.30**	**84.90 ± 0.60**	**86.30 ± 0.30**	**87.70 ± 0.20**	**88.50 ± 0.50**	**88.50 ± 0.50**
eye-movements	BiCART	45.40 ± 1.20	51.60 ± 0.70	52.20 ± 1.10	54.70 ± 1.60	56.30 ± 0.50	56.30 ± 0.50
	S^{2}GT-C	*57.80 ± 1.40*	*60.00 ± 2.00*	*61.70 ± 3.20*	*62.60 ± 3.30*	**64.80 ± 3.50**	**64.80 ± 3.50**
	S^{2}GT$_3$-C	**59.60 ± 2.40**	**63.60 ± 1.40**	**66.20 ± 1.90**	**67.50 ± 3.00**	*63.90 ± 2.40*	*63.90 ± 2.40*
	BiTAO	48.10 ± 2.00	51.60 ± 0.10	53.20 ± 0.40	55.80 ± 0.70	56.70 ± 0.40	56.70 ± 0.40
	S^{2}GT-T	*58.70 ± 0.60*	*60.10 ± 1.70*	**63.90 ± 1.10**	**66.10 ± 1.20**	**66.60 ± 1.40**	**66.60 ± 1.40**
	S^{2}GT$_3$-T	**59.80 ± 1.70**	**62.80 ± 1.10**	*56.90 ± 1.10*	*63.20 ± 1.20*	*64.90 ± 1.30*	*62.80 ± 1.10*
eye-state	BiCART	66.20 ± 2.40	69.20 ± 1.10	72.90 ± 0.60	74.10 ± 2.70	77.60 ± 0.80	77.60 ± 0.80
	S^{2}GT-C	*71.70 ± 1.10*	*72.80 ± 0.70*	*74.40 ± 2.10*	*76.10 ± 2.00*	*80.20 ± 0.30*	*80.20 ± 0.30*
	S^{2}GT$_3$-C	**73.10 ± 1.10**	**75.90 ± 0.40**	**79.30 ± 1.10**	**81.10 ± 0.60**	**80.60 ± 1.90**	**81.10 ± 0.60**
	BiTAO	68.80 ± 1.20	70.10 ± 0.70	74.50 ± 1.50	77.50 ± 0.40	79.00 ± 1.40	79.00 ± 1.40
	S^{2}GT-T	*72.40 ± 1.60*	*75.90 ± 1.20*	*77.20 ± 0.80*	*79.00 ± 1.70*	*80.90 ± 1.00*	*80.90 ± 1.00*

	S^{2}GT$_3$-T	**74.50 ± 1.20**	**76.30 ± 0.20**	**79.30 ± 1.80**	**80.50 ± 1.70**	**81.70 ± 1.20**	**81.70 ± 1.20**
fault	BiCART	—	61.40 ± 3.00	67.40 ± 1.90	68.80 ± 1.10	**73.40 ± 1.50**	**73.40 ± 1.50**
	S^{2}GT-C	—	*66.60 ± 5.80*	*69.00 ± 5.80*	*69.20 ± 1.00*	*71.90 ± 2.40*	*71.90 ± 2.40*
	S^{2}GT$_3$-C	—	**68.50 ± 2.50**	**70.30 ± 1.70**	**71.60 ± 2.80**	70.00 ± 1.90	71.60 ± 2.80
	BiTAO	—	62.30 ± 3.30	67.90 ± 3.00	68.00 ± 1.70	**73.40 ± 1.20**	**73.40 ± 1.20**
	S^{2}GT-T	—	*67.90 ± 1.20*	*70.40 ± 3.60*	*71.80 ± 1.50*	*72.40 ± 2.00*	71.80 ± 1.50
	S^{2}GT$_3$-T	—	**70.40 ± 3.10**	**73.40 ± 1.90**	**73.20 ± 3.40**	72.30 ± 1.50	*73.20 ± 3.40*
gas-drift	BiCART	—	*86.70 ± 1.10*	*95.40 ± 0.40*	**97.90 ± 0.10**	**98.60 ± 0.20**	**98.60 ± 0.20**
	S^{2}GT-C	—	83.60 ± 4.00	94.90 ± 1.20	96.80 ± 0.20	*97.20 ± 0.30*	*97.20 ± 0.30*
	S^{2}GT$_3$-C	—	**96.20 ± 0.50**	**97.00 ± 0.40**	*97.10 ± 0.30*	97.10 ± 0.40	97.10 ± 0.40
	BiTAO	—	91.50 ± 0.10	*96.20 ± 0.70*	97.20 ± 0.30	**98.20 ± 0.00**	**98.20 ± 0.00**
	S^{2}GT-T	—	*92.00 ± 1.10*	94.80 ± 1.20	*97.30 ± 0.60*	*98.00 ± 0.10*	*98.00 ± 0.10*
	S^{2}GT$_3$-T	—	**96.40 ± 0.50**	**97.90 ± 0.20**	**97.90 ± 0.20**	97.90 ± 0.20	97.90 ± 0.20
htru	BiCART	**97.90 ± 0.10**	**98.00 ± 0.10**	**98.10 ± 0.20**	**98.00 ± 0.20**	**98.00 ± 0.10**	**98.00 ± 0.10**
	S^{2}GT-C	*97.80 ± 0.00*	*97.80 ± 0.10*	97.80 ± 0.20	*97.80 ± 0.30*	*97.80 ± 0.30*	*97.80 ± 0.20*
	S^{2}GT$_3$-C	*97.80 ± 0.00*	**98.00 ± 0.00**	*98.00 ± 0.10*	**98.00 ± 0.10**	**98.00 ± 0.10**	**98.00 ± 0.00**
	BiTAO	**97.90 ± 0.10**	**98.10 ± 0.10**	*98.00 ± 0.30*	*98.00 ± 0.10*	*98.00 ± 0.00*	*98.00 ± 0.00*
	S^{2}GT-T	**97.90 ± 0.20**	*98.00 ± 0.20*	97.80 ± 0.20	**98.10 ± 0.10**	*98.00 ± 0.10*	*98.00 ± 0.20*
	S^{2}GT$_3$-T	*97.60 ± 0.10*	*98.00 ± 0.10*	**98.10 ± 0.10**	**98.10 ± 0.00**	**98.10 ± 0.00**	**98.10 ± 0.00**
magic	BiCART	77.50 ± 1.40	81.10 ± 0.30	81.10 ± 0.30	*82.90 ± 0.20*	**83.00 ± 0.60**	**82.90 ± 0.20**
	S^{2}GT-C	*81.10 ± 1.00*	*81.70 ± 0.90*	*81.20 ± 0.80*	81.90 ± 0.40	82.10 ± 0.10	*81.90 ± 0.40*
	S^{2}GT$_3$-C	**81.50 ± 0.80**	**82.90 ± 0.60**	**82.90 ± 0.40**	**83.50 ± 0.50**	*82.70 ± 0.70*	**82.90 ± 0.40**
	BiTAO	77.80 ± 1.30	81.70 ± 0.50	82.00 ± 0.40	*82.70 ± 0.30*	**83.30 ± 0.70**	**83.30 ± 0.70**
	S^{2}GT-T	*81.40 ± 0.10*	*82.10 ± 0.20*	*82.60 ± 0.70*	82.50 ± 0.40	*82.80 ± 0.60*	82.50 ± 0.40
	S^{2}GT$_3$-T	**82.20 ± 0.70**	**83.00 ± 0.80**	**83.60 ± 1.00**	**82.80 ± 0.20**	82.50 ± 0.60	*82.80 ± 0.20*
mini-boone	BiCART	87.20 ± 0.10	88.60 ± 0.20	89.50 ± 0.30	90.30 ± 0.10	*90.70 ± 0.20*	*90.70 ± 0.20*
	S^{2}GT-C	*87.60 ± 0.30*	*89.50 ± 0.10*	*90.10 ± 0.20*	*90.50 ± 0.20*	90.60 ± 0.20	90.60 ± 0.20
	S^{2}GT$_3$-C	**88.80 ± 0.30**	**90.00 ± 0.20**	**90.50 ± 0.20**	**90.90 ± 0.10**	**90.90 ± 0.20**	**90.90 ± 0.20**
	BiTAO	87.30 ± 0.10	88.40 ± 0.30	89.70 ± 0.40	90.20 ± 0.10	90.50 ± 0.20	90.50 ± 0.20
	S^{2}GT-T	*88.40 ± 0.50*	*89.70 ± 0.20*	*90.30 ± 0.20*	*90.80 ± 0.10*	*91.10 ± 0.10*	*91.10 ± 0.10*
	S^{2}GT$_3$-T	**89.00 ± 0.30**	**90.10 ± 0.20**	**90.60 ± 0.30**	**91.20 ± 0.30**	**91.20 ± 0.10**	**91.20 ± 0.10**
mushroom	BiCART	98.70 ± 0.10	**100.00 ± 0.00**	**100.00 ± 0.00**	**100.00 ± 0.00**	**100.00 ± 0.00**	**100.00 ± 0.00**
	S^{2}GT-C	*99.40 ± 0.20*	**100.00 ± 0.00**	**100.00 ± 0.00**	**100.00 ± 0.00**	**100.00 ± 0.00**	**100.00 ± 0.00**
	S^{2}GT$_3$-C	**100.00 ± 0.00**	**100.00 ± 0.00**	**100.00 ± 0.00**	**100.00 ± 0.00**	**100.00 ± 0.00**	**100.00 ± 0.00**
	BiTAO	98.70 ± 0.10	**100.00 ± 0.00**	**100.00 ± 0.00**	**100.00 ± 0.00**	**100.00 ± 0.00**	**100.00 ± 0.00**
	S^{2}GT-T	*99.40 ± 0.10*	**100.00 ± 0.00**	**100.00 ± 0.00**	**100.00 ± 0.00**	**100.00 ± 0.00**	**100.00 ± 0.00**
	S^{2}GT$_3$-T	**100.00 ± 0.00**	**100.00 ± 0.00**	**100.00 ± 0.00**	**100.00 ± 0.00**	**100.00 ± 0.00**	**100.00 ± 0.00**
occupancy	BiCART	99.00 ± 0.10	99.00 ± 0.10	99.10 ± 0.10	*99.20 ± 0.10*	*99.20 ± 0.10*	**99.20 ± 0.10**
	S^{2}GT-C	*99.10 ± 0.20*	*99.10 ± 0.10*	*99.20 ± 0.10*	**99.30 ± 0.10**	**99.30 ± 0.10**	*99.10 ± 0.10*
	S^{2}GT$_3$-C	**99.20 ± 0.20**	**99.30 ± 0.20**	**99.30 ± 0.10**	**99.30 ± 0.20**	**99.30 ± 0.20**	**99.20 ± 0.20**
	BiTAO	99.00 ± 0.10	99.00 ± 0.10	*99.10 ± 0.10*	*99.10 ± 0.10*	*99.10 ± 0.20*	*99.10 ± 0.20*
	S^{2}GT-T	*99.10 ± 0.20*	*99.10 ± 0.20*	**99.30 ± 0.20**	*99.10 ± 0.20*	**99.20 ± 0.20**	**99.20 ± 0.20**
	S^{2}GT$_3$-T	**99.20 ± 0.20**	**99.20 ± 0.20**	*99.10 ± 0.20*	**99.20 ± 0.20**	**99.20 ± 0.20**	**99.20 ± 0.20**
page	BiCART	—	*96.40 ± 0.30*	**97.20 ± 0.20**	*96.80 ± 0.50*	**97.10 ± 0.60**	*97.10 ± 0.60*
	S^{2}GT-C	—	**96.90 ± 0.10**	**97.20 ± 0.70**	**96.90 ± 1.20**	96.10 ± 0.90	**97.20 ± 0.70**
	S^{2}GT$_3$-C	—	96.20 ± 0.40	*96.80 ± 0.60*	*96.80 ± 0.30*	*96.80 ± 0.40*	96.80 ± 0.60
	BiTAO	—	*96.60 ± 0.60*	**97.40 ± 0.20**	**97.40 ± 0.40**	**96.80 ± 0.80**	*96.80 ± 0.80*
	S^{2}GT-T	—	**97.00 ± 0.20**	*96.90 ± 0.40*	*97.10 ± 0.80*	*96.60 ± 0.10*	**97.00 ± 0.20**
	S^{2}GT$_3$-T	—	96.50 ± 0.50	96.40 ± 0.60	96.40 ± 0.60	96.40 ± 0.60	96.40 ± 0.60
pendigits	BiCART	—	—	*87.40 ± 0.30*	*91.90 ± 1.30*	**94.50 ± 1.10**	*94.50 ± 1.10*
	S^{2}GT-C	—	—	87.20 ± 1.10	91.00 ± 0.80	93.30 ± 0.10	93.30 ± 0.10
	S^{2}GT$_3$-C	—	—	**91.80 ± 1.10**	**95.80 ± 0.70**	*94.20 ± 0.60*	**95.80 ± 0.70**
	BiTAO	—	—	88.60 ± 0.50	*93.80 ± 0.80*	**95.30 ± 0.90**	**95.30 ± 0.90**
	S^{2}GT-T	—	—	*89.00 ± 0.90*	92.10 ± 1.00	94.40 ± 0.20	94.40 ± 0.20

	S^2GT_3-T	—	—	**94.10 ± 0.40**	**94.10 ± 0.30**	*94.80 ± 0.20*	*94.80 ± 0.20*
raisin	BiCART	**89.40 ± 3.10**	**85.70 ± 1.70**	**86.50 ± 1.30**	**86.50 ± 3.70**	*85.40 ± 1.20*	**85.70 ± 1.70**
	S^2GT-C	85.40 ± 2.20	**85.70 ± 1.70**	*85.00 ± 3.50*	*85.00 ± 1.90*	**86.50 ± 1.30**	**85.70 ± 1.70**
	S^2GT_3-C	*85.70 ± 1.70*	*83.00 ± 1.20*	83.00 ± 1.20	83.00 ± 1.20	83.00 ± 1.20	**85.70 ± 1.70**
	BiTAO	**89.30 ± 3.40**	**88.50 ± 3.10**	**89.40 ± 3.50**	**89.40 ± 3.50**	**89.30 ± 3.40**	**88.50 ± 3.10**
	S^2GT-T	85.70 ± 3.70	*86.70 ± 2.40*	85.00 ± 3.10	85.00 ± 3.10	85.00 ± 3.10	85.70 ± 3.70
	S^2GT_3-T	*85.90 ± 3.70*	85.90 ± 3.70	*85.90 ± 3.70*	*85.90 ± 3.70*	*85.90 ± 3.70*	*85.90 ± 3.70*
rice	BiCART	**93.10 ± 0.50**	**93.10 ± 0.50**	**92.70 ± 0.40**	**92.80 ± 0.60**	**92.80 ± 0.50**	92.80 ± 0.60
	S^2GT-C	92.90 ± 0.90	*93.00 ± 0.60*	92.00 ± 0.60	*92.50 ± 0.60*	91.90 ± 0.60	*92.90 ± 0.90*
	S^2GT_3-C	*93.00 ± 0.50*	92.70 ± 0.40	*92.50 ± 0.60*	*92.50 ± 0.60*	*92.50 ± 0.60*	**93.00 ± 0.50**
	BiTAO	**93.10 ± 0.50**	**92.90 ± 0.50**	*92.90 ± 0.60*	**93.00 ± 0.50**	**93.00 ± 0.50**	**93.00 ± 0.50**
	S^2GT-T	*92.80 ± 0.20*	92.30 ± 1.40	**93.10 ± 0.60**	*92.90 ± 0.90*	*92.70 ± 0.20*	92.30 ± 1.40
	S^2GT_3-T	92.60 ± 1.40	*92.50 ± 0.10*	92.50 ± 0.10	92.50 ± 0.10	92.50 ± 0.10	*92.50 ± 0.10*
room	BiCART	93.30 ± 0.30	98.80 ± 0.20	**99.50 ± 0.20**	**99.50 ± 0.20**	*99.40 ± 0.10*	**99.50 ± 0.20**
	S^2GT-C	*94.60 ± 0.20*	*99.40 ± 0.10*	*99.40 ± 0.20*	*99.40 ± 0.20*	*99.40 ± 0.20*	*99.40 ± 0.20*
	S^2GT_3-C	**99.50 ± 0.00**	**99.50 ± 0.20**	**99.50 ± 0.20**	**99.50 ± 0.20**	**99.50 ± 0.20**	**99.50 ± 0.20**
	BiTAO	96.60 ± 0.00	*99.50 ± 0.20*	*99.30 ± 0.10*	**99.60 ± 0.20**	**99.50 ± 0.20**	*99.60 ± 0.20*
	S^2GT-T	*98.20 ± 0.50*	*99.50 ± 0.20*	**99.50 ± 0.00**	**99.60 ± 0.20**	**99.50 ± 0.20**	**99.50 ± 0.00**
	S^2GT_3-T	**99.70 ± 0.10**	**99.60 ± 0.10**	**99.50 ± 0.30**	*99.50 ± 0.10*	**99.50 ± 0.10**	**99.70 ± 0.10**
segment	BiCART	—	84.50 ± 6.60	*93.10 ± 1.20*	92.90 ± 2.00	*94.00 ± 1.10*	**94.00 ± 1.10**
	S^2GT-C	—	**92.90 ± 1.10**	**93.60 ± 0.50**	*93.50 ± 1.30*	93.90 ± 1.40	*93.90 ± 1.40*
	S^2GT_3-C	—	*92.60 ± 1.80*	*93.10 ± 1.20*	**94.50 ± 1.90**	**94.50 ± 1.90**	93.10 ± 1.20
	BiTAO	—	85.20 ± 6.80	92.70 ± 0.90	93.70 ± 2.30	*94.70 ± 0.50*	*94.70 ± 0.50*
	S^2GT-T	—	*93.40 ± 2.00*	*93.40 ± 1.50*	*94.30 ± 1.20*	94.40 ± 1.50	94.30 ± 1.20
	S^2GT_3-T	—	**94.40 ± 1.10**	**94.90 ± 0.50**	**94.80 ± 1.30**	**94.90 ± 1.20**	**94.80 ± 1.30**
skin	BiCART	98.60 ± 0.10	*99.40 ± 0.00*	*99.70 ± 0.00*	*99.80 ± 0.00*	*99.80 ± 0.00*	*99.80 ± 0.00*
	S^2GT-C	*99.80 ± 0.00*	**99.90 ± 0.00**	**99.90 ± 0.00**	**99.90 ± 0.00**	**99.90 ± 0.00**	**99.90 ± 0.00**
	S^2GT_3-C	**99.90 ± 0.00**	**99.90 ± 0.00**	**99.90 ± 0.00**	**99.90 ± 0.00**	**99.90 ± 0.00**	**99.90 ± 0.00**
	BiTAO	98.60 ± 0.10	*99.40 ± 0.00*	*99.80 ± 0.00*	*99.80 ± 0.00*	**99.90 ± 0.00**	**99.90 ± 0.00**
	S^2GT-T	*99.80 ± 0.00*	**99.90 ± 0.00**	**99.90 ± 0.00**	**99.90 ± 0.00**	**99.90 ± 0.00**	**99.90 ± 0.00**
	S^2GT_3-T	**99.90 ± 0.00**	**99.90 ± 0.00**	**99.90 ± 0.00**	**99.90 ± 0.00**	**99.90 ± 0.00**	**99.90 ± 0.00**
wilt	BiCART	*98.50 ± 0.20*	**98.50 ± 0.20**	**98.50 ± 0.20**	*98.50 ± 0.20*	**98.90 ± 0.50**	**98.90 ± 0.50**
	S^2GT-C	**98.80 ± 0.20**	**98.50 ± 0.10**	*98.20 ± 0.60*	**98.60 ± 0.40**	*98.60 ± 0.40*	*98.80 ± 0.20*
	S^2GT_3-C	98.30 ± 0.40	*98.30 ± 0.20*	**98.50 ± 0.40**	98.40 ± 0.30	98.40 ± 0.30	98.30 ± 0.20
	BiTAO	**98.50 ± 0.20**	98.40 ± 0.10	*98.50 ± 0.10*	*98.50 ± 0.20*	*98.50 ± 0.20*	*98.50 ± 0.20*
	S^2GT-T	**98.50 ± 0.10**	*98.50 ± 0.10*	98.10 ± 0.40	98.10 ± 0.40	98.10 ± 0.40	*98.50 ± 0.10*
	S^2GT_3-T	*98.40 ± 0.50*	**98.70 ± 0.20**	**98.70 ± 0.20**	**98.70 ± 0.20**	**98.70 ± 0.20**	**98.70 ± 0.20**

G.2 Additional Empirical Evaluation

G.2.1 Runtime

Table 6: Runtime (s ± std.) for all axis-aligned approaches separated into TDIDT and Non-Greedy approaches by dashed lines per dataset. Best approach is **bolded**, second-best is *italicized*.

dataset	model	2	3	4	5	6	Best
adult	CART	**0.036 ± 0.000**	*0.048 ± 0.000*	*0.059 ± 0.001*	*0.071 ± 0.001*	*0.083 ± 0.000*	*0.083 ± 0.000*
	HSTree	**0.036 ± 0.000**	**0.046 ± 0.001**	**0.058 ± 0.001**	**0.067 ± 0.000**	**0.077 ± 0.001**	**0.077 ± 0.001**
	SERDT	20.560 ± 0.037	30.489 ± 0.040	36.904 ± 0.157	44.494 ± 0.720	52.905 ± 0.963	52.905 ± 0.963
	SGT-C	*0.386 ± 0.009*	0.596 ± 0.009	0.894 ± 0.016	1.120 ± 0.023	1.144 ± 0.033	1.144 ± 0.033
	SGT_3-C	0.545 ± 0.005	1.069 ± 0.006	1.503 ± 0.013	2.723 ± 0.029	1.729 ± 0.082	1.729 ± 0.082
	AxTAO	*1.303 ± 0.004*	*1.708 ± 0.194*	*6.007 ± 0.445*	*7.710 ± 0.562*	9.812 ± 0.602	9.812 ± 0.602
	DPDT	**0.311 ± 0.003**	3.499 ± 0.187	7.731 ± 0.032	9.249 ± 0.088	*9.276 ± 0.667*	*9.276 ± 0.667*
	SPLIT	1.363 ± 0.516	**1.353 ± 0.511**	7.286 ± 2.613	**3.477 ± 0.208**	**7.823 ± 1.706**	**7.823 ± 1.706**
	SGT-T	2.029 ± 0.020	2.522 ± 0.879	**4.038 ± 1.353**	37.314 ± 1.389	41.237 ± 23.798	41.237 ± 23.798
	SGT_3-T	2.806 ± 0.123	7.232 ± 0.066	22.743 ± 19.981	50.972 ± 34.416	49.766 ± 28.622	49.766 ± 28.622
avila	CART	—	—	**0.050 ± 0.000**	**0.061 ± 0.002**	**0.069 ± 0.000**	**0.069 ± 0.000**

	HSTree	—	—	*0.054 ± 0.002*	**0.061 ± 0.000**	*0.072 ± 0.002*	*0.072 ± 0.002*
	SERDT	—	—	2.734 ± 0.010	3.344 ± 0.021	3.995 ± 0.012	3.995 ± 0.012
	SGT-C	—	—	1.711 ± 0.036	*2.343 ± 0.007*	2.733 ± 0.088	2.733 ± 0.088
	SGT$_3$-C	—	—	6.553 ± 0.210	8.060 ± 0.358	7.817 ± 0.096	7.817 ± 0.096
	AxTAO	—	—	**0.970 ± 0.319**	**1.681 ± 0.033**	**3.038 ± 1.320**	**3.038 ± 1.320**
	DPDT	—	—	*3.042 ± 0.201*	*7.466 ± 0.303*	*10.148 ± 0.460*	*10.148 ± 0.460*
	SPLIT	—	—	48.450 ± 9.734	104.178 ± 1.324	70.139 ± 8.502	70.139 ± 8.502
	SGT-T	—	—	6.837 ± 1.515	16.545 ± 3.764	31.646 ± 22.865	31.646 ± 22.865
	SGT$_3$-T	—	—	27.996 ± 7.018	28.331 ± 1.424	21.534 ± 0.983	21.534 ± 0.983
bank	CART	**0.002 ± 0.000**	**0.002 ± 0.000**	**0.002 ± 0.000**	**0.003 ± 0.000**	**0.003 ± 0.000**	**0.003 ± 0.000**
	HSTree	**0.002 ± 0.000**	*0.003 ± 0.000*	*0.003 ± 0.000*	**0.003 ± 0.000**	**0.003 ± 0.000**	**0.003 ± 0.000**
	SERDT	*0.033 ± 0.000*	0.050 ± 0.000	0.068 ± 0.000	*0.085 ± 0.003*	*0.093 ± 0.002*	*0.093 ± 0.002*
	SGT-C	0.101 ± 0.001	0.138 ± 0.004	0.165 ± 0.015	0.184 ± 0.008	0.179 ± 0.010	0.165 ± 0.015
	SGT$_3$-C	0.142 ± 0.000	0.187 ± 0.002	0.217 ± 0.008	0.220 ± 0.013	0.216 ± 0.016	0.217 ± 0.008
	AxTAO	**0.036 ± 0.017**	*0.115 ± 0.025*	**0.147 ± 0.022**	**0.256 ± 0.062**	*0.259 ± 0.083*	*0.256 ± 0.062*
	DPDT	*0.040 ± 0.007*	**0.041 ± 0.001**	*0.617 ± 0.027*	*0.308 ± 0.003*	**0.128 ± 0.001**	**0.128 ± 0.001**
	SPLIT	0.653 ± 0.609	0.648 ± 0.601	0.757 ± 0.538	2.495 ± 0.512	1.369 ± 0.302	2.495 ± 0.512
	SGT-T	0.726 ± 0.228	2.917 ± 0.473	3.262 ± 0.610	7.584 ± 7.667	3.388 ± 1.137	7.584 ± 7.667
	SGT$_3$-T	1.107 ± 0.339	4.162 ± 4.690	2.019 ± 0.634	2.130 ± 0.663	2.101 ± 0.646	2.019 ± 0.634
bean	CART	—	*0.107 ± 0.001*	*0.135 ± 0.001*	*0.160 ± 0.001*	*0.186 ± 0.002*	*0.186 ± 0.002*
	HSTree	—	**0.093 ± 0.002**	**0.119 ± 0.004**	**0.138 ± 0.001**	**0.161 ± 0.003**	**0.161 ± 0.003**
	SERDT	—	3.861 ± 0.007	4.996 ± 0.009	6.197 ± 0.009	7.345 ± 0.007	7.345 ± 0.007
	SGT-C	—	1.892 ± 0.027	2.420 ± 0.071	1.797 ± 0.041	2.328 ± 0.061	2.328 ± 0.061
	SGT$_3$-C	—	1.179 ± 0.009	2.670 ± 0.076	4.684 ± 0.085	7.103 ± 0.125	7.103 ± 0.125
	AxTAO	—	**1.367 ± 0.054**	**2.008 ± 0.048**	**3.189 ± 0.589**	**4.472 ± 0.106**	**4.472 ± 0.106**
	DPDT	—	*3.258 ± 0.174*	*5.503 ± 0.286*	*7.565 ± 0.361*	*5.889 ± 0.337*	*5.889 ± 0.337*
	SPLIT	—	38.276 ± 7.431	42.074 ± 18.018	55.909 ± 14.860	71.596 ± 12.543	71.596 ± 12.543
	SGT-T	—	6.180 ± 0.111	19.833 ± 9.656	18.729 ± 4.516	43.396 ± 24.977	43.396 ± 24.977
	SGT$_3$-T	—	8.404 ± 0.343	14.332 ± 2.636	43.177 ± 2.059	26.883 ± 1.676	43.177 ± 2.059
bidding	CART	**0.005 ± 0.000**	**0.005 ± 0.000**	**0.006 ± 0.000**	**0.005 ± 0.000**	**0.005 ± 0.000**	**0.005 ± 0.000**
	HSTree	**0.005 ± 0.000**	**0.005 ± 0.000**	**0.006 ± 0.000**	*0.006 ± 0.000*	*0.006 ± 0.000*	*0.006 ± 0.000*
	SERDT	0.190 ± 0.002	0.311 ± 0.001	0.334 ± 0.007	0.341 ± 0.002	0.353 ± 0.003	0.353 ± 0.003
	SGT-C	*0.132 ± 0.001*	*0.207 ± 0.002*	*0.208 ± 0.004*	0.256 ± 0.004	0.333 ± 0.011	0.333 ± 0.011
	SGT$_3$-C	0.276 ± 0.007	0.479 ± 0.025	0.533 ± 0.040	0.534 ± 0.042	0.544 ± 0.043	0.479 ± 0.025
	AxTAO	*0.070 ± 0.001*	**0.186 ± 0.141**	**0.123 ± 0.032**	**0.234 ± 0.091**	**0.204 ± 0.064**	**0.234 ± 0.091**
	DPDT	**0.020 ± 0.001**	*0.426 ± 0.068*	*0.264 ± 0.001*	*0.955 ± 0.143*	*0.243 ± 0.012*	*0.264 ± 0.001*
	SPLIT	0.636 ± 0.107	0.647 ± 0.111	1.013 ± 0.145	1.077 ± 0.176	1.031 ± 0.151	1.031 ± 0.151
	SGT-T	0.632 ± 0.175	1.212 ± 0.532	1.325 ± 0.043	1.656 ± 0.494	4.025 ± 0.473	1.325 ± 0.043
	SGT$_3$-T	1.090 ± 0.009	2.184 ± 1.188	2.432 ± 1.080	2.393 ± 0.967	2.472 ± 1.033	2.432 ± 1.080
covtype	CART	—	*1.008 ± 0.009*	*1.321 ± 0.011*	*1.636 ± 0.022*	*1.977 ± 0.021*	*1.977 ± 0.021*
	HSTree	—	**0.913 ± 0.011**	**1.236 ± 0.103**	**1.466 ± 0.025**	**1.723 ± 0.012**	**1.723 ± 0.012**
	SERDT	—	281.991 ± 0.979	360.049 ± 1.806	447.986 ± 0.312	534.572 ± 1.955	534.572 ± 1.955
	SGT-C	—	6.135 ± 0.034	11.224 ± 0.014	10.618 ± 0.064	15.770 ± 0.096	15.770 ± 0.096
	SGT$_3$-C	—	8.910 ± 0.052	14.011 ± 0.071	19.099 ± 0.151	29.561 ± 0.430	29.561 ± 0.430
	AxTAO	—	**30.698 ± 0.183**	**52.465 ± 12.625**	**99.446 ± 16.476**	*170.256 ± 28.126*	*170.256 ± 28.126*
	DPDT	—	124.065 ± 0.671	207.358 ± 1.485	298.735 ± 1.185	415.134 ± 1.714	415.134 ± 1.714
	SPLIT	—	912.950 ± 157.383	901.083 ± 169.281	877.478 ± 164.931	881.974 ± 153.045	912.950 ± 157.383
	SGT-T	—	*34.679 ± 7.011*	*56.332 ± 5.875*	*100.787 ± 11.809*	**148.474 ± 9.684**	**148.474 ± 9.684**
	SGT$_3$-T	—	73.772 ± 15.480	122.400 ± 38.379	397.392 ± 85.282	728.959 ± 118.892	728.959 ± 118.892
electricity	CART	*0.031 ± 0.000*	*0.047 ± 0.000*	*0.062 ± 0.000*	*0.077 ± 0.000*	*0.093 ± 0.001*	*0.093 ± 0.001*
	HSTree	**0.029 ± 0.000**	**0.043 ± 0.001**	**0.057 ± 0.000**	**0.070 ± 0.001**	**0.085 ± 0.000**	**0.085 ± 0.000**
	SERDT	2.923 ± 0.036	4.184 ± 0.010	5.262 ± 0.046	6.237 ± 0.025	7.454 ± 0.093	7.454 ± 0.093
	SGT-C	0.396 ± 0.002	0.438 ± 0.006	0.880 ± 0.007	1.356 ± 0.011	2.145 ± 0.177	2.145 ± 0.177
	SGT$_3$-C	0.646 ± 0.014	1.138 ± 0.012	2.301 ± 0.081	4.603 ± 0.381	7.767 ± 0.918	7.767 ± 0.918
	AxTAO	**0.438 ± 0.003**	**1.408 ± 0.008**	**2.020 ± 0.007**	**6.282 ± 2.817**	**10.311 ± 0.628**	**10.311 ± 0.628**
	DPDT	1.539 ± 0.008	*3.158 ± 0.016*	*8.492 ± 0.024*	13.254 ± 0.028	*19.481 ± 0.057*	*19.481 ± 0.057*
	SPLIT	*0.458 ± 0.115*	3.509 ± 0.578	12.528 ± 2.394	*11.515 ± 0.450*	22.478 ± 0.111	22.478 ± 0.111
	SGT-T	1.505 ± 0.374	4.662 ± 0.122	11.463 ± 1.274	31.993 ± 5.000	72.724 ± 18.726	72.724 ± 18.726
	SGT$_3$-T	6.664 ± 1.547	20.198 ± 7.617	30.156 ± 8.124	79.497 ± 26.969	92.449 ± 6.446	92.449 ± 6.446
eucalyptus	CART	—	**0.006 ± 0.000**	**0.007 ± 0.000**	**0.008 ± 0.000**	**0.009 ± 0.000**	**0.009 ± 0.000**
	HSTree	—	*0.007 ± 0.000*	*0.009 ± 0.000*	*0.010 ± 0.000*	*0.011 ± 0.000*	*0.011 ± 0.000*
	SERDT	—	4.464 ± 0.019	5.694 ± 0.082	7.129 ± 0.144	8.441 ± 0.177	8.441 ± 0.177
	SGT-C	—	0.319 ± 0.048	0.523 ± 0.063	0.799 ± 0.046	0.995 ± 0.030	0.995 ± 0.030
	SGT$_3$-C	—	0.688 ± 0.048	2.559 ± 0.275	2.658 ± 0.305	1.765 ± 0.119	2.559 ± 0.275
	AxTAO	—	4.184 ± 0.028	8.124 ± 4.652	7.608 ± 0.738	33.022 ± 12.345	33.022 ± 12.345
	DPDT	—	**0.099 ± 0.006**	**0.096 ± 0.002**	**0.952 ± 0.225**	**3.289 ± 0.128**	*3.289 ± 0.128*
	SPLIT	—	*0.267 ± 0.003*	3.009 ± 0.936	*2.925 ± 0.568*	8.046 ± 2.917	8.046 ± 2.917
	SGT-T	—	1.878 ± 0.407	7.580 ± 6.658	6.044 ± 1.326	*7.649 ± 1.954*	7.649 ± 1.954
	SGT$_3$-T	—	3.240 ± 1.273	*2.730 ± 0.543*	15.882 ± 9.963	14.908 ± 8.775	**3.240 ± 1.273**
	CART	*0.023 ± 0.000*	*0.034 ± 0.000*	*0.044 ± 0.000*	*0.053 ± 0.000*	*0.062 ± 0.000*	*0.062 ± 0.000*
	HSTree	**0.021 ± 0.000**	**0.031 ± 0.001**	**0.040 ± 0.000**	**0.051 ± 0.002**	**0.060 ± 0.003**	**0.060 ± 0.003**
	SERDT	1.427 ± 0.002	2.177 ± 0.004	2.844 ± 0.008	3.491 ± 0.017	4.302 ± 0.013	4.302 ± 0.013
	SGT-C	0.464 ± 0.009	0.910 ± 0.010	1.540 ± 0.020	2.501 ± 0.018	3.879 ± 0.329	3.879 ± 0.329

eye-movements

	SGT$_3$-C	0.661 ± 0.015	2.216 ± 0.179	4.876 ± 0.325	6.152 ± 0.443	12.470 ± 0.314	12.470 ± 0.314
	AxTAO	**0.227 ± 0.004**	**0.748 ± 0.444**	**1.074 ± 0.358**	**2.180 ± 0.571**	**3.849 ± 0.049**	**3.849 ± 0.049**
	DPDT	*0.973 ± 0.018*	*3.191 ± 0.031*	*5.777 ± 0.023*	9.090 ± 0.044	*5.727 ± 0.943*	*5.727 ± 0.943*
	SPLIT	4.920 ± 1.249	7.691 ± 2.536	6.656 ± 1.058	*6.736 ± 0.976*	12.934 ± 1.627	6.736 ± 0.976
	SGT-T	2.330 ± 0.574	5.937 ± 1.198	12.002 ± 3.378	24.338 ± 4.959	54.067 ± 25.371	54.067 ± 25.371
	SGT$_3$-T	4.173 ± 0.033	12.936 ± 1.726	16.618 ± 5.723	32.929 ± 8.677	62.689 ± 18.553	62.689 ± 18.553
eye-state	CART	*0.015 ± 0.000*	*0.022 ± 0.000*	*0.028 ± 0.000*	*0.036 ± 0.000*	*0.044 ± 0.001*	*0.044 ± 0.001*
	HSTree	**0.014 ± 0.000**	**0.020 ± 0.000**	**0.026 ± 0.000**	**0.033 ± 0.000**	**0.040 ± 0.000**	**0.040 ± 0.000**
	SERDT	0.905 ± 0.036	1.318 ± 0.029	1.615 ± 0.033	2.047 ± 0.032	2.495 ± 0.071	2.495 ± 0.071
	SGT-C	0.339 ± 0.003	0.505 ± 0.002	0.678 ± 0.005	1.171 ± 0.005	2.087 ± 0.100	2.087 ± 0.100
	SGT$_3$-C	0.574 ± 0.007	1.063 ± 0.008	2.511 ± 0.133	4.777 ± 0.111	6.192 ± 0.148	6.192 ± 0.148
	AxTAO	**0.449 ± 0.081**	*1.122 ± 0.191*	*1.808 ± 0.049*	**2.954 ± 0.564**	*5.547 ± 1.728*	*5.547 ± 1.728*
	DPDT	0.773 ± 0.012	**0.485 ± 0.101**	**1.461 ± 0.005**	*3.796 ± 1.080*	**3.550 ± 0.032**	**3.550 ± 0.032**
	SPLIT	*0.465 ± 0.251*	2.575 ± 0.490	2.502 ± 0.443	112.005 ± 25.574	44.632 ± 11.038	44.632 ± 11.038
	SGT-T	2.187 ± 0.956	4.029 ± 0.029	9.571 ± 2.318	26.239 ± 6.816	38.509 ± 12.263	38.509 ± 12.263
	SGT$_3$-T	4.998 ± 1.079	14.493 ± 4.296	23.130 ± 0.825	37.413 ± 1.708	84.647 ± 14.679	84.647 ± 14.679
fault	CART	—	**0.012 ± 0.000**	**0.015 ± 0.000**	**0.018 ± 0.000**	**0.020 ± 0.000**	**0.020 ± 0.000**
	HSTree	—	**0.012 ± 0.000**	*0.016 ± 0.000*	*0.019 ± 0.000*	*0.021 ± 0.000*	*0.021 ± 0.000*
	SERDT	—	*0.455 ± 0.003*	0.605 ± 0.004	0.777 ± 0.004	0.958 ± 0.006	0.958 ± 0.006
	SGT-C	—	0.641 ± 0.032	1.044 ± 0.045	1.945 ± 0.153	2.599 ± 0.102	2.599 ± 0.102
	SGT$_3$-C	—	1.928 ± 0.047	2.356 ± 0.170	4.842 ± 0.093	5.925 ± 0.192	5.925 ± 0.192
	AxTAO	—	**0.282 ± 0.108**	*0.461 ± 0.082*	**0.624 ± 0.134**	**1.128 ± 0.190**	**1.128 ± 0.190**
	DPDT	—	*0.609 ± 0.001*	**0.332 ± 0.006**	*1.336 ± 0.010*	*1.217 ± 0.008*	*1.217 ± 0.008*
	SPLIT	—	9.265 ± 5.923	6.138 ± 0.328	9.549 ± 5.396	8.209 ± 0.269	8.209 ± 0.269
	SGT-T	—	4.148 ± 0.724	7.013 ± 1.576	12.704 ± 1.537	64.566 ± 1.261	64.566 ± 1.261
	SGT$_3$-T	—	5.172 ± 0.935	12.787 ± 0.413	10.829 ± 1.168	42.420 ± 8.558	42.420 ± 8.558
gas-drift	CART	—	*0.891 ± 0.005*	*1.149 ± 0.002*	*1.387 ± 0.013*	*1.569 ± 0.014*	*1.569 ± 0.014*
	HSTree	—	**0.763 ± 0.011**	**0.980 ± 0.003**	**1.217 ± 0.058**	**1.325 ± 0.004**	**1.325 ± 0.004**
	SERDT	—	29.884 ± 0.096	39.047 ± 0.190	48.294 ± 0.116	57.239 ± 0.289	57.239 ± 0.289
	SGT-C	—	7.714 ± 0.016	14.076 ± 0.137	17.205 ± 0.505	20.722 ± 0.314	20.722 ± 0.314
	SGT$_3$-C	—	35.316 ± 0.725	26.835 ± 0.653	40.630 ± 1.449	47.566 ± 0.873	47.566 ± 0.873
	AxTAO	—	**8.720 ± 1.664**	**13.863 ± 2.509**	**25.127 ± 6.892**	**34.319 ± 7.415**	**34.319 ± 7.415**
	DPDT	—	36.866 ± 0.395	*40.200 ± 0.063*	*29.836 ± 0.182*	*37.349 ± 0.300*	*37.349 ± 0.300*
	SPLIT	—	135.935 ± 4.754	120.914 ± 8.115	371.082 ± 39.808	141.962 ± 6.909	141.962 ± 6.909
	SGT-T	—	*30.638 ± 7.954*	43.388 ± 7.772	109.836 ± 24.944	89.735 ± 5.680	89.735 ± 5.680
	SGT$_3$-T	—	89.856 ± 31.211	101.685 ± 61.669	92.602 ± 9.560	257.699 ± 186.309	257.699 ± 186.309
higgs	CART	**0.045 ± 1.535**	**0.057 ± 1.134**	*0.076 ± 2.312*	**0.112 ± 2.103**	**0.127 ± 1.230**	**0.127 ± 1.230**
	HSTree	*37.872 ± 1.412*	*51.436 ± 2.121*	**71.554 ± 1.768**	*87.323 ± 1.203*	*111.087 ± 2.392*	*111.087 ± 2.392*
	SERDT	54.929 ± 2.123	60.801 ± 3.237	82.336 ± 2.899	107.199 ± 4.434	127.199 ± 5.187	127.199 ± 5.187
	SGT-C	38.987 ± 5.122	65.121 ± 5.102	84.432 ± 6.939	103.653 ± 7.729	124.762 ± 8.092	103.653 ± 7.729
	SGT$_3$-C	67.214 ± 4.032	75.952 ± 7.323	83.548 ± 7.122	111.954 ± 8.892	141.062 ± 9.321	187.612 ± 11.321
	AxTAO	*174.298 ± 12.321*	*296.307 ± 19.010*	**361.494 ± 21.210**	**448.253 ± 19.453**	**587.211 ± 20.227**	**587.211 ± 20.227**
	DPDT	**103.342 ± 9.101**	**270.478 ± 18.23**	*430.524 ± 24.434*	*499.492 ± 22.112*	*645.241 ± 29.110*	*645.241 ± 29.110*
	SPLIT	643.232 ± 29.211	764.445 ± 22.867	900.000 ± 0.000	900.000 ± 0.000	900.000 ± 0.000	900.000 ± 0.000
	SGT-T	299.308 ± 7.472	425.915 ± 12.825	563.486 ± 32.081	743.802 ± 24.001	900.000 ± 0.000	900.000 ± 0.000
	SGT$_3$-T	389.313 ± 22.072	476.130 ± 11.432	628.492 ± 34.403	900.000 ± 0.000	900.000 ± 0.000	900.000 ± 0.000
htru	CART	**0.026 ± 0.000**	**0.037 ± 0.001**	**0.049 ± 0.000**	**0.064 ± 0.004**	**0.058 ± 0.002**	**0.049 ± 0.000**
	HSTree	*0.027 ± 0.001*	*0.039 ± 0.001*	*0.050 ± 0.000*	*0.068 ± 0.007*	*0.059 ± 0.003*	*0.068 ± 0.007*
	SERDT	0.983 ± 0.030	1.504 ± 0.005	1.930 ± 0.006	2.340 ± 0.008	2.754 ± 0.103	1.930 ± 0.006
	SGT-C	0.328 ± 0.002	0.456 ± 0.004	0.646 ± 0.020	0.586 ± 0.065	0.561 ± 0.020	0.456 ± 0.004
	SGT$_3$-C	0.495 ± 0.003	0.763 ± 0.018	0.731 ± 0.100	0.996 ± 0.035	0.882 ± 0.119	0.731 ± 0.100
	AxTAO	**0.278 ± 0.084**	*0.430 ± 0.145*	*0.842 ± 0.122*	*1.275 ± 0.679*	*1.164 ± 0.626*	*1.164 ± 0.626*
	DPDT	*0.304 ± 0.079*	**0.054 ± 0.001**	**0.483 ± 0.044**	**0.051 ± 0.001**	**0.055 ± 0.001**	**0.483 ± 0.044**
	SPLIT	5.767 ± 3.391	0.757 ± 0.085	2.783 ± 0.315	9.423 ± 3.014	9.901 ± 2.383	9.901 ± 2.383
	SGT-T	1.516 ± 0.019	1.819 ± 0.601	5.049 ± 1.393	16.676 ± 10.774	17.290 ± 2.296	17.290 ± 2.296
	SGT$_3$-T	1.566 ± 0.341	1.352 ± 0.293	1.635 ± 0.351	1.586 ± 0.319	1.665 ± 0.335	1.352 ± 0.293
magic	CART	**0.023 ± 0.000**	**0.034 ± 0.001**	**0.044 ± 0.000**	**0.064 ± 0.001**	**0.074 ± 0.001**	**0.074 ± 0.001**
	HSTree	**0.023 ± 0.001**	**0.034 ± 0.000**	*0.045 ± 0.000*	**0.064 ± 0.000**	*0.075 ± 0.001*	*0.075 ± 0.001*
	SERDT	0.824 ± 0.001	1.239 ± 0.006	1.605 ± 0.004	2.078 ± 0.010	2.447 ± 0.007	2.447 ± 0.007
	SGT-C	*0.312 ± 0.000*	*0.477 ± 0.003*	0.689 ± 0.003	*1.071 ± 0.042*	1.876 ± 0.061	1.876 ± 0.061
	SGT$_3$-C	0.325 ± 0.006	0.948 ± 0.028	1.621 ± 0.135	2.710 ± 0.089	3.284 ± 0.353	2.710 ± 0.089
	AxTAO	*0.349 ± 0.081*	**0.502 ± 0.002**	**1.173 ± 0.036**	**2.349 ± 0.095**	**2.645 ± 0.151**	**2.645 ± 0.151**
	DPDT	**0.231 ± 0.059**	1.884 ± 0.007	*2.812 ± 0.004*	*8.062 ± 0.050*	*11.521 ± 0.121*	*11.521 ± 0.121*
	SPLIT	2.514 ± 0.667	*0.667 ± 0.047*	3.353 ± 1.291	240.554 ± 202.408	69.764 ± 29.671	69.764 ± 29.671
	SGT-T	1.687 ± 0.336	4.590 ± 1.273	7.290 ± 4.003	18.635 ± 7.555	38.378 ± 36.280	38.378 ± 36.280
	SGT$_3$-T	3.670 ± 0.536	9.933 ± 1.604	20.429 ± 2.513	27.240 ± 7.119	52.910 ± 15.146	52.910 ± 15.146
mini-boone	CART	*1.327 ± 0.003*	*2.377 ± 0.006*	*3.169 ± 0.001*	*3.292 ± 0.013*	*3.920 ± 0.012*	*3.920 ± 0.012*
	HSTree	**1.234 ± 0.010**	**2.112 ± 0.006**	**2.923 ± 0.260**	**2.987 ± 0.008**	**3.561 ± 0.015**	**3.561 ± 0.015**
	SERDT	59.664 ± 0.425	94.866 ± 0.362	121.947 ± 0.338	148.979 ± 0.959	146.750 ± 0.547	146.750 ± 0.547
	SGT-C	11.023 ± 0.078	12.995 ± 0.129	16.074 ± 0.116	20.609 ± 0.135	25.352 ± 0.062	25.352 ± 0.062
	SGT$_3$-C	13.670 ± 0.121	18.370 ± 0.194	20.669 ± 0.178	25.379 ± 1.723	66.695 ± 4.619	66.695 ± 4.619
	AxTAO	**3.156 ± 0.058**	**10.769 ± 1.910**	**19.074 ± 2.473**	**28.574 ± 3.315**	**36.061 ± 5.404**	**36.061 ± 5.404**

	DPDT	9.395 ± 1.738	148.946 ± 1.520	256.252 ± 1.234	*47.860 ± 0.151*	453.668 ± 4.310	453.668 ± 4.310
	SPLIT	*8.502 ± 0.052*	83.926 ± 33.161	188.186 ± 19.342	212.160 ± 16.792	152.526 ± 14.973	212.160 ± 16.792
	SGT-T	26.137 ± 5.566	*33.979 ± 2.929*	*53.121 ± 7.172*	66.677 ± 12.084	*148.090 ± 52.451*	*148.090 ± 52.451*
	SGT$_3$-T	63.035 ± 8.172	60.582 ± 45.599	71.228	125.311 ± 14.876	256.178 ± 7.425	256.178 ± 7.425
mushroom	CART	**0.007 ± 0.000**	**0.009 ± 0.000**	**0.010 ± 0.000**	**0.009 ± 0.000**	**0.009 ± 0.000**	**0.009 ± 0.000**
	HSTree	**0.007 ± 0.000**	**0.009 ± 0.000**	**0.010 ± 0.001**	**0.009 ± 0.000**	*0.010 ± 0.001*	**0.009 ± 0.000**
	SERDT	2.501 ± 0.030	3.648 ± 0.029	4.413 ± 0.083	5.367 ± 0.089	6.145 ± 0.225	6.145 ± 0.225
	SGT-C	*0.185 ± 0.003*	0.331 ± 0.008	0.399 ± 0.026	*0.327 ± 0.004*	0.330 ± 0.004	*0.327 ± 0.004*
	SGT$_3$-C	0.274 ± 0.003	*0.326 ± 0.005*	*0.392 ± 0.028*	0.395 ± 0.003	0.400 ± 0.002	0.392 ± 0.028
	AxTAO	1.110 ± 0.011	1.324 ± 0.549	1.471 ± 0.004	*1.463 ± 0.004*	3.212 ± 0.009	1.463 ± 0.004
	DPDT	*0.264 ± 0.015*	**0.742 ± 0.024**	1.504 ± 0.085	1.718 ± 0.176	**0.725 ± 0.029**	1.504 ± 0.085
	SPLIT	**0.123 ± 0.011**	1.065 ± 0.484	**1.123 ± 0.470**	**0.865 ± 0.241**	*0.895 ± 0.210*	**0.865 ± 0.241**
	SGT-T	0.557 ± 0.002	10.795 ± 0.073	1.596 ± 0.020	1.981 ± 0.212	2.027 ± 0.206	1.981 ± 0.212
	SGT$_3$-T	0.919 ± 0.007	*1.017 ± 0.021*	*1.462 ± 0.020*	1.490 ± 0.012	1.535 ± 0.019	*1.462 ± 0.020*
occupancy	CART	**0.012 ± 0.000**	**0.012 ± 0.000**	**0.012 ± 0.000**	**0.012 ± 0.000**	*0.025 ± 0.002*	*0.025 ± 0.002*
	HSTree	**0.012 ± 0.001**	*0.016 ± 0.000*	*0.018 ± 0.000*	*0.019 ± 0.001*	**0.017 ± 0.003**	**0.017 ± 0.003**
	SERDT	0.546 ± 0.011	0.801 ± 0.004	1.113 ± 0.055	1.254 ± 0.103	1.405 ± 0.154	1.113 ± 0.055
	SGT-C	*0.148 ± 0.002*	0.186 ± 0.003	0.176 ± 0.004	0.197 ± 0.006	0.405 ± 0.024	0.405 ± 0.024
	SGT$_3$-C	0.216 ± 0.002	0.222 ± 0.036	0.365 ± 0.015	0.511 ± 0.033	0.579 ± 0.068	0.365 ± 0.015
	AxTAO	*0.183 ± 0.001*	**0.098 ± 0.002**	**0.111 ± 0.009**	**1.085 ± 0.068**	**1.626 ± 0.475**	**1.626 ± 0.475**
	DPDT	**0.088 ± 0.001**	*1.757 ± 0.002*	*1.722 ± 0.300*	4.697 ± 0.181	5.932 ± 0.196	4.697 ± 0.181
	SPLIT	0.206 ± 0.019	4.228 ± 1.873	4.165 ± 1.847	*4.192 ± 1.823*	*4.248 ± 1.824*	*4.192 ± 1.823*
	SGT-T	0.541 ± 0.013	5.539 ± 4.348	2.112 ± 0.388	20.543 ± 11.216	27.321 ± 16.985	27.321 ± 16.985
	SGT$_3$-T	1.292 ± 0.249	2.159 ± 1.011	2.262 ± 0.160	14.579 ± 7.958	7.077 ± 7.276	7.077 ± 7.276
page	CART	—	**0.007 ± 0.000**	**0.012 ± 0.000**	**0.012 ± 0.000**	**0.014 ± 0.000**	**0.012 ± 0.000**
	HSTree	—	*0.008 ± 0.000*	*0.013 ± 0.000*	*0.013 ± 0.000*	*0.015 ± 0.000*	*0.013 ± 0.000*
	SERDT	—	0.335 ± 0.002	0.477 ± 0.018	0.589 ± 0.017	0.711 ± 0.022	0.711 ± 0.022
	SGT-C	—	0.263 ± 0.001	0.437 ± 0.022	0.696 ± 0.075	0.933 ± 0.015	0.696 ± 0.075
	SGT$_3$-C	—	0.817 ± 0.063	1.053 ± 0.122	1.318 ± 0.105	1.798 ± 0.142	1.318 ± 0.105
	AxTAO	—	**0.399 ± 0.096**	**0.347 ± 0.137**	*0.601 ± 0.143*	*0.976 ± 0.366*	*0.976 ± 0.366*
	DPDT	—	*0.905 ± 0.007*	*1.071 ± 0.017*	**0.315 ± 0.010**	**0.423 ± 0.015**	**0.423 ± 0.015**
	SPLIT	—	5.425 ± 2.155	8.316 ± 0.927	5.511 ± 1.992	9.737 ± 1.043	5.511 ± 1.992
	SGT-T	—	3.422 ± 1.302	4.174 ± 0.396	11.024 ± 9.302	24.833 ± 23.466	24.833 ± 23.466
	SGT$_3$-T	—	4.892 ± 0.064	9.753 ± 1.842	11.594 ± 8.558	23.490 ± 15.246	9.753 ± 1.842
pendigits	CART	—	—	*0.021 ± 0.000*	*0.027 ± 0.000*	*0.033 ± 0.000*	*0.033 ± 0.000*
	HSTree	—	—	**0.020 ± 0.000**	**0.025 ± 0.000**	**0.030 ± 0.000**	**0.030 ± 0.000**
	SERDT	—	—	2.127 ± 0.017	2.628 ± 0.032	3.216 ± 0.037	3.216 ± 0.037
	SGT-C	—	—	2.312 ± 0.020	3.443 ± 0.053	4.788 ± 0.033	4.788 ± 0.033
	SGT$_3$-C	—	—	4.421 ± 0.009	7.037 ± 0.124	8.468 ± 0.429	8.468 ± 0.429
	AxTAO	—	—	*1.653 ± 0.364*	**3.087 ± 1.128**	**4.157 ± 0.779**	**4.157 ± 0.779**
	DPDT	—	—	**0.811 ± 0.004**	*3.948 ± 0.021*	*9.062 ± 0.068*	*9.062 ± 0.068*
	SPLIT	—	—	28.828 ± 1.348	35.454 ± 1.105	48.427 ± 1.831	48.427 ± 1.831
	SGT-T	—	—	10.774 ± 1.335	18.070 ± 0.007	48.994 ± 24.878	48.994 ± 24.878
	SGT$_3$-T	—	—	32.178 ± 5.256	180.997 ± 9.845	282.237 ± 20.653	282.237 ± 20.653
raisin	CART	**0.002 ± 0.000**	**0.002 ± 0.000**	**0.003 ± 0.000**	**0.003 ± 0.000**	**0.003 ± 0.000**	**0.003 ± 0.000**
	HSTree	**0.002 ± 0.000**	*0.003 ± 0.000*	**0.003 ± 0.000**	**0.003 ± 0.000**	**0.003 ± 0.000**	**0.003 ± 0.000**
	SERDT	*0.038 ± 0.000*	0.058 ± 0.001	*0.080 ± 0.000*	*0.096 ± 0.002*	*0.106 ± 0.001*	*0.080 ± 0.000*
	SGT-C	0.137 ± 0.002	0.196 ± 0.011	0.263 ± 0.029	0.249 ± 0.034	0.317 ± 0.087	0.249 ± 0.034
	SGT$_3$-C	0.137 ± 0.001	0.241 ± 0.026	0.275 ± 0.037	0.129 ± 0.003	0.136 ± 0.002	0.241 ± 0.026
	AxTAO	*0.040 ± 0.018*	**0.071 ± 0.057**	**0.110 ± 0.052**	**0.098 ± 0.025**	**0.081 ± 0.038**	**0.110 ± 0.052**
	DPDT	**0.016 ± 0.000**	*0.276 ± 0.001*	*0.542 ± 0.048*	0.779 ± 0.064	1.060 ± 0.112	1.060 ± 0.112
	SPLIT	0.780 ± 0.394	0.613 ± 0.353	0.741 ± 0.303	*0.485 ± 0.144*	*0.115 ± 0.024*	*0.741 ± 0.303*
	SGT-T	0.764 ± 0.259	1.336 ± 0.303	2.336 ± 0.817	2.859 ± 0.880	2.654 ± 1.199	2.336 ± 0.817
	SGT$_3$-T	0.650 ± 0.260	1.859 ± 0.844	2.006 ± 0.631	2.078 ± 0.649	2.106 ± 0.676	1.859 ± 0.844
rice	CART	**0.005 ± 0.000**	**0.007 ± 0.000**	**0.008 ± 0.000**	*0.010 ± 0.000*	*0.012 ± 0.001*	*0.010 ± 0.000*
	HSTree	**0.005 ± 0.000**	**0.007 ± 0.000**	*0.009 ± 0.000*	**0.008 ± 0.000**	**0.009 ± 0.001**	**0.009 ± 0.000**
	SERDT	0.176 ± 0.021	0.255 ± 0.019	0.326 ± 0.002	0.414 ± 0.006	0.457 ± 0.002	0.326 ± 0.002
	SGT-C	*0.134 ± 0.002*	*0.239 ± 0.003*	0.337 ± 0.029	0.441 ± 0.062	0.541 ± 0.049	0.541 ± 0.049
	SGT$_3$-C	0.204 ± 0.002	0.311 ± 0.022	0.236 ± 0.018	0.232 ± 0.013	0.232 ± 0.017	0.204 ± 0.002
	AxTAO	**0.058 ± 0.023**	**0.065 ± 0.024**	*0.279 ± 0.033*	*0.354 ± 0.117*	*0.527 ± 0.114*	*0.527 ± 0.114*
	DPDT	*0.121 ± 0.021*	*0.182 ± 0.006*	**0.176 ± 0.005**	**0.049 ± 0.006**	**0.059 ± 0.006**	**0.182 ± 0.006**
	SPLIT	1.334 ± 0.386	0.648 ± 0.177	0.645 ± 0.167	0.644 ± 0.157	0.655 ± 0.148	1.334 ± 0.386
	SGT-T	0.550 ± 0.006	2.356 ± 1.251	5.808 ± 4.953	3.399 ± 0.706	7.415 ± 1.940	5.808 ± 4.953
	SGT$_3$-T	0.933 ± 0.349	6.232 ± 5.830	1.991 ± 0.849	2.316 ± 1.014	2.158 ± 0.941	1.991 ± 0.849
room	CART	**0.006 ± 0.000**	**0.008 ± 0.000**	**0.010 ± 0.001**	**0.010 ± 0.001**	**0.010 ± 0.001**	**0.010 ± 0.001**
	HSTree	*0.007 ± 0.000*	*0.009 ± 0.000*	*0.011 ± 0.001*	*0.011 ± 0.000*	*0.011 ± 0.001*	*0.011 ± 0.000*
	SERDT	0.541 ± 0.019	0.795 ± 0.005	1.069 ± 0.006	1.288 ± 0.009	1.546 ± 0.018	1.546 ± 0.018
	SGT-C	0.238 ± 0.004	0.535 ± 0.004	0.704 ± 0.027	0.770 ± 0.014	0.773 ± 0.012	0.773 ± 0.012
	SGT$_3$-C	0.478 ± 0.017	0.884 ± 0.053	0.938 ± 0.069	0.967 ± 0.075	0.932 ± 0.085	0.938 ± 0.069
	AxTAO	*0.308 ± 0.001*	**0.506 ± 0.002**	*0.871 ± 0.166*	**0.751 ± 0.260**	**0.804 ± 0.272**	**0.804 ± 0.272**
	DPDT	**0.084 ± 0.007**	0.738 ± 0.089	**0.578 ± 0.006**	*2.410 ± 0.044*	*1.021 ± 0.072*	*2.410 ± 0.044*
	SPLIT	0.327 ± 0.032	*0.614 ± 0.129*	5.658 ± 0.178	7.797 ± 0.979	6.261 ± 0.343	6.261 ± 0.343
	SGT-T	2.344 ± 0.318	3.408 ± 0.033	9.386 ± 5.627	6.525 ± 1.961	6.014 ± 2.769	6.014 ± 2.769

	SGT$_3$-T	1.972 ± 0.101	3.035 ± 0.150	3.632 ± 0.132	8.988 ± 4.116	12.089 ± 7.349	3.632 ± 0.132
segment	CART	—	**0.008 ± 0.000**	**0.010 ± 0.000**	**0.010 ± 0.000**	**0.011 ± 0.000**	**0.011 ± 0.000**
	HSTree	—	*0.009 ± 0.000*	**0.010 ± 0.000**	*0.011 ± 0.000*	*0.012 ± 0.000*	*0.012 ± 0.000*
	SERDT	—	0.346 ± 0.001	*0.442 ± 0.012*	0.504 ± 0.010	0.580 ± 0.018	0.580 ± 0.018
	SGT-C	—	0.410 ± 0.015	0.468 ± 0.016	0.844 ± 0.053	1.009 ± 0.109	1.009 ± 0.109
	SGT$_3$-C	—	0.545 ± 0.017	1.271 ± 0.084	1.234 ± 0.038	1.908 ± 0.096	1.234 ± 0.038
	AxTAO	—	**0.198 ± 0.094**	**0.524 ± 0.158**	*0.790 ± 0.207*	**0.732 ± 0.038**	**0.732 ± 0.038**
	DPDT	—	*0.329 ± 0.030*	*1.110 ± 0.011*	**0.516 ± 0.012**	*1.142 ± 0.064*	*1.142 ± 0.064*
	SPLIT	—	4.735 ± 1.463	4.778 ± 1.408	4.999 ± 1.451	5.115 ± 1.427	5.115 ± 1.427
	SGT-T	—	2.355 ± 0.157	4.999 ± 1.288	7.528 ± 1.169	7.641 ± 0.787	7.641 ± 0.787
	SGT$_3$-T	—	2.777 ± 0.930	7.510 ± 0.555	9.224 ± 2.099	19.645 ± 15.345	9.224 ± 2.099
skin	CART	**0.043 ± 0.001**	**0.059 ± 0.000**	**0.067 ± 0.001**	**0.081 ± 0.000**	**0.091 ± 0.000**	**0.091 ± 0.000**
	HSTree	*0.049 ± 0.001*	*0.064 ± 0.001*	*0.080 ± 0.001*	*0.090 ± 0.002*	*0.099 ± 0.001*	*0.099 ± 0.001*
	SERDT	2.930 ± 0.044	4.439 ± 0.101	5.699 ± 0.068	6.902 ± 0.101	8.007 ± 0.374	8.007 ± 0.374
	SGT-C	0.399 ± 0.009	0.520 ± 0.010	0.645 ± 0.008	0.776 ± 0.009	0.919 ± 0.018	0.919 ± 0.018
	SGT$_3$-C	0.398 ± 0.014	0.537 ± 0.009	0.717 ± 0.026	0.944 ± 0.013	1.117 ± 0.013	1.117 ± 0.013
	AxTAO	*3.356 ± 0.022*	10.456 ± 1.594	*20.172 ± 8.560*	*21.687 ± 6.169*	*62.218 ± 3.298*	*62.218 ± 3.298*
	DPDT	**2.691 ± 0.023**	**1.058 ± 0.011**	**13.309 ± 0.004**	**19.033 ± 0.066**	**20.969 ± 0.209**	**20.969 ± 0.209**
	SPLIT	82.441 ± 25.752	77.346 ± 23.421	96.253 ± 22.971	269.301 ± 47.638	86.591 ± 8.351	86.591 ± 8.351
	SGT-T	4.319 ± 1.118	*9.555 ± 0.206*	31.501 ± 0.513	41.956 ± 8.365	84.671 ± 0.898	84.671 ± 0.898
	SGT$_3$-T	9.801 ± 2.874	24.299 ± 10.724	83.188 ± 1.171	78.788 ± 26.254	176.502 ± 16.665	176.502 ± 16.665
wilt	CART	**0.005 ± 0.000**	**0.007 ± 0.000**	**0.008 ± 0.000**	**0.009 ± 0.001**	**0.008 ± 0.001**	**0.009 ± 0.001**
	HSTree	*0.006 ± 0.000*	**0.007 ± 0.000**	*0.009 ± 0.000*	*0.010 ± 0.001*	*0.010 ± 0.001*	*0.010 ± 0.001*
	SERDT	0.159 ± 0.019	0.212 ± 0.000	0.289 ± 0.002	0.368 ± 0.013	0.394 ± 0.022	0.368 ± 0.013
	SGT-C	0.127 ± 0.002	*0.169 ± 0.001*	0.252 ± 0.009	0.292 ± 0.033	0.316 ± 0.059	0.252 ± 0.009
	SGT$_3$-C	0.183 ± 0.006	0.242 ± 0.021	0.352 ± 0.024	0.251 ± 0.010	0.256 ± 0.009	0.242 ± 0.021
	AxTAO	*0.087 ± 0.028*	**0.128 ± 0.040**	**0.421 ± 0.125**	*0.584 ± 0.083*	**0.462 ± 0.117**	**0.584 ± 0.083**
	DPDT	**0.078 ± 0.008**	*0.239 ± 0.005*	*1.501 ± 0.011*	**0.134 ± 0.008**	*0.627 ± 0.035*	*0.627 ± 0.035*
	SPLIT	1.612 ± 0.771	0.761 ± 0.545	1.685 ± 0.718	1.898 ± 0.157	1.684 ± 0.100	1.898 ± 0.157
	SGT-T	0.894 ± 0.390	1.666 ± 0.538	2.890 ± 0.713	13.621 ± 10.497	4.850 ± 2.549	4.850 ± 2.549
	SGT$_3$-T	2.030 ± 0.609	2.338 ± 0.916	8.042 ± 6.568	10.688 ± 10.439	10.251 ± 10.054	10.688 ± 10.439

Table 7: Runtime (s ± std.) for all bivariate approaches separated into TDIDT and Non-Greedy approaches by dashed lines per dataset. Best approach is **bolded**, second-best is *italicized*.

dataset	model	2	3	4	5	6	Best
adult	BiCART	161.982 ± 4.528	230.208 ± 2.447	208.602 ± 2.611	164.421 ± 1.459	244.966 ± 6.894	244.966 ± 6.894
	S^{2}GT-C	**0.914 ± 0.023**	**1.466 ± 0.018**	**1.785 ± 0.013**	**2.138 ± 0.251**	**2.883 ± 0.237**	**2.883 ± 0.237**
	S^{2}GT$_3$-C	*1.018 ± 0.011*	*2.766 ± 0.069*	*5.652 ± 0.187*	*9.798 ± 0.353*	*9.137 ± 0.356*	*9.137 ± 0.356*
	BiTAO	519.138 ± 9.067	660.103 ± 10.453	835.272 ± 438.190	676.755 ± 254.419	715.373 ± 277.318	676.755 ± 254.419
	S^{2}GT-T	**3.048 ± 0.475**	**5.817 ± 0.526**	**10.216 ± 0.996**	**8.596 ± 0.906**	**29.082 ± 19.674**	**8.596 ± 0.906**
	S^{2}GT$_3$-T	*8.479 ± 1.166*	*16.804 ± 3.316*	*28.323 ± 7.263*	*58.823 ± 7.955*	*227.868 ± 25.558*	*58.823 ± 7.955*
avila	BiCART	—	—	**3.605 ± 0.016**	**2.272 ± 0.004**	**2.646 ± 0.010**	**2.646 ± 0.010**
	S^{2}GT-C	—	—	*4.248 ± 0.131*	*5.380 ± 0.214*	*6.402 ± 0.171*	*6.402 ± 0.171*
	S^{2}GT$_3$-C	—	—	9.139 ± 0.178	10.774 ± 0.165	9.608 ± 0.245	9.608 ± 0.245
	BiTAO	—	—	**8.205 ± 0.404**	**13.076 ± 1.953**	*27.271 ± 4.852*	*27.271 ± 4.852*
	S^{2}GT-T	—	—	*16.503 ± 11.068*	*18.244 ± 2.260*	**23.580 ± 1.872**	**23.580 ± 1.872**
	S^{2}GT$_3$-T	—	—	19.400 ± 0.481	22.246 ± 4.050	32.641 ± 0.356	32.641 ± 0.356
bank	BiCART	**0.011 ± 0.000**	**0.015 ± 0.001**	**0.010 ± 0.001**	**0.011 ± 0.001**	**0.011 ± 0.001**	**0.010 ± 0.001**
	S^{2}GT-C	*0.132 ± 0.001*	*0.144 ± 0.012*	*0.149 ± 0.009*	*0.142 ± 0.011*	*0.141 ± 0.009*	*0.132 ± 0.001*
	S^{2}GT$_3$-C	0.170 ± 0.008	0.212 ± 0.017	0.209 ± 0.021	0.213 ± 0.016	0.214 ± 0.020	0.170 ± 0.008
	BiTAO	**0.437 ± 0.170**	**0.539 ± 0.056**	1.560 ± 0.410	1.577 ± 0.412	1.538 ± 0.364	1.560 ± 0.410
	S^{2}GT-T	0.680 ± 0.034	*0.546 ± 0.137*	**0.531 ± 0.176**	**0.515 ± 0.152**	**0.476 ± 0.159**	**0.546 ± 0.137**
	S^{2}GT$_3$-T	*0.635 ± 0.277*	0.718 ± 0.202	*0.860 ± 0.271*	*0.877 ± 0.259*	*1.106 ± 0.353*	*0.635 ± 0.277*
bean	BiCART	—	*5.241 ± 0.034*	*4.492 ± 0.016*	**5.400 ± 0.063**	**6.030 ± 0.085**	**6.030 ± 0.085**
	S^{2}GT-C	—	**4.264 ± 0.059**	**4.134 ± 0.057**	*5.789 ± 0.114*	7.849 ± 0.426	*7.849 ± 0.426*
	S^{2}GT$_3$-C	—	6.099 ± 0.066	9.546 ± 0.254	9.039 ± 0.777	*6.448 ± 0.122*	9.546 ± 0.254
	BiTAO	—	*13.466 ± 0.089*	*17.550 ± 3.502*	**21.262 ± 4.176**	**17.836 ± 5.087**	**17.836 ± 5.087**
	S^{2}GT-T	—	**10.078 ± 0.063**	**14.549 ± 2.278**	*35.814 ± 17.026*	49.716 ± 23.694	49.716 ± 23.694
	S^{2}GT$_3$-T	—	25.607 ± 0.510	28.688 ± 5.987	45.855 ± 0.793	*36.229 ± 4.994*	*45.855 ± 0.793*
bidding	BiCART	**0.122 ± 0.000**	**0.226 ± 0.004**	**0.087 ± 0.000**	**0.088 ± 0.000**	**0.087 ± 0.001**	**0.087 ± 0.000**
	S^{2}GT-C	*0.379 ± 0.062*	*0.420 ± 0.076*	*0.453 ± 0.089*	*0.444 ± 0.084*	*0.444 ± 0.085*	*0.420 ± 0.076*
	S^{2}GT$_3$-C	0.520 ± 0.007	0.631 ± 0.043	0.643 ± 0.040	0.641 ± 0.041	0.634 ± 0.045	0.520 ± 0.007
	BiTAO	**0.455 ± 0.155**	2.854 ± 1.296	**0.881 ± 0.103**	**0.968 ± 0.127**	**0.956 ± 0.122**	**0.881 ± 0.103**
	S^{2}GT-T	*3.742 ± 2.479*	*1.552 ± 0.201*	1.886 ± 0.069	2.064 ± 0.305	2.151 ± 0.424	1.552 ± 0.201
	S^{2}GT$_3$-T	3.784 ± 2.417	**1.336 ± 0.026**	*1.449 ± 0.033*	*1.363 ± 0.031*	*1.847 ± 0.070*	*1.336 ± 0.026*
electricity	BiCART	**1.710 ± 0.013**	**2.459 ± 0.015**	*4.716 ± 0.011*	**4.399 ± 0.060**	**4.468 ± 0.027**	**4.468 ± 0.027**

	S^{2}GT-C	*1.751 ± 0.020*	*3.068 ± 0.041*	**3.943 ± 0.022**	*6.214 ± 0.068*	*7.709 ± 0.056*	*7.709 ± 0.056*
	S^{2}GT$_3$-C	2.077 ± 0.024	4.083 ± 0.066	6.865 ± 0.109	13.089 ± 0.404	16.725 ± 0.356	16.725 ± 0.356
	BiTAO	**3.090 ± 0.013**	**5.217 ± 0.982**	**19.134 ± 2.517**	**25.496 ± 15.712**	**23.716 ± 5.873**	**23.716 ± 5.873**
	S^{2}GT-T	*4.900 ± 0.901*	*13.187 ± 2.958*	*26.192 ± 8.955*	*35.407 ± 5.905*	*64.266 ± 27.552*	*64.266 ± 27.552*
	S^{2}GT$_3$-T	16.278 ± 1.949	29.913 ± 8.363	38.181 ± 0.606	58.046 ± 15.761	186.041 ± 81.833	186.041 ± 81.833
	BiCART	*2.343 ± 0.006*	*5.074 ± 0.073*	*6.529 ± 0.029*	**5.365 ± 0.003**	**6.213 ± 0.023**	**6.213 ± 0.023**
	S^{2}GT-C	**1.882 ± 0.068**	**3.410 ± 0.018**	**5.833 ± 0.091**	*9.208 ± 0.331*	*14.078 ± 0.496*	*14.078 ± 0.496*
eye-movements	S^{2}GT$_3$-C	2.973 ± 0.024	6.749 ± 0.222	14.320 ± 0.381	23.759 ± 3.123	41.232 ± 2.209	41.232 ± 2.209
	BiTAO	**5.639 ± 1.477**	**10.443 ± 1.853**	**12.694 ± 3.756**	**25.351 ± 15.615**	**30.017 ± 7.258**	**30.017 ± 7.258**
	S^{2}GT-T	*5.723 ± 0.934*	*13.424 ± 2.150*	*20.808 ± 2.432*	*40.531 ± 6.476*	70.415 ± 28.127	70.415 ± 28.127
	S^{2}GT$_3$-T	13.826 ± 1.436	31.005 ± 7.743	30.284 ± 4.121	55.390 ± 7.432	*69.564 ± 6.342*	*31.005 ± 7.743*
	BiCART	*1.575 ± 0.018*	**2.290 ± 0.085**	**3.017 ± 0.008**	**2.397 ± 0.016**	**1.431 ± 0.008**	**1.431 ± 0.008**
	S^{2}GT-C	**1.428 ± 0.009**	*2.650 ± 0.068*	*4.042 ± 0.019*	*6.192 ± 0.074*	*5.843 ± 0.092*	*5.843 ± 0.092*
eye-state	S^{2}GT$_3$-C	1.998 ± 0.009	3.895 ± 0.009	6.083 ± 0.386	7.614 ± 0.383	14.603 ± 0.709	7.614 ± 0.383
	BiTAO	*5.084 ± 0.763*	**6.086 ± 0.920**	**15.055 ± 3.777**	**16.758 ± 3.696**	**17.236 ± 4.397**	**17.236 ± 4.397**
	S^{2}GT-T	**4.785 ± 1.786**	*10.767 ± 5.110*	*20.799 ± 3.613*	*25.682 ± 10.657*	*39.077 ± 5.903*	*39.077 ± 5.903*
	S^{2}GT$_3$-T	10.356 ± 2.611	13.256 ± 0.249	36.587 ± 3.486	84.161 ± 64.111	83.416 ± 22.508	83.416 ± 22.508
	BiCART	—	**0.671 ± 0.004**	**0.858 ± 0.020**	**1.056 ± 0.021**	**2.960 ± 0.041**	**2.960 ± 0.041**
	S^{2}GT-C	—	*1.612 ± 0.073*	*3.789 ± 0.147*	*4.264 ± 0.128*	*3.640 ± 0.253*	*3.640 ± 0.253*
fault	S^{2}GT$_3$-C	—	2.670 ± 0.381	5.217 ± 0.624	4.927 ± 0.401	15.148 ± 1.188	4.927 ± 0.401
	BiTAO	—	27.657 ± 8.662	63.598 ± 13.320	37.251 ± 2.027	**9.754 ± 3.397**	**9.754 ± 3.397**
	S^{2}GT-T	—	**6.341 ± 1.211**	*11.313 ± 7.714*	**11.403 ± 3.118**	*18.722 ± 1.558*	*11.403 ± 3.118*
	S^{2}GT$_3$-T	—	*9.007 ± 1.816*	**7.998 ± 0.319**	*17.878 ± 0.855*	28.492 ± 5.414	17.878 ± 0.855
	BiCART	—	306.141 ± 1.082	549.345 ± 1.295	595.498 ± 2.316	687.982 ± 21.935	687.982 ± 21.935
	S^{2}GT-C	—	**63.441 ± 2.416**	**85.418 ± 5.980**	**89.618 ± 1.188**	**107.478 ± 2.900**	**107.478 ± 2.900**
gas-drift	S^{2}GT$_3$-C	—	*69.479 ± 0.213*	*177.539 ± 4.145*	*100.374 ± 2.373*	*110.818 ± 1.290*	*110.818 ± 1.290*
	BiTAO	—	383.562 ± 93.594	1327.892 ± 366.219	582.853 ± 87.410	1090.152 ± 121.334	1090.152 ± 121.334
	S^{2}GT-T	—	**202.147 ± 53.643**	**192.221 ± 68.401**	**208.110 ± 44.917**	**186.536 ± 20.301**	**186.536 ± 20.301**
	S^{2}GT$_3$-T	—	*212.746 ± 133.915*	*202.622 ± 15.431*	*249.498 ± 18.637*	*253.412 ± 18.672*	*202.622 ± 15.431*
	BiCART	**0.465 ± 0.000**	**0.691 ± 0.008**	**1.050 ± 0.065**	**1.035 ± 0.115**	**1.175 ± 0.210**	**1.175 ± 0.210**
	S^{2}GT-C	*1.375 ± 0.019*	1.614 ± 0.023	*1.867 ± 0.009*	*1.838 ± 0.239*	3.212 ± 0.266	1.867 ± 0.009
htru	S^{2}GT$_3$-C	1.706 ± 0.039	*1.496 ± 0.091*	2.098 ± 0.188	2.490 ± 0.329	*2.681 ± 0.201*	*1.496 ± 0.091*
	BiTAO	**0.490 ± 0.004**	*4.274 ± 0.386*	*7.087 ± 2.078*	**3.572 ± 0.883**	**6.305 ± 0.846**	*6.305 ± 0.846*
	S^{2}GT-T	*1.559 ± 0.254*	**3.521 ± 0.623**	**4.992 ± 0.509**	11.568 ± 2.664	*12.452 ± 3.665*	**3.521 ± 0.623**
	S^{2}GT$_3$-T	3.907 ± 1.259	4.842 ± 1.006	7.089 ± 1.676	*9.252 ± 1.575*	13.567 ± 1.836	9.252 ± 1.575
	BiCART	**0.532 ± 0.003**	**0.761 ± 0.004**	**0.986 ± 0.004**	**1.214 ± 0.005**	**1.399 ± 0.007**	**1.214 ± 0.005**
	S^{2}GT-C	*1.222 ± 0.006*	*2.023 ± 0.016*	*2.579 ± 0.042*	*3.417 ± 0.036*	*5.149 ± 0.293*	*3.417 ± 0.036*
magic	S^{2}GT$_3$-C	1.853 ± 0.015	2.336 ± 0.033	3.632 ± 0.243	5.462 ± 0.175	6.613 ± 0.503	3.632 ± 0.243
	BiTAO	**2.312 ± 1.436**	*7.309 ± 1.476*	**5.492 ± 2.836**	**11.394 ± 1.136**	**12.020 ± 6.460**	**12.020 ± 6.460**
	S^{2}GT-T	*3.670 ± 0.175*	**6.565 ± 2.845**	*8.800 ± 1.447*	*19.018 ± 4.394*	*22.002 ± 2.200*	*19.018 ± 4.394*
	S^{2}GT$_3$-T	6.552 ± 0.972	11.303 ± 3.233	28.370 ± 18.524	64.631 ± 32.421	49.323 ± 4.491	64.631 ± 32.421
	BiCART	205.993 ± 1.017	283.306 ± 3.623	421.122 ± 6.973	585.503 ± 2.113	685.981 ± 1.666	685.981 ± 1.666
	S^{2}GT-C	*87.626 ± 0.976*	**87.751 ± 0.520**	**105.152 ± 0.643**	**135.392 ± 4.667**	**196.851 ± 0.727**	**196.851 ± 0.727**
mini-boone	S^{2}GT$_3$-C	**77.147 ± 0.087**	*131.214 ± 0.526*	*184.391 ± 2.667*	*182.661 ± 4.632*	*275.842 ± 1.822*	*275.842 ± 1.822*
	BiTAO	*513.002 ± 218.327*	695.079 ± 137.696	1580.557 ± 159.385	746.081 ± 90.647	692.239 ± 108.287	692.239 ± 108.287
	S^{2}GT-T	**255.640 ± 60.646**	**240.491 ± 36.959**	**249.069 ± 31.002**	**364.934 ± 26.289**	**254.313 ± 11.954**	**254.313 ± 11.954**
	S^{2}GT$_3$-T	547.680 ± 454.771	*674.206 ± 232.831*	*268.206 ± 40.527*	*375.451 ± 48.913*	*659.697 ± 88.394*	*659.697 ± 88.394*
	BiCART	9.876 ± 0.035	11.360 ± 0.076	11.661 ± 0.285	11.900 ± 0.104	11.424 ± 0.047	11.360 ± 0.076
	S^{2}GT-C	**0.450 ± 0.004**	**0.574 ± 0.058**	**0.574 ± 0.060**	**0.573 ± 0.060**	**0.567 ± 0.054**	**0.574 ± 0.058**
mushroom	S^{2}GT$_3$-C	*0.674 ± 0.002*	*0.677 ± 0.008*	*0.676 ± 0.010*	*0.671 ± 0.003*	*0.664 ± 0.007*	*0.674 ± 0.002*
	BiTAO	23.650 ± 0.082	32.016 ± 0.068	31.680 ± 0.114	31.644 ± 0.217	30.900 ± 0.695	32.016 ± 0.068
	S^{2}GT-T	**0.903 ± 0.051**	**1.237 ± 0.153**	**1.257 ± 0.165**	**1.254 ± 0.178**	**1.228 ± 0.168**	**1.237 ± 0.153**
	S^{2}GT$_3$-T	*1.725 ± 0.026*	*1.708 ± 0.009*	*1.700 ± 0.012*	*1.717 ± 0.039*	*1.708 ± 0.034*	*1.725 ± 0.026*
	BiCART	**0.165 ± 0.002**	**0.236 ± 0.002**	**0.242 ± 0.027**	**0.396 ± 0.011**	**0.181 ± 0.002**	**0.181 ± 0.002**
	S^{2}GT-C	*0.653 ± 0.025*	0.939 ± 0.061	*0.744 ± 0.021*	*0.590 ± 0.050*	*0.585 ± 0.052*	0.939 ± 0.061
occupancy	S^{2}GT$_3$-C	0.739 ± 0.014	*0.680 ± 0.002*	0.991 ± 0.057	1.741 ± 0.049	1.879 ± 0.047	*0.739 ± 0.014*
	BiTAO	**0.358 ± 0.007**	**0.592 ± 0.279**	**0.966 ± 0.297**	**2.024 ± 1.027**	**2.756 ± 1.003**	**2.756 ± 1.003**
	S^{2}GT-T	*2.334 ± 0.224*	3.354 ± 1.055	10.974 ± 7.008	8.160 ± 1.116	8.196 ± 1.756	8.196 ± 1.756
	S^{2}GT$_3$-T	3.550 ± 0.639	*3.333 ± 1.181*	*4.591 ± 1.160*	*3.789 ± 1.850*	*3.924 ± 2.057*	*3.550 ± 0.639*
	BiCART	—	**0.136 ± 0.001**	**0.265 ± 0.002**	**0.568 ± 0.048**	**0.624 ± 0.088**	**0.624 ± 0.088**
	S^{2}GT-C	—	*0.647 ± 0.005*	1.219 ± 0.055	1.820 ± 0.025	1.951 ± 0.072	1.219 ± 0.055
page	S^{2}GT$_3$-C	—	1.553 ± 0.106	*0.974 ± 0.004*	*1.120 ± 0.110*	*1.441 ± 0.129*	*0.974 ± 0.004*
	BiTAO	—	**2.071 ± 0.330**	**2.233 ± 0.756**	**2.252 ± 0.853**	**3.958 ± 2.572**	*3.958 ± 2.572*
	S^{2}GT-T	—	*3.085 ± 0.805*	*8.576 ± 8.214*	13.182 ± 11.022	*6.672 ± 1.158*	**3.085 ± 0.805**
	S^{2}GT$_3$-T	—	6.055 ± 1.312	10.564 ± 2.250	*10.963 ± 1.690*	15.098 ± 2.583	10.564 ± 2.250

pendigits	BiCART	—	—	**3.703 ± 0.029**	**4.409 ± 0.038**	**4.979 ± 0.132**	**4.979 ± 0.132**
	S^{2}GT-C	—	—	*5.447 ± 0.137*	*5.681 ± 0.077*	*5.999 ± 0.100*	*5.999 ± 0.100*
	S^{2}GT$_3$-C	—	—	13.424 ± 0.194	11.251 ± 0.546	16.132 ± 0.661	11.251 ± 0.546
	BiTAO	—	—	**16.041 ± 1.840**	*27.429 ± 2.592*	**39.368 ± 6.442**	**39.368 ± 6.442**
	S^{2}GT-T	—	—	*21.442 ± 11.148*	**20.195 ± 3.336**	*41.947 ± 12.994*	*41.947 ± 12.994*
	S^{2}GT$_3$-T	—	—	31.893 ± 6.406	163.337 ± 7.436	56.912 ± 9.267	56.912 ± 9.267
raisin	BiCART	**0.019 ± 0.000**	**0.037 ± 0.001**	**0.041 ± 0.001**	**0.030 ± 0.001**	**0.041 ± 0.001**	**0.037 ± 0.001**
	S^{2}GT-C	*0.180 ± 0.001*	*0.329 ± 0.003*	0.465 ± 0.014	0.520 ± 0.028	0.560 ± 0.063	0.329 ± 0.003
	S^{2}GT$_3$-C	0.269 ± 0.001	0.388 ± 0.064	*0.391 ± 0.061*	*0.382 ± 0.063*	*0.381 ± 0.055*	*0.269 ± 0.001*
	BiTAO	**0.285 ± 0.219**	**0.635 ± 0.211**	**0.471 ± 0.088**	**0.480 ± 0.092**	1.322 ± 0.369	*0.635 ± 0.211*
	S^{2}GT-T	*0.509 ± 0.154*	1.571 ± 0.680	*0.992 ± 0.376*	1.216 ± 0.535	**1.137 ± 0.567**	**0.509 ± 0.154**
	S^{2}GT$_3$-T	0.727 ± 0.285	*0.932 ± 0.477*	1.159 ± 0.605	*0.948 ± 0.491*	*1.317 ± 0.714*	0.727 ± 0.285
rice	BiCART	**0.117 ± 0.000**	**0.168 ± 0.001**	**0.213 ± 0.006**	**0.236 ± 0.004**	**0.169 ± 0.002**	**0.236 ± 0.004**
	S^{2}GT-C	*0.317 ± 0.006*	*0.468 ± 0.008*	*0.715 ± 0.060*	1.082 ± 0.077	1.335 ± 0.025	*0.317 ± 0.006*
	S^{2}GT$_3$-C	0.359 ± 0.002	0.804 ± 0.007	0.815 ± 0.074	*0.839 ± 0.083*	*0.841 ± 0.079*	0.359 ± 0.002
	BiTAO	**0.391 ± 0.001**	**0.595 ± 0.363**	**1.089 ± 0.348**	**1.103 ± 0.452**	**0.897 ± 0.303**	**1.103 ± 0.452**
	S^{2}GT-T	*0.728 ± 0.013*	*1.912 ± 0.823*	5.103 ± 3.741	4.694 ± 1.198	*2.002 ± 0.473*	*1.912 ± 0.823*
	S^{2}GT$_3$-T	1.425 ± 0.322	3.249 ± 3.737	*3.242 ± 3.695*	*3.186 ± 3.657*	3.047 ± 3.429	3.249 ± 3.737
room	BiCART	**0.245 ± 0.002**	**0.329 ± 0.001**	**0.354 ± 0.007**	**0.371 ± 0.006**	**1.095 ± 0.039**	**0.354 ± 0.007**
	S^{2}GT-C	*0.529 ± 0.010*	*1.018 ± 0.131*	*1.145 ± 0.033*	1.299 ± 0.073	*1.278 ± 0.065*	*1.145 ± 0.033*
	S^{2}GT$_3$-C	0.802 ± 0.016	1.259 ± 0.076	1.284 ± 0.063	*1.274 ± 0.061*	1.286 ± 0.068	1.259 ± 0.076
	BiTAO	4.212 ± 0.520	*2.872 ± 0.386*	**1.356 ± 0.090**	*5.522 ± 0.832*	**3.008 ± 1.874**	5.522 ± 0.832
	S^{2}GT-T	*2.757 ± 0.664*	**2.666 ± 0.581**	*3.444 ± 0.002*	**4.148 ± 1.386**	*4.337 ± 0.795*	*3.444 ± 0.002*
	S^{2}GT$_3$-T	**2.726 ± 0.176**	2.930 ± 0.463	6.014 ± 4.492	9.987 ± 7.450	13.029 ± 9.741	**2.726 ± 0.176**
segment	BiCART	—	**0.713 ± 0.018**	**0.856 ± 0.008**	**0.928 ± 0.034**	**0.986 ± 0.050**	**0.986 ± 0.050**
	S^{2}GT-C	—	*1.404 ± 0.020*	*1.555 ± 0.106*	*2.007 ± 0.044*	*2.454 ± 0.174*	*2.454 ± 0.174*
	S^{2}GT$_3$-C	—	2.722 ± 0.065	3.512 ± 0.235	3.526 ± 0.332	3.515 ± 0.317	3.512 ± 0.235
	BiTAO	—	*3.508 ± 1.662*	**2.871 ± 1.091**	**4.486 ± 1.403**	**5.786 ± 0.956**	**5.786 ± 0.956**
	S^{2}GT-T	—	**3.402 ± 0.607**	*4.658 ± 0.903*	6.702 ± 1.683	*6.846 ± 0.676*	6.702 ± 1.683
	S^{2}GT$_3$-T	—	6.858 ± 1.575	5.228 ± 0.796	*6.383 ± 1.162*	8.472 ± 1.177	*6.383 ± 1.162*
skin	BiCART	**0.550 ± 0.004**	**0.778 ± 0.010**	**0.837 ± 0.012**	**0.300 ± 0.005**	**0.840 ± 0.010**	**0.840 ± 0.010**
	S^{2}GT-C	1.529 ± 0.086	*1.572 ± 0.126*	2.164 ± 0.047	2.281 ± 0.059	2.371 ± 0.097	2.371 ± 0.097
	S^{2}GT$_3$-C	*1.244 ± 0.173*	1.668 ± 0.109	*1.843 ± 0.028*	*1.975 ± 0.152*	*1.716 ± 0.089*	*1.716 ± 0.089*
	BiTAO	**1.343 ± 0.007**	**2.537 ± 0.034**	**4.490 ± 0.230**	**4.175 ± 1.884**	*24.620 ± 4.906*	24.620 ± 4.906
	S^{2}GT-T	*3.948 ± 0.217*	10.320 ± 4.136	6.232 ± 0.635	*7.273 ± 0.468*	**6.485 ± 1.392**	*7.273 ± 0.468*
	S^{2}GT$_3$-T	4.443 ± 0.053	*6.694 ± 0.465*	*5.812 ± 1.213*	39.704 ± 31.111	54.114 ± 41.059	**5.812 ± 1.213**
wilt	BiCART	**0.061 ± 0.001**	**0.064 ± 0.001**	**0.066 ± 0.001**	**0.066 ± 0.001**	**0.079 ± 0.002**	**0.079 ± 0.002**
	S^{2}GT-C	*0.280 ± 0.003*	*0.366 ± 0.019*	*0.479 ± 0.028*	*0.401 ± 0.027*	*0.396 ± 0.034*	*0.280 ± 0.003*
	S^{2}GT$_3$-C	0.313 ± 0.007	0.480 ± 0.020	0.595 ± 0.057	0.672 ± 0.038	0.680 ± 0.035	0.480 ± 0.020
	BiTAO	**0.413 ± 0.122**	**0.432 ± 0.164**	**0.376 ± 0.109**	*0.764 ± 0.213*	**0.768 ± 0.209**	**0.413 ± 0.122**
	S^{2}GT-T	*0.781 ± 0.193*	0.867 ± 0.197	1.424 ± 0.627	1.501 ± 0.732	1.373 ± 0.615	0.781 ± 0.193
	S^{2}GT$_3$-T	0.825 ± 0.293	*0.678 ± 0.174*	*0.940 ± 0.358*	**0.762 ± 0.272**	*1.056 ± 0.434*	*0.678 ± 0.174*

G.2.2 Optimization Procedure Ablation

In this section, we examine our bin-to-branch optimization procedure. Here, we provide two ablations: removing the coordinate descent procedure and only replying on Weighted K-Means to assign bins to branches (denoted as “No CD”) and replacing the Weighted K-Means initialization with a random initialization (denoted as “No WKM”). For these experiments, we work with a subset of our datasets - Electricity, Eye-Movements, and Eye-State. We run hyperparameter tuning for both ablations and choose the model with the lowest validation loss for each depth. We report the average test accuracy for the ablated TDIDT approaches in Table 8 and provide the runtimes for these approaches in Table 9. In these tables, “All” denotes using the full optimization procedure. In general, we observe that both ablations consistently achieve lower test accuracy than the full models across most depths and tested datasets, especially at depths above two, with a minimal sacrifice in runtime.

Table 8: Test Accuracy (% ± std.) results for the optimization ablation analysis. Best approach for each model and dataset is **bolded**.

	Model	2	3	4	5	6	Overall
ShapeCART							
electricity	All	**75.5±0.1**	**78.5±0.4**	**81.3±0.8**	**84.4±0.1**	**84.8±0.6**	**84.8±0.6**
	No CD	74.9±0.2	76.5±0.3	79.6±0.5	83.7±1.2	83.4±0.2	83.4±0.2
	No WKM	74.9±0.2	76.5±0.3	79.4±0.1	83.2±0.4	83.3±0.5	83.3±0.5
eye-movements	All	**48.1±2.1**	**53±0.7**	**54.9±1.2**	**53.9±0.7**	**57.4±1.2**	**57.4±1.2**
	No CD	47.1±3.3	52.5±1.3	52.4±2.7	47.4±1.6	51±0.5	51±0.5
	No WKM	47.3±1.2	51.8±1	51.5±0.7	47.2±0.8	50.1±1.3	50.1±1.3
eye-state	All	64.3±0.9	**69±0.2**	**70.5±1.2**	**72.4±1.3**	**74.5±1.1**	**74.5±1.1**
	No CD	62.5±0.3	68.6±0.9	70.3±1	71.9±0.9	73.7±0.7	73.7±0.7
	No WKM	**64.4±1.2**	68.5±1	**70.5±1.2**	**72.4±1.3**	**74.5±1.1**	**74.5±1.1**
ShapeCART$_3$							
electricity	All	**76.5±0.3**	**80.6±0.6**	**84±1.2**	**86±0.4**	87.8±1	87.8±1
	No CD	73.5±1.2	78.5±0.3	82.3±0.1	85.7±0.3	88±0.5	88±0.5
	No WKM	73±0.4	78.1±0.3	82±0.4	84.8±0.5	**88.3±0.3**	**88.3±0.3**
eye-movements	All	**47.1±0.5**	54.4±0.8	56±0.3	**57.5±1.6**	**60.9±2.6**	**60.9±2.6**
	No CD	46±0.5	54.8±1.4	56.1±1.4	54.4±1.7	56.5±3	56.5±3
	No WKM	45.6±0.4	**55.3±1.9**	**56.2±2.3**	56±1.2	57.2±1.9	57.2±1.9
eye-state	All	**66.1±0.7**	**70.8±1.4**	73.3±1	76.8±1.3	77.5±0.5	77.5±0.5
	No CD	64.6±0.3	69.3±1	**73.7±1.5**	**78.4±0.1**	76.7±0.5	76.7±0.5
	No WKM	65.1±0.8	70.7±1.1	73±1	77.5±1.3	**77.7±0.2**	**77.7±0.2**
Shape^{2}CART							
electricity	All	**80.6±0.6**	**82±0.6**	**83.9±0.3**	**86.5±1.2**	**87.5±0.5**	**87.5±0.5**
	No CD	78.3±0.4	77.4±0.7	79.8±0.5	84.8±0.5	86.3±0.3	86.3±0.3
	No WKM	78.5±0.6	77.4±0.2	79.8±1	84.2±1	85.7±0.4	85.7±0.4
eye-movements	All	**57.8±1.4**	**60±2**	**61.7±3.2**	**62.6±3.3**	**64.8±3.5**	**64.8±3.5**
	No CD	57.7±3.2	59±1.5	58.2±3.1	58.4±2.9	60.5±0.5	60.5±0.5
	No WKM	56.4±2	57.5±1.6	58.7±0.7	57.1±0.2	61.1±1	61.1±1
eye-state	All	**71.7±1.1**	**72.8±0.7**	**74.4±2.1**	**76.1±2**	80.2±0.3	80.2±0.3
	No CD	71.5±0.5	72.1±1.3	71.9±0.9	74.5±0.9	**80.3±0.4**	**80.3±0.4**
	No WKM	71.2±0.3	71.8±1.4	71.7±1.2	73.4±1.8	80.2±1.2	80.2±1.2
Shape^{2}CART$_3$							
electricity	All	**81.8±0.2**	**84.5±0.3**	**86.6±0.8**	**87.3±1**	88.8±0.2	88.8±0.2
	No CD	79.8±0.5	81.8±0.3	85±0.6	86±0.3	**89±0.3**	89±0.3
	No WKM	80±0.4	81.2±0.3	85.1±0.6	85.8±0.9	89.1±0.5	**89.1±0.5**
eye-movements	All	**59.6±2.4**	**63.6±1.4**	**66.2±1.9**	**67.5±3**	**63.9±2.4**	**63.9±2.4**
	No CD	55.1±1	58±0	58±1.7	57.4±3.4	51.9±1.8	51.9±1.8
	No WKM	56.6±1.1	58±2	60.3±3	62.7±6.3	55.4±3.6	55.4±3.6
eye-state	All	73.1±1.1	**75.9±0.4**	79.3±1.1	81.1±0.6	**80.6±1.9**	81.1±0.6
	No CD	**74±0.8**	75.4±1.8	**80.2±0.2**	81.5±0.4	80.3±1.1	**81.5±0.4**
	No WKM	73.3±1.1	75.3±2	79±3	**81.7±6.3**	78.8±3.6	78.8±3.6

Table 9: Runtime (s. ± std.) results for the optimization ablation analysis. Best approach for each model and dataset is **bolded**.

	Model	2	3	4	5	6	Overall
				ShapeCART			
electricity	All	0.396±0.002	**0.438±0.006**	0.88±0.007	1.356±0.011	2.145±0.177	2.145±0.177
	No CD	**0.283±0.018**	0.439±0.017	**0.692±0.06**	0.883±0.018	**1.385±0.097**	**1.385±0.097**
	No WKM	0.294±0.011	0.481±0.009	0.722±0.016	**0.809±0.012**	1.463±0.043	1.463±0.043
eye-movements	All	0.464±0.009	0.91±0.01	1.54±0.02	2.501±0.018	3.879±0.329	3.879±0.329
	No CD	**0.277±0.011**	**0.48±0.018**	**0.846±0.033**	**1.421±0.046**	**2.382±0.473**	**2.382±0.473**
	No WKM	0.31±0.012	0.622±0.022	1.576±0.159	1.847±0.039	2.693±0.2	2.693±0.2
eye-state	All	0.339±0.003	0.505±0.002	0.678±0.005	1.171±0.005	2.087±0.1	2.087±0.1
	No CD	**0.165±0.011**	0.292±0.007	0.457±0.029	0.88±0.094	1.306±0.089	1.306±0.089
	No WKM	0.172±0.006	**0.238±0.034**	**0.283±0.008**	**0.501±0.038**	**0.834±0.039**	**0.834±0.039**
				ShapeCART_3			
electricity	All	0.646±0.014	1.138±0.012	2.301±0.081	4.603±0.381	7.767±0.918	7.767±0.918
	No CD	**0.318±0.014**	**0.546±0.014**	**1.087±0.054**	**1.992±0.045**	3.01±0.35	3.01±0.35
	No WKM	0.438±0.004	1.118±0.052	1.903±0.068	2.098±0.12	**2.688±0.02**	**2.688±0.02**
eye-movements	All	0.661±0.015	2.216±0.179	4.876±0.325	6.152±0.443	12.47±0.314	12.47±0.314
	No CD	**0.352±0.027**	**0.656±0.105**	**1.201±0.03**	**1.749±0.193**	**2.762±0.078**	**2.762±0.078**
	No WKM	0.629±0.07	1.564±0.264	3.672±0.31	3.811±0.331	4.829±0.155	4.829±0.155
eye-state	All	0.574±0.007	1.063±0.008	2.511±0.133	4.777±0.111	6.192±0.148	6.192±0.148
	No CD	0.192±0.008	0.48±0.044	1.071±0.144	1.975±0.048	4.265±0.132	4.265±0.132
	No WKM	**0.136±0.007**	**0.478±0.014**	**0.59±0.029**	**1.167±0.073**	**1.86±0.154**	**1.86±0.154**
				$\text{Shape}^2\text{CART}$			
electricity	All	1.751±0.02	3.068±0.041	3.943±0.022	6.214±0.068	7.709±0.056	7.709±0.056
	No CD	**1.585±0.005**	2.759±0.052	**3.713±0.17**	4.962±0.154	**5.619±0.056**	**5.619±0.056**
	No WKM	1.885±0.007	**2.36±0.004**	3.816±0.123	**4.508±0.047**	5.876±0.025	5.876±0.025
eye-movements	All	1.882±0.068	3.41±0.018	5.833±0.091	9.208±0.331	14.078±0.496	14.078±0.496
	No CD	**1.553±0.124**	2.845±0.055	5.288±0.141	**7.391±0.063**	9.512±0.076	9.512±0.076
	No WKM	1.698±0.046	**3.278±0.165**	**4.849±0.063**	9.436±0.206	**9.116±0.577**	**9.116±0.577**
eye-state	All	1.428±0.009	2.65±0.068	4.042±0.019	6.192±0.074	5.843±0.092	5.843±0.092
	No CD	1.301±0.05	**1.454±0.014**	2.261±0.017	3.397±0.191	4.196±0.163	4.196±0.163
	No WKM	**1.048±0.022**	1.762±0.029	**2.223±0.002**	**2.62±0.08**	**3.191±0.099**	**3.191±0.099**
				$\text{Shape}^2\text{CART}_3$			
electricity	All	**2.077±0.024**	4.083±0.066	6.865±0.109	13.089±0.404	16.725±0.356	16.725±0.356
	No CD	2.274±0.035	**3.113±0.104**	**4.469±0.124**	**5.756±0.742**	**8.358±0.733**	**5.756±0.742**
	No WKM	2.253±0.035	4.182±0.025	5.976±0.013	6.594±0.101	8.824±0.615	8.824±0.615
eye-movements	All	2.973±0.024	6.749±0.222	14.32±0.381	23.759±3.123	41.232±2.209	41.232±2.209
	No CD	2.533±0.071	**4.393±0.277**	**7.732±0.387**	**9.818±0.516**	**13.094±0.479**	**9.818±0.516**
	No WKM	**2.344±0.071**	6.604±0.165	16.5±1.009	23.284±0.671	21.673±1.054	21.673±1.054
eye-state	All	1.998±0.009	3.895±0.009	6.083±0.386	7.614±0.383	14.603±0.709	7.614±0.383
	No CD	**1.077±0.008**	**1.994±0.008**	3.078±0.041	4.739±0.317	9.667±0.879	**4.739±0.317**
	No WKM	1.386±0.004	2.247±0.017	**2.959±0.05**	**3.863±0.527**	**6.192±0.195**	6.192±0.195

G.2.3 Pairwise Selection Heuristic Ablation

In this section, we examine the benefits of utilizing our pairwise selection heuristic. To do this, we do not score pairs of features and instead allow $\text{Shape}^2\text{CART}$ and $\text{Shape}^2\text{CART}_3$ to construct all bivariate shape functions at each node. Like in the previous ablation, we work with a subset of our datasets and run hyperparameter tuning to choose the model with the highest validation accuracy at each depth. We report the average test accuracy in 10 and training runtime in 11.

We observe that utilizing our heuristic has significant benefits in improving the training runtime for both $\text{Shape}^2\text{CART}$ and $\text{Shape}^2\text{CART}_3$ across all datasets and depth. This improvement is very apparent on the eye-movements dataset where $\text{Shape}^2\text{CART}$ and $\text{Shape}^2\text{CART}_3$ have an $\sim 5\times$ and $\sim 6\times$ reduction, respectively, in training runtime at depth 6. When looking at test accuracy, we observe that allowing for all pairs does benefit test accuracy. Interestingly, the accuracy of $\text{Shape}^2\text{CART}_3$ benefits from limiting pairs on most depths on the eye-state dataset.

Table 10: Test accuracy results (% ± std.) for the pairwise heuristic ablation.

Dataset	Model	2	3	4	5	6	Overall
				Shape^{2}CART			
electricity	Heur.	80.6 ± 0.6	82 ± 0.6	83.9 ± 0.3	86.5 ± 1.2	87.5 ± 0.5	87.5 ± 0.5
	No Heur.	$\mathbf{83.1 \pm 0.8}$	$\mathbf{85.8 \pm 0.2}$	$\mathbf{86.3 \pm 0.3}$	$\mathbf{87 \pm 0.1}$	$\mathbf{88.1 \pm 1}$	$\mathbf{88.1 \pm 1}$
eye-movements	Heur.	57.8 ± 1.4	60 ± 2	61.7 ± 3.2	62.6 ± 3.3	64.8 ± 3.5	64.8 ± 3.5
	No Heur.	$\mathbf{59.3 \pm 1.2}$	$\mathbf{63.6 \pm 2.5}$	$\mathbf{68.4 \pm 1.6}$	$\mathbf{75.2 \pm 3}$	$\mathbf{77.8 \pm 2.7}$	$\mathbf{77.8 \pm 2.7}$
eye-state	Heur.	$\mathbf{71.7 \pm 1.1}$	72.8 ± 0.7	74.4 ± 2.1	76.1 ± 2	80.2 ± 0.3	80.2 ± 0.3
	No Heur.	70.8 ± 0.8	$\mathbf{73.7 \pm 0.7}$	$\mathbf{76.1 \pm 1}$	$\mathbf{77 \pm 2.1}$	$\mathbf{81 \pm 1}$	$\mathbf{81 \pm 1}$
				Shape^{2}CART$_3$			
electricity	Heur.	81.8 ± 0.2	84.5 ± 0.3	86.6 ± 0.8	87.3 ± 1	$\mathbf{88.8 \pm 20}$	$\mathbf{88.8 \pm 20}$
	No Heur.	$\mathbf{84.7 \pm 0.8}$	$\mathbf{88.9 \pm 0.2}$	$\mathbf{89 \pm 1}$	$\mathbf{89 \pm 0.1}$	88.3 ± 0.1	88.9 ± 0.2
eye-movements	Heur.	59.6 ± 2.4	63.6 ± 1.4	66.2 ± 1.9	67.5 ± 3	63.9 ± 2.4	63.9 ± 2.4
	No Heur.	$\mathbf{62 \pm 1.2}$	$\mathbf{69.9 \pm 2.5}$	$\mathbf{78.6 \pm 1.6}$	$\mathbf{79.7 \pm 3}$	$\mathbf{74.9 \pm 2.7}$	$\mathbf{74.9 \pm 2.7}$
eye-state	Heur.	$\mathbf{73.1 \pm 1.1}$	75.9 ± 0.4	$\mathbf{79.3 \pm 1.1}$	$\mathbf{81.1 \pm 0.6}$	$\mathbf{80.6 \pm 1.9}$	$\mathbf{81.1 \pm 0.6}$
	No Heur.	$\mathbf{73 \pm 0.8}$	$\mathbf{76.3 \pm 0.7}$	77.2 ± 0.1	78.9 ± 2.1	76.1 ± 1	78.9 ± 2.1

Table 11: Runtime results (s. ± std.) for the pairwise heuristic ablation.

Dataset	Model	2	3	4	5	6	Overall
				Shape^{2}CART			
electricity	Heur.	$\mathbf{1.751 \pm 0.02}$	$\mathbf{3.068 \pm 0.041}$	$\mathbf{3.943 \pm 0.022}$	$\mathbf{6.214 \pm 0.068}$	$\mathbf{7.709 \pm 0.056}$	$\mathbf{7.709 \pm 0.056}$
	No Heur.	3.989 ± 0.037	7.202 ± 0.123	9.121 ± 0.142	13.878 ± 0.319	16.101 ± 0.187	16.101 ± 0.187
eye-movements	Heur.	$\mathbf{1.882 \pm 0.068}$	$\mathbf{3.41 \pm 0.018}$	$\mathbf{5.833 \pm 0.091}$	$\mathbf{9.208 \pm 0.331}$	$\mathbf{14.078 \pm 0.496}$	$\mathbf{14.078 \pm 0.496}$
	No Heur.	16.716 ± 0.204	28.674 ± 0.132	41.5 ± 0.361	75.599 ± 4.085	77.686 ± 4.074	77.686 ± 4.074
eye-state	Heur.	$\mathbf{1.428 \pm 0.009}$	$\mathbf{2.65 \pm 0.068}$	$\mathbf{4.042 \pm 0.019}$	$\mathbf{6.192 \pm 0.074}$	$\mathbf{5.843 \pm 0.092}$	$\mathbf{5.843 \pm 0.092}$
	No Heur.	8.321 ± 0.127	9.455 ± 0.201	11.765 ± 0.312	13.482 ± 0.483	14.123 ± 0.336	14.123 ± 0.336
				Shape^{2}CART$_3$			
electricity	Heur.	$\mathbf{2.077 \pm 0.024}$	$\mathbf{4.083 \pm 0.066}$	$\mathbf{6.865 \pm 0.109}$	$\mathbf{13.089 \pm 0.404}$	$\mathbf{16.725 \pm 0.356}$	16.725 ± 0.356
	No Heur.	5.084 ± 0.037	11.164 ± 0.123	18.321 ± 0.101	26.528 ± 0.319	42.123 ± 0.331	$\mathbf{11.164 \pm 0.123}$
eye-movements	Heur.	$\mathbf{2.973 \pm 0.024}$	$\mathbf{6.749 \pm 0.222}$	$\mathbf{14.32 \pm 0.381}$	$\mathbf{23.759 \pm 3.123}$	$\mathbf{41.232 \pm 2.209}$	$\mathbf{41.232 \pm 2.209}$
	No Heur.	30.616 ± 0.204	56.75 ± 0.132	155.597 ± 0.361	201.283 ± 4.085	224.403 ± 4.074	224.403 ± 4.074
eye-state	Heur.	$\mathbf{1.998 \pm 0.009}$	$\mathbf{3.895 \pm 0.009}$	$\mathbf{6.083 \pm 0.386}$	$\mathbf{7.614 \pm 0.383}$	$\mathbf{14.603 \pm 0.709}$	$\mathbf{7.614 \pm 0.383}$
	No Heur.	7.594 ± 0.127	9.84 ± 0.201	17.761 ± 0.413	21.993 ± 0.483	33.826 ± 0.651	21.993 ± 0.483

H Visualized Trees

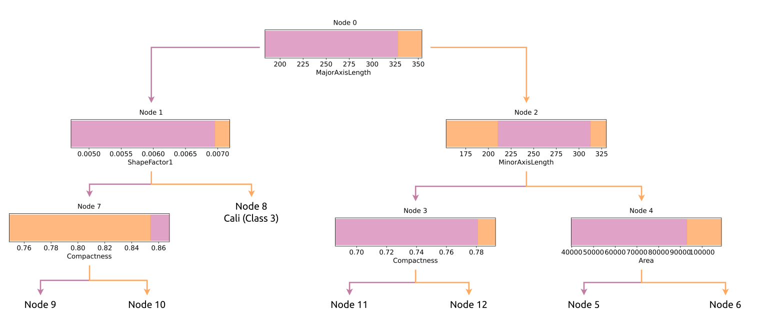

Figure H.5: ShapeCART (Depth 3) trained on Bean

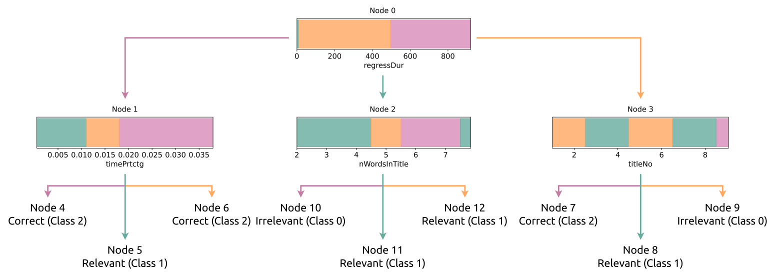

Figure H.6: ShapeCART$_3$ (Depth 2) trained on Eye-Movements

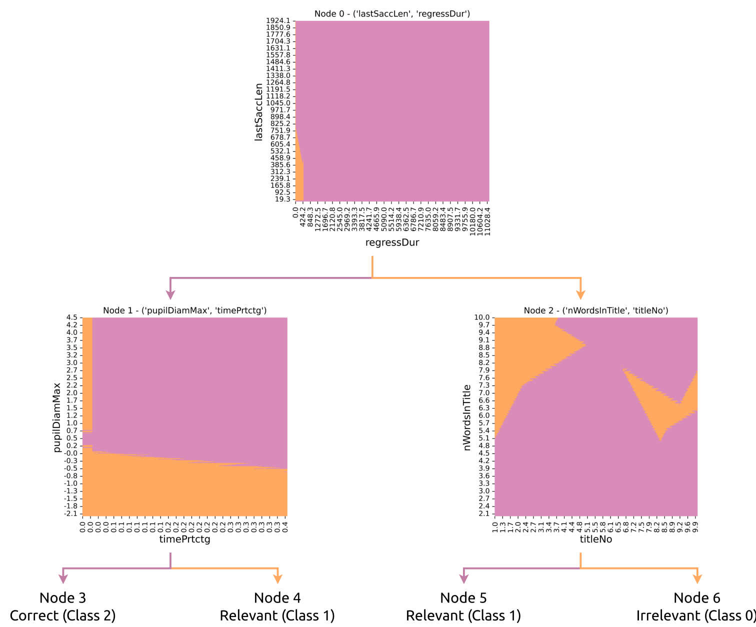

Figure H.7: Shape^{2}CART (Depth 2) Trained on the Eye-Movements dataset

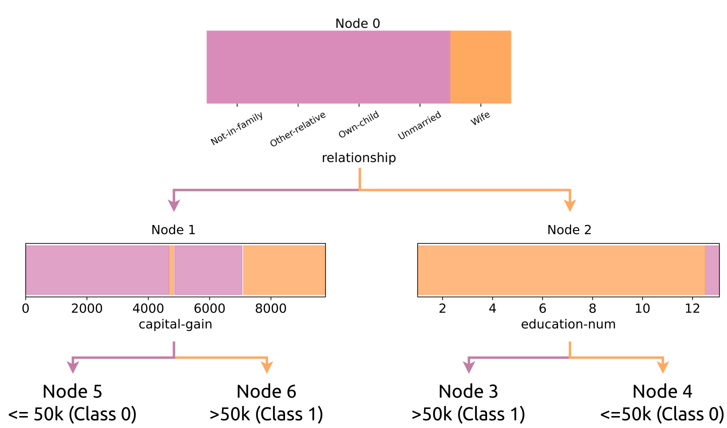

Figure H.8: ShapeCART (Depth 2) Trained on the Adult dataset

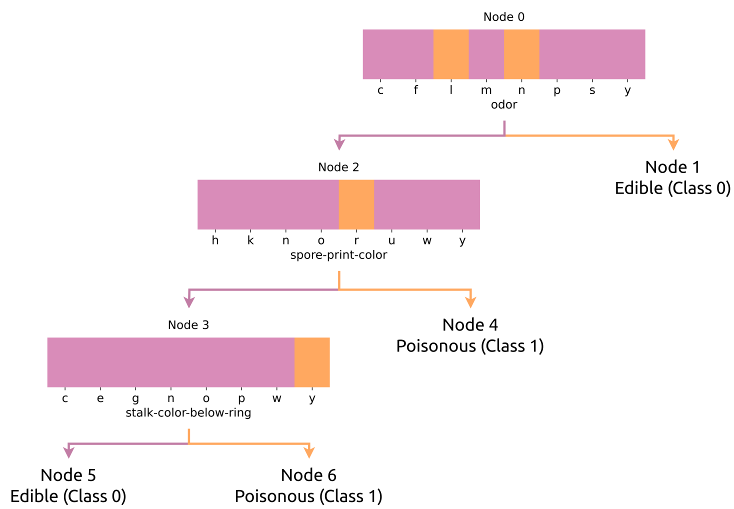

Figure H.9: ShapeCART (Depth 3) Trained on the Mushroom dataset

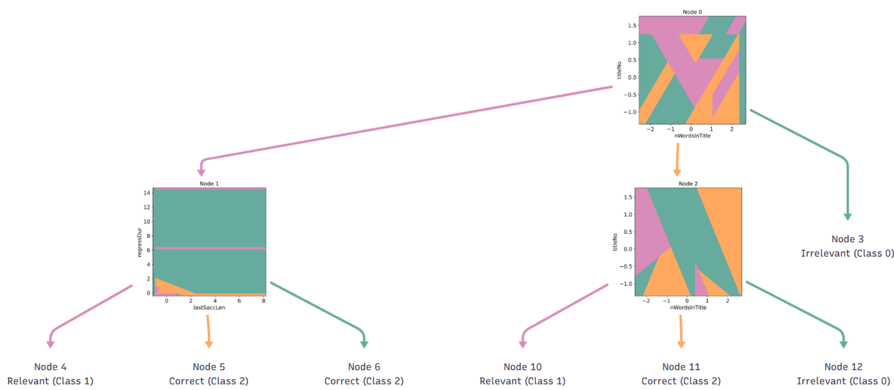

Figure H.10: Shape^{2}CART$_3$ (Depth 2) Trained on Eye-Movements

I Other Shape Function Candidates

While our approach uses CART to construct the internal tree, our two-stage approach can be applied to any algorithm that can group samples, including other trees. To demonstrate this, we present a version of the ShapeCART algorithm that constructs the internal tree via DPDT [29] (denoted as SGT-C (D)). Note that we exclude Higgs from this evaluation as the DPDT version did not finish on most depths. Test accuracy results for this algorithm per dataset can be seen in Table 12 and runtime results in Table 13. Overall, we observe minor accuracy differences between constructing the internal tree with CART and DPDT. However, we observe that the runtime of the DPDT variant is much higher across all depths and datasets.

J Regression

To adapt ShapeCART to the regression setting ($y_n \in \mathbb{R} \quad \forall n = 1, \ldots, N$), we simply need to modify the superadditive impurity metric $\mathcal{H}$ from Gini/Entropy (class-based impurity measures), to one adapted for a regression setting, such as squared-error or absolute error. To accommodate this, we must modify the calculation of the empirical distribution of a set of samples (Equation (7)) to instead calculate the mean value of the target in the set of samples.

Table 12: Test Accuracy comparison (% ± std.) between ShapeCART and ShapeCART with DPDT internal tree.

Dataset	Model	2	3	4	5	6	Overall
adult	SGT-C	**82.80 ± 0.20**	**84.10 ± 0.30**	84.00 ± 0.30	**84.30 ± 0.40**	**84.60 ± 0.60**	**84.60 ± 0.60**
	SGT-C (D)	81.30 ± 1.90	83.90 ± 0.20	**84.10 ± 0.30**	84.20 ± 0.60	84.50 ± 0.60	84.50 ± 0.60
avila	SGT-C	—	—	64.50 ± 2.90	71.70 ± 1.80	82.00 ± 2.10	82.00 ± 2.10
	SGT-C (D)	—	—	**67.30 ± 2.80**	**75.50 ± 2.80**	**83.80 ± 3.30**	**83.80 ± 3.30**
bank	SGT-C	**88.50 ± 2.30**	**89.50 ± 3.20**	**97.00 ± 0.90**	**96.70 ± 0.00**	**96.70 ± 0.00**	**97.00 ± 0.90**
	SGT-C (D)	88.00 ± 2.00	89.00 ± 2.80	90.90 ± 2.20	92.40 ± 1.60	89.30 ± 4.10	92.40 ± 1.60
bean	SGT-C	—	85.10 ± 1.20	**88.80 ± 0.40**	89.70 ± 0.40	89.80 ± 0.10	89.80 ± 0.10
	SGT-C (D)	—	**85.20 ± 0.90**	88.70 ± 0.30	**90.40 ± 0.90**	**90.90 ± 0.60**	**90.90 ± 0.60**
bidding	SGT-C	**98.10 ± 0.70**	**98.40 ± 0.60**	**99.70 ± 0.20**	**99.60 ± 0.30**	**99.60 ± 0.10**	**99.60 ± 0.10**
	SGT-C (D)	**98.10 ± 0.70**	98.20 ± 0.70	99.50 ± 0.20	99.20 ± 0.20	**99.60 ± 0.20**	**99.60 ± 0.20**
covtype	SGT-C	—	**68.90 ± 0.20**	70.40 ± 0.10	72.10 ± 0.50	73.70 ± 0.20	73.70 ± 0.20
	SGT-C (D)	—	68.80 ± 0.70	**70.50 ± 0.20**	**72.40 ± 0.10**	**73.80 ± 0.20**	**73.80 ± 0.20**
electricity	SGT-C	75.50 ± 0.10	78.50 ± 0.40	81.30 ± 0.80	84.40 ± 0.10	84.80 ± 0.60	84.80 ± 0.60
	SGT-C (D)	**75.60 ± 0.20**	**79.30 ± 0.60**	**82.50 ± 0.40**	**85.10 ± 0.60**	**86.60 ± 0.40**	**86.60 ± 0.40**
eucalyptus	SGT-C	—	53.60 ± 3.30	55.90 ± 4.00	56.30 ± 4.60	**58.80 ± 7.20**	**58.80 ± 7.20**
	SGT-C (D)	—	**54.10 ± 3.50**	**56.30 ± 4.80**	**57.20 ± 7.20**	56.10 ± 1.20	57.20 ± 7.20
eye-movements	SGT-C	**48.10 ± 2.10**	53.00 ± 0.70	54.90 ± 1.20	53.90 ± 0.70	57.40 ± 1.20	57.40 ± 1.20
	SGT-C (D)	47.30 ± 0.30	**53.20 ± 0.40**	**55.00 ± 1.20**	**57.00 ± 0.10**	**60.40 ± 0.20**	**60.40 ± 0.20**
eye-state	SGT-C	64.30 ± 0.90	69.00 ± 0.20	70.50 ± 1.20	72.40 ± 1.30	74.50 ± 1.10	74.50 ± 1.10
	SGT-C (D)	**66.60 ± 0.60**	**70.20 ± 0.50**	**72.50 ± 0.90**	**74.10 ± 0.10**	**75.30 ± 0.40**	**75.30 ± 0.40**
fault	SGT-C	—	59.70 ± 3.90	**65.30 ± 1.80**	68.00 ± 0.40	69.70 ± 3.60	69.70 ± 3.60
	SGT-C (D)	—	**60.20 ± 5.70**	**65.30 ± 1.40**	**70.10 ± 1.70**	**69.90 ± 2.50**	**69.90 ± 2.50**
gas-drift	SGT-C	—	**66.30 ± 1.30**	76.00 ± 1.00	83.10 ± 2.00	**89.00 ± 0.90**	**89.00 ± 0.90**
	SGT-C (D)	—	66.00 ± 2.10	**76.80 ± 1.20**	**83.80 ± 0.90**	87.70 ± 2.70	87.70 ± 2.70
htru	SGT-C	**97.80 ± 0.10**	97.80 ± 0.10	97.80 ± 0.20	**97.90 ± 0.20**	97.60 ± 0.10	**97.80 ± 0.10**
	SGT-C (D)	**97.80 ± 0.10**	**97.90 ± 0.30**	**97.90 ± 0.20**	97.70 ± 0.10	**97.80 ± 0.10**	**97.80 ± 0.10**
magic	SGT-C	73.90 ± 1.00	77.10 ± 0.10	**79.60 ± 1.10**	80.10 ± 1.70	**81.00 ± 0.50**	**81.00 ± 0.50**
	SGT-C (D)	**74.90 ± 1.50**	**77.60 ± 1.00**	78.90 ± 1.00	**80.20 ± 0.30**	80.70 ± 0.70	80.70 ± 0.70
mini-boone	SGT-C	**84.80 ± 0.20**	87.10 ± 0.50	88.30 ± 0.30	**89.20 ± 0.20**	**89.70 ± 0.10**	**89.70 ± 0.10**
	SGT-C (D)	84.70 ± 0.20	**87.40 ± 0.50**	**88.40 ± 0.30**	89.10 ± 0.30	89.60 ± 0.30	89.60 ± 0.30
mushroom	SGT-C	98.60 ± 0.30	99.30 ± 0.10	99.80 ± 0.20	**99.90 ± 0.10**	99.90 ± 0.10	99.90 ± 0.10
	SGT-C (D)	**98.90 ± 0.30**	**99.60 ± 0.20**	**99.90 ± 0.10**	**99.90 ± 0.10**	**100.00 ± 0.00**	**100.00 ± 0.00**
occupancy	SGT-C	**99.00 ± 0.10**	**98.90 ± 0.10**	99.00 ± 0.10	**99.00 ± 0.20**	**99.20 ± 0.20**	**99.20 ± 0.20**
	SGT-C (D)	**99.00 ± 0.10**	**98.90 ± 0.10**	**99.10 ± 0.20**	**99.00 ± 0.20**	99.00 ± 0.20	99.00 ± 0.20
page	SGT-C	—	95.20 ± 0.30	96.40 ± 0.20	**96.30 ± 1.20**	96.20 ± 0.40	96.30 ± 1.20
	SGT-C (D)	—	**95.60 ± 0.20**	**96.70 ± 0.20**	96.00 ± 0.20	**96.40 ± 0.20**	**96.70 ± 0.20**
pendigits	SGT-C	—	—	**79.30 ± 3.90**	86.40 ± 0.70	88.30 ± 1.20	88.30 ± 1.20
	SGT-C (D)	—	—	78.10 ± 1.20	**86.70 ± 0.10**	**90.10 ± 0.30**	**90.10 ± 0.30**
raisin	SGT-C	85.70 ± 1.40	**85.90 ± 2.30**	84.30 ± 3.90	84.30 ± 2.90	84.40 ± 2.90	84.30 ± 2.90
	SGT-C (D)	**85.90 ± 1.40**	85.60 ± 2.20	**85.90 ± 1.40**	**85.70 ± 2.20**	**85.70 ± 2.20**	**85.60 ± 2.20**
rice	SGT-C	**93.10 ± 0.40**	**92.70 ± 0.80**	**92.50 ± 0.90**	92.10 ± 0.90	92.50 ± 0.50	92.50 ± 0.50
	SGT-C (D)	**93.10 ± 0.40**	**92.70 ± 0.40**	92.20 ± 0.90	**93.00 ± 0.60**	**93.00 ± 0.60**	**93.00 ± 0.60**
room	SGT-C	93.00 ± 0.40	**98.30 ± 0.20**	**99.40 ± 0.10**	**99.40 ± 0.00**	**99.60 ± 0.00**	**99.60 ± 0.00**
	SGT-C (D)	**93.20 ± 0.60**	98.20 ± 0.30	99.20 ± 0.20	99.20 ± 0.20	99.50 ± 0.30	99.50 ± 0.30
segment	SGT-C	—	**83.30 ± 3.60**	**88.90 ± 0.80**	**89.80 ± 2.50**	**91.50 ± 1.90**	**91.50 ± 1.90**
	SGT-C (D)	—	**83.30 ± 3.70**	87.80 ± 1.00	89.60 ± 2.50	91.10 ± 0.60	91.10 ± 0.60
skin	SGT-C	93.20 ± 0.20	**97.70 ± 0.10**	**98.50 ± 0.00**	**98.90 ± 0.10**	**99.20 ± 0.20**	**99.20 ± 0.20**
	SGT-C (D)	**93.40 ± 0.30**	97.60 ± 0.40	98.30 ± 0.20	**98.90 ± 0.00**	**99.20 ± 0.30**	**99.20 ± 0.30**
wilt	SGT-C	97.10 ± 0.60	97.10 ± 0.10	**97.90 ± 0.50**	97.60 ± 0.20	97.60 ± 0.20	**97.90 ± 0.50**
	SGT-C (D)	**97.30 ± 0.40**	**97.20 ± 0.40**	97.80 ± 0.50	**97.90 ± 0.60**	**97.90 ± 0.60**	**97.90 ± 0.60**

Table 13: Runtime comparison (s. ± std.) between SGT-C and SGT-C with DPDT internal tree.

Dataset	Model	2	3	4	5	6	Overall
adult	SGT-C	**0.386** ± **0.009**	**0.596** ± **0.009**	**0.894** ± **0.016**	**1.120** ± **0.023**	**1.144** ± **0.033**	**1.144** ± **0.033**
	SGT-C (D)	12.129 ± 0.425	21.990 ± 0.318	33.145 ± 2.011	42.382 ± 5.490	47.805 ± 7.702	47.805 ± 7.702
avila	SGT-C	—	—	**1.711** ± **0.036**	**2.343** ± **0.007**	**2.733** ± **0.088**	**2.733** ± **0.088**
	SGT-C (D)	—	—	79.209 ± 1.388	117.866 ± 2.197	147.429 ± 3.796	147.429 ± 3.796
bank	SGT-C	**0.101** ± **0.001**	**0.138** ± **0.004**	**0.165** ± **0.015**	**0.184** ± **0.008**	**0.179** ± **0.010**	**0.165** ± **0.015**
	SGT-C (D)	1.878 ± 0.051	3.073 ± 0.234	1.203 ± 0.145	1.334 ± 0.202	3.492 ± 0.586	1.334 ± 0.202
bean	SGT-C	—	**1.892** ± **0.027**	**2.420** ± **0.071**	**1.797** ± **0.041**	**2.328** ± **0.061**	**2.328** ± **0.061**
	SGT-C (D)	—	35.693 ± 0.138	14.431 ± 0.125	22.438 ± 0.111	32.694 ± 0.614	32.694 ± 0.614
bidding	SGT-C	**0.132** ± **0.001**	**0.207** ± **0.002**	**0.208** ± **0.004**	**0.256** ± **0.004**	**0.333** ± **0.011**	**0.333** ± **0.011**
	SGT-C (D)	0.998 ± 0.116	1.516 ± 0.195	2.172 ± 0.249	2.395 ± 0.414	2.660 ± 0.374	2.660 ± 0.374
covtype	SGT-C	—	**6.135** ± **0.034**	**11.224** ± **0.014**	**10.618** ± **0.064**	**15.770** ± **0.096**	**15.770** ± **0.096**
	SGT-C (D)	—	439.259 ± 2.396	227.655 ± 2.720	496.196 ± 4.219	603.667 ± 7.049	603.667 ± 7.049
electricity	SGT-C	**0.396** ± **0.002**	**0.438** ± **0.006**	**0.880** ± **0.007**	**1.356** ± **0.011**	**2.145** ± **0.177**	**2.145** ± **0.177**
	SGT-C (D)	5.202 ± 0.177	55.811 ± 0.318	89.526 ± 0.634	142.068 ± 0.423	197.176 ± 10.258	197.176 ± 10.258
eucalyptus	SGT-C	—	**0.319** ± **0.048**	**0.523** ± **0.063**	**0.799** ± **0.046**	**0.995** ± **0.030**	**0.995** ± **0.030**
	SGT-C (D)	—	9.549 ± 1.072	12.593 ± 1.672	21.382 ± 2.201	8.036 ± 0.352	21.382 ± 2.201
eye-movements	SGT-C	**0.464** ± **0.009**	**0.910** ± **0.010**	**1.540** ± **0.020**	**2.501** ± **0.018**	**3.879** ± **0.329**	**3.879** ± **0.329**
	SGT-C (D)	39.528 ± 0.188	74.187 ± 0.853	125.956 ± 2.508	193.079 ± 8.774	272.248 ± 22.320	272.248 ± 22.320
eye-state	SGT-C	**0.339** ± **0.003**	**0.505** ± **0.002**	**0.678** ± **0.005**	**1.171** ± **0.005**	**2.087** ± **0.100**	**2.087** ± **0.100**
	SGT-C (D)	7.504 ± 0.050	6.531 ± 0.032	10.843 ± 0.071	17.596 ± 0.487	27.433 ± 1.789	27.433 ± 1.789
fault	SGT-C	—	**0.641** ± **0.032**	**1.044** ± **0.045**	**1.945** ± **0.153**	**2.599** ± **0.102**	**2.599** ± **0.102**
	SGT-C (D)	—	12.921 ± 1.536	22.719 ± 2.346	15.749 ± 1.534	21.990 ± 1.183	21.990 ± 1.183
gas-drift	SGT-C	—	**7.714** ± **0.016**	**14.076** ± **0.137**	**17.205** ± **0.505**	**20.722** ± **0.314**	**20.722** ± **0.314**
	SGT-C (D)	—	167.784 ± 2.558	490.627 ± 2.307	763.837 ± 24.354	552.024 ± 10.415	552.024 ± 10.415
htru	SGT-C	**0.328** ± **0.002**	**0.456** ± **0.004**	**0.646** ± **0.020**	**0.586** ± **0.065**	**0.561** ± **0.020**	**0.456** ± **0.004**
	SGT-C (D)	9.063 ± 0.021	4.563 ± 0.040	6.069 ± 0.382	24.929 ± 4.588	7.213 ± 0.460	7.213 ± 0.460
magic	SGT-C	**0.312** ± **0.000**	**0.477** ± **0.003**	**0.689** ± **0.003**	**1.071** ± **0.042**	**1.876** ± **0.061**	**1.876** ± **0.061**
	SGT-C (D)	2.937 ± 0.019	5.079 ± 0.021	50.830 ± 0.901	28.735 ± 0.621	17.214 ± 1.284	17.214 ± 1.284
mini-boone	SGT-C	**11.023** ± **0.078**	**12.995** ± **0.129**	**16.074** ± **0.116**	**20.609** ± **0.135**	**25.352** ± **0.062**	**25.352** ± **0.062**
	SGT-C (D)	297.692 ± 1.729	153.416 ± 2.880	236.032 ± 2.896	284.030 ± 2.886	738.861 ± 24.597	738.861 ± 24.597
mushroom	SGT-C	**0.185** ± **0.003**	**0.331** ± **0.008**	**0.399** ± **0.026**	**0.327** ± **0.004**	**0.330** ± **0.004**	**0.327** ± **0.004**
	SGT-C (D)	3.644 ± 0.108	4.357 ± 0.128	4.824 ± 0.229	3.400 ± 0.045	4.881 ± 0.258	4.881 ± 0.258
occupancy	SGT-C	**0.148** ± **0.002**	**0.186** ± **0.003**	**0.176** ± **0.004**	**0.197** ± **0.006**	**0.405** ± **0.024**	**0.405** ± **0.024**
	SGT-C (D)	1.821 ± 0.010	7.952 ± 0.093	7.419 ± 0.673	9.229 ± 1.337	7.998 ± 0.908	7.998 ± 0.908
page	SGT-C	—	**0.263** ± **0.001**	**0.437** ± **0.022**	**0.696** ± **0.075**	**0.933** ± **0.015**	**0.696** ± **0.075**
	SGT-C (D)	—	6.266 ± 0.109	5.173 ± 0.086	13.694 ± 0.449	6.238 ± 0.361	5.173 ± 0.086
pendigits	SGT-C	—	—	**2.312** ± **0.020**	**3.443** ± **0.053**	**4.788** ± **0.033**	**4.788** ± **0.033**
	SGT-C (D)	—	—	128.053 ± 2.424	203.633 ± 0.778	70.396 ± 0.761	70.396 ± 0.761
raisin	SGT-C	**0.137** ± **0.002**	**0.196** ± **0.011**	**0.263** ± **0.029**	**0.249** ± **0.034**	**0.317** ± **0.087**	**0.249** ± **0.034**
	SGT-C (D)	1.620 ± 0.017	1.262 ± 0.275	2.892 ± 0.513	1.762 ± 0.414	1.832 ± 0.348	1.262 ± 0.275
rice	SGT-C	**0.134** ± **0.002**	**0.239** ± **0.003**	**0.337** ± **0.029**	**0.441** ± **0.062**	**0.541** ± **0.049**	**0.541** ± **0.049**
	SGT-C (D)	1.073 ± 0.015	1.987 ± 0.017	3.106 ± 0.356	3.663 ± 0.810	3.592 ± 0.679	3.663 ± 0.810
room	SGT-C	**0.238** ± **0.004**	**0.535** ± **0.004**	**0.704** ± **0.027**	**0.770** ± **0.014**	**0.773** ± **0.012**	**0.773** ± **0.012**
	SGT-C (D)	20.538 ± 0.232	9.141 ± 0.236	19.394 ± 0.328	22.729 ± 1.789	7.997 ± 0.356	7.997 ± 0.356
segment	SGT-C	—	**0.410** ± **0.015**	**0.468** ± **0.016**	**0.844** ± **0.053**	**1.009** ± **0.109**	**1.009** ± **0.109**
	SGT-C (D)	—	7.757 ± 0.310	20.347 ± 0.481	12.982 ± 0.307	16.016 ± 0.189	16.016 ± 0.189
skin	SGT-C	**0.399** ± **0.009**	**0.520** ± **0.010**	**0.645** ± **0.008**	**0.776** ± **0.009**	**0.919** ± **0.018**	**0.919** ± **0.018**
	SGT-C (D)	9.559 ± 0.388	21.933 ± 0.846	29.639 ± 0.523	35.859 ± 0.545	23.851 ± 2.256	23.851 ± 2.256
wilt	SGT-C	**0.127** ± **0.002**	**0.169** ± **0.001**	**0.252** ± **0.009**	**0.292** ± **0.033**	**0.316** ± **0.059**	**0.252** ± **0.009**
	SGT-C (D)	1.772 ± 0.048	1.539 ± 0.027	2.165 ± 0.260	2.814 ± 0.336	3.213 ± 0.159	3.213 ± 0.159

We provide regression results for ShapeCART, ShapeCART$_3$, Shape^{2}CART, and Shape^{2}CART$_3$. We benchmark our axis-aligned approaches against CART and our Bivariate approaches against BiCART. Our hyperparameter tuning approach and hyperparameter search in this setting are similar to the classification setting. One key modification is that we only use the MSE criterion (rather than tuning for a splitting criterion like in the classification setting). We report the mean squared error (MSE) of each model on five open source regression datasets - Ailerons (OpenML ID: 44137), Black Friday (OpenML ID: 41540), California Housing (OpenML ID: 44025), and Diamonds (OpenML ID: 42225) - broken down by depth and overall best model, chosen by best validation MSE, in Table 14. We scale the target to zero mean and one standard deviation for all datasets to ensure stability during training. We observe that ShapeCART consistently outperforms CART on all datasets except Ailerons, while ShapeCART$_3$ outperforms CART on all datasets. A similar trend can be seen in the Bivariate approaches, where Shape^{2}CART outperforms BiCART on all datasets except Ailerons. Interestingly, Shape^{2}CART also outperforms Shape^{2}CART$_3$ on California Housing and Ailerons, while achieving similar performance on Black-Friday and Diamonds.

Table 14: Test MSE Results (MSE ± std.) on regression datasets. Approaches are split into axis-aligned and bivariate by the dotted line. Best approach is **bolded**, second best is *italicized*.

dataset	Model	2	3	4	5	6	Overall
ailerons	CART	0.453 ± 0.011	0.368 ± 0	*0.302 ± 0.001*	*0.257 ± 0.006*	*0.235 ± 0.004*	*0.235 ± 0.004*
	SGT-C	*0.452 ± 0.012*	*0.364 ± 0.004*	0.312 ± 0.003	0.258 ± 0.007	0.238 ± 0.005	0.238 ± 0.005
	SGT$_3$-C	**0.375 ± 0.002**	**0.321 ± 0.004**	**0.263 ± 0.004**	**0.23 ± 0.004**	**0.229 ± 0.006**	**0.229 ± 0.006**
	BiCART	*0.363 ± 0.004*	**0.28 ± 0.006**	**0.231 ± 0.016**	**0.206 ± 0.008**	**0.197 ± 0.008**	**0.197 ± 0.008**
	S^{2}GT-C	**0.358 ± 0.008**	*0.296 ± 0.005*	*0.256 ± 0*	*0.233 ± 0.001*	*0.231 ± 0.009*	*0.231 ± 0.009*
	S^{2}GT$_3$-C	0.37 ± 0.002	0.311 ± 0.005	0.265 ± 0.001	0.237 ± 0.008	0.236 ± 0.003	0.236 ± 0.001
black-friday	CART	0.728 ± 0.012	0.608 ± 0.008	0.567 ± 0.018	0.513 ± 0.011	0.502 ± 0.009	0.502 ± 0.009
	SGT-C	*0.548 ± 0.019*	*0.528 ± 0.002*	*0.512 ± 0.001*	*0.504 ± 0.016*	*0.496 ± 0.016*	*0.496 ± 0.016*
	SGT$_3$-C	**0.528 ± 0.002**	**0.507 ± 0.008**	**0.492 ± 0.008**	**0.487 ± 0.017**	**0.484 ± 0.022**	**0.484 ± 0.022**
	BiCART	0.728 ± 0.011	0.606 ± 0.012	0.561 ± 0.001	0.508 ± 0.011	0.499 ± 0.013	0.499 ± 0.013
	S^{2}GT-C	*0.546 ± 0.001*	*0.511 ± 0.002*	*0.504 ± 0.012*	**0.491 ± 0.011**	*0.487 ± 0.013*	*0.487 ± 0.013*
	S^{2}GT$_3$-C	**0.519 ± 0.002**	**0.502 ± 0.003**	**0.49 ± 0.008**	*0.492 ± 0.007*	**0.485 ± 0.021**	**0.485 ± 0.021**
california	CART	0.54 ± 0.015	0.459 ± 0.008	0.418 ± 0.006	0.377 ± 0.001	0.338 ± 0.004	0.338 ± 0.004
	SGT-C	*0.508 ± 0.005*	*0.43 ± 0.007*	*0.354 ± 0.002*	*0.305 ± 0.001*	*0.272 ± 0.008*	*0.272 ± 0.008*
	SGT$_3$-C	**0.426 ± 0.007**	**0.33 ± 0.001**	**0.271 ± 0.002**	**0.254 ± 0.006**	**0.245 ± 0.001**	**0.245 ± 0.001**
	BiCART	0.442 ± 0.001	0.345 ± 0.003	0.297 ± 0.002	0.267 ± 0.007	0.243 ± 0.009	0.243 ± 0.009
	S^{2}GT-C	**0.358 ± 0.008**	**0.272 ± 0.001**	**0.228 ± 0.001**	**0.224 ± 0.008**	**0.213 ± 0.012**	**0.213 ± 0.012**
	S^{2}GT$_3$-C	*0.415 ± 0.002*	*0.332 ± 0*	*0.276 ± 0.007*	*0.243 ± 0.008*	*0.236 ± 0.001*	*0.236 ± 0.001*
diamonds	CART	0.169 ± 0.001	0.125 ± 0.001	0.105 ± 0	0.092 ± 0	0.081 ± 0	0.081 ± 0
	SGT-C	*0.169 ± 0.001*	*0.11 ± 0*	*0.084 ± 0.002*	*0.062 ± 0.001*	*0.047 ± 0.001*	*0.047 ± 0.001*
	SGT$_3$-C	**0.116 ± 0**	**0.079 ± 0.001**	**0.048 ± 0.001**	**0.038 ± 0.003**	**0.031 ± 0.001**	**0.031 ± 0.001**
	BiCART	0.163 ± 0.001	0.113 ± 0.002	0.084 ± 0.001	0.066 ± 0.001	0.051 ± 0.001	0.051 ± 0.001
	S^{2}GT-C	*0.128 ± 0.002*	**0.064 ± 0.001**	*0.044 ± 0.003*	*0.042 ± 0.001*	*0.036 ± 0*	*0.036 ± 0*
	S^{2}GT$_3$-C	**0.106 ± 0.001**	*0.07 ± 0.001*	**0.041 ± 0.002**	**0.034 ± 0.002**	**0.031 ± 0.002**	**0.031 ± 0.002**

K Extra Pseudocode

In this section, we provide pseudocode for the TDIDT induction of a tree (Algorithm 3) and of our coordinate descent procedure (Algorithm 4).

Algorithm 3: ShapeCART (TDIDT Pseudocode)

Input: Features $\mathcal{X}$, Target $\mathcal{Y}$, Branching Factor K, Pairwise Candidate Limit P, Coordinate Descent Iterations R, Pairwise Reg. γ, Branching Reg. λ, Impurity $\mathcal{H}(\cdot)$, Weighted Impurity $\mathcal{L}(\cdot)$, Max Depth M_{max}, Minimum Impurity Improvement $\mathcal{L}_{\text{min}}$, Min. Samples Leaf S_{leaf}, Min. Samples Split S_{split}
Output: $\mathcal{I}, \mathcal{T}$

```
I ← {};   T ← {}
Q ← Initialize Empty Priority Queue
L^init ← L(Y)
(D^0, L^0, f^0(·)) ← SelectShapeFunc( X, Y, K, P, R, γ, λ, H(·), L(·) )
Q.add({0 : (D^0, L^init − L^0, f^0(·), 0, X × Y)})
while |Q| > 0 do
    i, (D^i, L̃^i, f^i(·), M^i, D) ← Pop(Q)
    if L̃^i < L_min then
        Add node i to T, assign the label as the dominant class in D, continue to next node
    end
    if M = M_max then
        Add node i to T, assign the label as the dominant class in D, continue to next node
    end
    if |D| < S_split then
        Add node i to T, assign the label as the dominant class in D, continue to next node
    end
    if ∃D^j ∈ D : |D^j| < S_leaf then
        Add node i to T, assign the label as the dominant class in D, continue to next node
    end
    Add node i and corresponding shape function f^i(·) to I
    foreach D^j ∈ D do
        Mark j as child of i
        X^j, Y^j ← D^j
        (D^j, L^j, f^j(·)) ← SelectShapeFunc( X^j, Y^j, K, P, R, γ, λ, H(·), L(·))
        Q.add(j : {D^j, L^j − L^i, f^j(·), M^i + 1, D^j})
    end
end
return I, T
```

Algorithm 4: Coordinate Descent

Input: $\mathbf{a}, [\pi_1, \ldots, \pi_L], [W_1, \ldots, W_L], K, \mathcal{H}(\cdot), R$
Output: $\mathbf{a}, \boldsymbol{L}$

```
for k ← 1 to K do
    W_k ← Σ_{ℓ=1}^{L} W_ℓ 1(a_ℓ = k)
    P_k ← Σ_{ℓ=1}^{L} 1(a_ℓ = k) (W_ℓ π_ℓ)
end
L* ← ∞ for r ← 1 to R do
    foreach ℓ in RandomizedOrder(1,...,L) do
        P_{a_ℓ} ← P_{a_ℓ} − W_ℓ π_ℓ; W_{a_ℓ} ← W_{a_ℓ} − W_ℓ
        L ← Σ_{j=1}^{k} W_k H(P_k / W_k)
        Store P̃_k ← P_k, W̃_k ← W_k   ∀k = 1, ..., K
        for k ← 1 to K do                          // Iterate through all Branches
            W_k ← W̃_k + W_ℓ; P_k ← P̃_k + W_ℓ π_ℓ
            L_k ← L − W̃_k H(P̃_k / W̃_k) + W_k H(P_k / W_k)
            if L_k ≤ L* then                      // Commit if weighted impurity improves
                L* ← L_k; a_ℓ ← i
                StoreState(P_1, W_1, ..., P_K, W_K)
            end
        end
        (P_1, W_1, ..., P_K, W_K) ← RetrieveState()
    end
end
return a, L
```